Order Number 9510656

Characterization and regulation of basement membrane heparan sulfate proteoglycan

Eisler, Jesse Grant, Ph.D.

City University of New York, 1994

U·M·I
300 N. Zeeb Rd.
Ann Arbor, MI 48106

Characterization and Regulation of Basement Membrane Heparan Sulfate Proteoglycan

Jesse Grant Eisler

A dissertation submitted to the Graduate Faculty in Biomedical Sciences in partial fulfillment of the requirements for the degree of Doctor of Philosophy, granted by the City University of New York.

1994

Approval Page

This manuscript has been read and accepted by the Graduate Faculty in Biomedical Sciences in satisfaction of the dissertation requirement for the degree of Doctor of Philosophy.

9/29/94
Date

L. Rotwein
Chair of Examining Committee

10/3/94
Date

Executive Officer

Howard Fillit, MD

Stephen Salton, MD, PhD

Mariann Blum, PhD
Supervisory Committee

The City University of New York

Abstract

Characterization and Regulation of Basement Membrane Heparan Sulfate Proteoglycan

by

Jesse G. Eisler

Advisor: Professor Howard Fillit

Heparan sulfate proteoglycans (HSPG) are integral components of the extracellular matrix of basement membranes (BM). BMs may support polarized cells, being deposited at the basal side of endothelial or epithelial cells, or they may surround such cells as muscle cells, or neurons. As constituents of the BM, HSPGs play a role in several important physiologic processes, including BM structure and permeability, regulating the activity of protease inhibitors and growth factors, and they have been implicated in the pathogenesis of Alzheimer's Disease. Despite their significance we do not have a complete understanding of the structure of all basement membrane HSPGs, or of the factors that may regulate the metabolism of these molecules.

We examined the relationship between the two major forms of basement membrane HSPGs, perlecan and vascular HSPG (vHSPG). Immunological methods revealed a high degree of antigenic uniqueness, and protein precursor studies demonstrated different precursor sizes for the two basement membrane HSPGs. The data suggests that these molecules are unique gene products. While the cDNA sequence of perlecan is known, there is no DNA sequence available for vHSPG to date, and the elucidation of the exact relationship between perlecan and vHSPG awaits this information.

The regulation of basement membrane proteoglycans produced by mouse endothelial cells exposed to various relevant factors was examined. Our analysis employed RNA analysis, ion exchange, gel filtration, and A4-affinity chromatography. We determined that the relative proportion of proteoglycans with high net negative charges was susceptible to alteration when cells were treated with IL-1β, TGF-β, and low molecular weight hyaluronic

acid, whereas the proteoglycans with a lower net negative charge were not altered significantly. IL-1β (10 ng/ml) increased the proportion of secreted proteoglycans, TGF-β (5 ng/ml) increased the relative amount of cellular proteoglycans, while low molecular weight hyaluronic acid had the opposite effect and decreased the amount of cellular proteoglycans with a high net negative charge. These results suggest that proteoglycans are subject to specific regulation by various cellular/extracellular factors, and fluctuations in the levels of these factors that can occur in disease processes may have important consequences for the regulation of proteoglycans.

Acknowledgments

There are many people who have been invaluable to me in my Ph.D. training. My sincere appreciation goes to Dr. Howard Fillit for giving me the opportunity to conduct my graduate work in his laboratory in the Department of Geriatrics. As members of Dr. Fillit's lab, Beatrice Leveugle, Maja Matic, Wan Hong Ding, and Chang Pei Yang were both colleagues and friends and the time we spent together was quite memorable. Over the past few years Dr. Stephen Salton has been a role model without equal as both a scientist and an individual. I thank him for all the guidance he provided and for all the meaningful discussions we had. I hope that other students have the opportunity to interact with someone like Dr. Salton in their training. His graduate student, Suzie Snyder, was very supportive all along the way and I am very grateful to her. I would also like to thank Dr. Mariann Blum and her graduate student Cynthia Shannon for all of their assistance; they have been wonderful to work with, and I look forward to future projects together.Thanks to everyone in the Fishberg Center for Neurobiology whom I had the pleasure to work with. As chairman of the Neurobiology Department, Professor Jim Roberts is the best. It was an honor and a joy to be a member of his department as a graduate student.

Of course, my family; Mom, Dad, Joe and Glenna, and Amy were patient, supportive, and loving throughout my training. Thanks for listening me talk about proteoglycans and the blood-brain barrier. I know you understood more than you say you did. Thank you all for everything.

Table of Contents

List of Figures

Introduction

Basement membranes are ubiquitous structures found throughout the body supporting polarized cells such as endothelium and epithelium or surrounding cells such as muscle, or nerve cells. Heparan sulfate proteoglycans are a family of molecules which are integral components of the cell surface and the basement membrane They play a role in several important physiologic processes including basement membrane structure and permeability, binding and regulating the activity of protease inhibitors (such as antithrombin III thereby providing a nonthrombogenic surface in the vasculature) and various growth factors. Basement membrane heparan sulfate proteoglycans have also been implicated in the pathogenesis of Alzheimer's Disease. Despite their involvement in many important biological events we do not have a complete understanding of the structure of all BM heparan sulfate proteoglycans, or of the factors that may regulate the metabolism of these molecules.

The focus of much of my graduate study has been to elucidate the nature of the relationship between the two major forms of basement membrane heparan sulfate proteoglycan, perlecan and what is referred to here as vHSPG, and to investigate the regulation of endothelial proteoglycans by various relevant factors. To investigate the nature of the relationship between perlecan and vHSPG I employed several methodologies. Immunological methods revealed a high degree of antigenic uniqueness, and protein precursor studies demonstrated different precursor sizes for the two basement membrane heparan sulfate proteoglycans. The full cDNA and genomic DNA sequence of perlecan is known, and since the amino acid sequences obtained from peptide fragments of vHSPG did not share significant homology to the published sequence of

perlecan or any other protein in the protein databases, we decided to attempt to clone the cDNA for vHSPG.

In chapter 1 the background related to my thesis is presented. Chapter 2 describes the methods utilized in this study. Chapter 3 is divided into three sections of results:1. immunohistochemical evidence for the localization of vHSPG in the pathologic alterations of aging and AD, 2. the characterization of basement membrane HSPGs, and 3. the biochemical and molecular regulation of endothelial cell proteoglycans by several factors that play a role in disease processes. In Chapter 4. I discuss these results and attempt to put them into a larger context.

Chapter 1. Background and Significance

I. Structure of Proteoglycans

Proteoglycans (PGs) are widely distributed throughout the animal phyla [1]. PGs are molecules which contain a protein core to which glycosaminoglycans are covalently linked via an O-glycosidic linkage. They are a complex and heterogeneous class of molecules with a wide distribution in intracellular granules, on cell surfaces and in the basement membranes of many cell types. A limited number of the core proteins of proteoglycans have been isolated and their structures determined. Among the proteoglycans of the extracellular matrix are the large proteoglycans perlecan, aggrecan,and versican, and the small proteoglycans decorin and fibromodulin. Syndecan is a proteoglycan with a membrane-embedded core protein. The polypeptide core of a proteoglycan determines the type of glycosaminoglycan (GAG) chains associated with the core protein and the cellular localization of the proteoglycan. The protein core contains amino acid consensus sequences for the attachment of xylose from UDP-xylose onto serine residues in glutamic acid/aspartic acid-X-serine-glycine sequences, or in serine-glycine repeats after such a sequence which are attachment sites for glycosaminoglycan chains.

Important structural and functional diversity in the proteoglycans stems from the heterogeneity of their GAG composition. Each glycosaminoglycan is a linear heteropolysaccharide possessing characteristic disaccharide subunits. Each subunit has a hexosamine (D-glucosamine or D-galactosamine) and either hexuronic acid (D-glucuronic acid or L-iduronic acid) or galactose units (in keratan sulfate). These GAG units are arranged in alternating, unbranched sequence. The number of GAGs covalently linked to any particular proteoglycan varies greatly.

The types of glycosaminoglycans are heparan sulfate/heparin, chondroitin sulfate dermatan sulfate, keratan sulfate. Glycosaminoglycans are linear polysaccharide chains generally 20-200 sugars in length, which are attached via the linkage region (see above) to serine residues by the sequential addition of identical disaccharides. There may be 1-100 chains on a given core protein, of one or mixed types, and this number may vary in a cell type-specific manner. The sulfated residues on GAGs confer proteoglycans with a highly negative net charge, making them the most highly anionic molecules present in vertebrate tissues [2], and are widely distributed throughout the animal phyla [3]. These long GAG chains are then usually further modified by either O-sulfation, N-deacetylation/N-sulfation, and/or epimerization of the glucuronic acid to iduronic acid, generating an enormous amount of diversity.

Proteoglycans bind nearly all extracellular matrix components. The major components of the extracellular molecules (ECM) include the cell adhesion proteins, fibronectin, vitronectin, thrombospondin, and laminin; the structural components, collagens and elastin; and the proteoglycans. Non-specific electrostatic interactions in which the positive charge on basic amino acids couples with the highly negative charge of sulfate groups plays an important physiologic role. Through these binding interactions proteoglycans act as organizers of the extracellular matrix.

There is a large class of glycosaminoglycan binding proteins that appear to involve specific binding interactions. Models of these binding interactions describe the alignment of positive charges in the protein so as to interact with repetitive carboxyl units spaced evenly along the glycosaminoglycan chain. Unique patterns of sulfation in specific oligosaccharide sequences play a role in the binding between a spatially matched arrangement of basic amino acids, creating well-defined recognition sequences. Peptides with specific affinities for

heparan sulfate/heparin include the serpins (serine protease inhibitors), lipoprotein lipases, antithrombin III, and fibroblast growth factor I (acidic FGF) and II (basic FGF) [4]. Proteoglycans act as 'catalysts' of serpin action . Antithrombin III, heparin cofactor II, and protease nexin I all bind and inactivate serine proteases when GAGs are present.

II. Role of Proteoglycans in Cellular Processes

Proteoglycans have been found to bind many growth factors, and play a variety of roles in cellular processes such as the regulation of hemostasis, lipid metabolism, cell adhesion, migration, growth regulation, and in the structure and function of the extracellular matrix [1,2,5-10].

A. Modulation of Growth Factor Activity

The binding of FGFs to heparin or heparan sulfate chains of proteoglycans appears to protect the growth factors from degradation and enhance their affinity for their primary receptor [11]. A more direct physiologic role for heparan sulfate in modulating FGF activity exists. Binding of FGF to its high affinity receptor requires previous binding of FGF to the heparan sulfate chains of a membrane heparan sulfate proteoglycan or to free heparan sulfate [12]. In addition, proteoglycan binding may provide a matrix-bound or cell surface-bound reservoir of FGFs. From this reservoir, active FGF-GAG complex can be generated by proteolysis of the proteoglycan core proteins or partial degradation of the heparan sulfate component [13,14].

Using affinity chromatography, a develomental change in the specificity of HSPG for FGF-2 and FGF-1 was observed in neuroepithelium. Embryonic day 9-derived HSPG (20 GAG chains of 20 kd each) preferentially binds and

potentiates the action of FGF-2, whereas embryonic day 11-derived HSPG (12 GAG chains of 35 kD each) preferentially binds and potentiates the action of FGF-1 coinciding with the developmental regulation of these two FGFs in the neuroepithelium [15]. The synthesis of FGF-1 by precursor cells is closely coordinated with the modification of heparan sulfate side chains on a specific protein core that had not undergone alterations in size. This finding contrasts with previous findings that all heparan sulfate molecules bind to FGF with nearly equal affinity [16].

The binding of transforming growth factor-ß (TGF-ß) to its cellular receptor involves the protein core of the proteoglycan betaglycan. Betaglycan is thought to bind TGF-ß for the subsequent delivery to the signal transduction receptors responsive to this growth factor [17]. The extracellular matrix proteoglycan decorin binds TGF-ß through its protein core, and can neutralize its activity, presumably by competing with TGF-ß for the binding sites of the TGF-ß receptor. The synthesis of decorin is stimulated by TGF-ß suggesting that decorin is playing a role in a negative feedback loop governing TGF-ß activity [18].

B. Functions in the Vasculature

Proteoglycans constitute a minor component of vascular tissue but have been shown to influence a number of important vascular properties, such as viscoelasticity, permeability, thrombosis and lipid metabolism. Endothelial cells synthesize at least five types of heparan sulfate proteoglycans. Syndecan-1, syndecan-2 (fibroglycan) and syndecan-4 (ryudocan) are type 1 integral cell membrane proteoglycans. Glypican is anchored to the cell surface by a glycosylphosphatidylinositol (GPI) linkage [4]. Perlecan, a large (400-6000 kDa) heparan sulfate proteoglycan, is part of endothelial cell basement membranes.

Another basement membrane HSPG, referred to as vHSPG, is also present in vascular basement membrane [19,20]. The exact relationship between vHSPG and perlecan is unclear. There are conflicting reports, some suggesting that these two proteoglycans share the same precursor [21,22], and others demonstrating a lack of immunologic cross-reactivity [20,23,24].

Heparan sulfate contributes to the process of hemostasis in the vasculature, by facilitating the interaction of the protease inhibitor antithrombin III (AT III) with its substrate, thrombin, thereby inactivating the protease thrombin and inhibiting the clotting cascade. The binding of heparan sulfate to AT III accelerates the enzyme-inhibitor complex by 1000-fold [10]. In this way heparan sulfate is thought to provide a non-thrombogenic surface for the vascular endothelium. Lipoprotein lipase associates with heparan sulfate on the endothelial cell surface, making the enzyme accessible to di- and triglycerides that circulate with very low density lipoproteins [7]. PGs/GAGs have also been isolated from the atherosclerotic lesions of humans and have been shown to precipitate low density lipoproteins [25], indicating their role in vascular diseases.

As mentioned above, the sulfate esters on heparan sulfate side chains make HSPG the most highly charged structure in vertebrate tissue, and in the basement membrane, these fixed charges are responsible for conferring the selective filtration properties of the basement membrane. It is this filtration barrier which establishes the ionic filtration properties of the glomerular basement membrane [26-28].

Depletion of heparan sulfate by heparinase I and heparinase III, but not heparinase II, have been shown to inhibit angiogenesis [29]. This finding is surprising since degradation of the basement membrane might be expected to release bFGF and lead to neovascularization. However it appears that the

depletion of positionally fixed heparan sulfate growth factor receptors outweighs the angiogenic effect of free heparan sulfate. Both enzymes modulate the availability of specific bFGF binding sites that are required for bFGF-mediated bovine capillary endothelial cell angiogenesis.

C. Functions in the Nervous System

In the brain, proteoglycans are produced by neurons, glial and endothelial cells. Proteoglycans contribute to the establishment and regulation of cell-cell and cell-matrix interactions in the nervous system. Proteoglycans usually faciliate interactions mediated by integrins or cell adhesion molecules. A proteoglycan has been shown to promote neural crest migration in vitro [30]. Certain proteoglycans can be either permissive for (allow but not actively stimulate), or promote (actively stimulate) neuronal elongation [31,32]. Astrocytes, which provide a substratum to which nerve cells attach and elongate *in vivo* and *in vitro,* express a number of PGs on their cell surface and also secrete them into the extracellular environment. Of these proteoglycans, only HSPG enhances neurite outgrowth by sensory neurons on laminin [33].

A neuronal heparan sulfate proteoglycan was found to be present in basement membranes at early stages of chick development (E2 and E4) . At E4 the HSPG was also localized to the optic fibres in the optic stalk and then disappeared from this location by E10 but was maintained in the basement membrane structures [34].

III. Proteoglycans as Major Components of Basement Membrane

Basement membrane (BM) is a specialized form of extracellular matrix which occurs wherever cells meet connective tissue, and occurs underlying endothelia of capillaries and venules; around neurons, Schwann cells, adipocytes, skeletal and cardiac muscle cells; at the dermal-epidermal border of

the skin; at the base of all lumen-lining epithelia throughout the digestive, respiratory, reproductive, and urinary tracts; and at the base of parenchymatous cells of exocrine (pancreas, salivary glands) and endocrine (pituitary, thyroid, adrenal) glands [25].

A. Basement Membrane Proteoglycans

The proteoglycans found in the specialized form of the extracellular matrix known as the basement membrane (basal lamina) are heparan sulfate proteoglycans (HSPGs). There are numerous species of HSPG found within the cell and within the cellular membrane, and the extracellular matrix (see above). Heparan sulfate proteoglycans derived from the EHS tumor and the bovine glomerulus are two forms that have been described extensively [19,35-38]. In addition, they have been described for certain types of cultured cells. Significant differences exist in hydrodynamic size, the number and length of side chains, and in the size of the core protein. The actual relationship between the various described basement membrane HSPGs is still being examined. Whether these proteoglycans share a common gene product, and are related by a precursor product relationship, or are distinct proteins coded for by separate genes is unknown and is addressed in chapter 3. HSPG, laminin, type IV collagen, and entactin, are considered to be the predominant components of basement membrane. Two major forms of basement membrane HSPG are known. One form of basement membrane HSPG has a protein core of approximately 110,000 Daltons (Da), and an intact molecular weight of approximately 200,000 Da (herein referred to as vHSPG). Studies [39] demonstrated the presence of this heparan sulfate proteoglycan in glomerular basement membrane. As a component of the basement membrane, HSPG occupies a volume largely filled with water to which molecules or ions have access, whereas larger molecules are excluded, providing a selective filtration of macromolecules.

The other well characterized form of basement membrane HSPG is known as "perlecan". Due to its abundance in the mouse Engelbert-Holm-Swarm tumor, this form of HSPG has been the subject of much study. It has been well characterized and the cDNA has been fully sequenced [32]. The cDNA is 12 kilobases, and codes for a protein core of approximately 400,000 Daltons. The intact proteoglycan has a molecular weight of 600,000 Daltons. The complex structure of perlecan protein core, consists of five domains, including N-CAM-like domains containing immunoglobulin-like motifs, laminin-like, and LDL receptor-like regions, and a unique N-terminal domain suggests a multitude of possible functions which will only be elucidated with future studies.

B. Evidence for precursor-product relationship between the EHS HSPG and bmHSPG

Hassell et al. have described two forms of HSPG produced by the EHS tumor sarcoma [35]. The first is a high molecular weight/low density HSPG that had a protein core of ~400 kDa and an intact molecular weight of 600 to 800 Da. The low molecular weight high density HSPG had a protein core of ~90-130, kDa, and an intact molecular weight of ~350kDa. Antibodies to both large and small forms of bmHSPGs precipitated the protein that served as their biosynthetic precursor. These same antibodies precipitated the same size proteoglycans in bovine glomerular basement membrane preparations [22].

B. Evidence against a precursor-product relationship

Kato et al. [24] have attempted to further clarify the relationship between the low density and high density HSPG from the EHS tumor. Pulse-chase experiments yielded results that demonstrated the ratio of low density/high density did not change throughout the time course of the experiment. The

results suggest that the HD form is distinct from that of the LD form. The authors suggest that the immunogen used for the production of antibodies to BM HSPG were a mixture of the LD and HD form, and data suggesting that these BM HSPGs are related must be interpreted in this context.

Others [23] have identified two immunologically related basement membrane proteoglycans in bovine glomerulus, calf lens capsule and cultured lens epithelial cells [40]. The HSPGs ranged in size from 250,000 to 350,000 for the lens capsule, 350-kDa and 210-kD for the GBM, and 200-KDa and 400 kDa for the cultured lens epithelial cells. These HSPGs were all immunologically related but antibodies to them show limited affinity for the EHS proteoglycan. EHS antibodies, likewise, demonstrate minimal reaction with GBM proteoglycan and modest interaction with the lens capsule HSPG. In addition to the alterations in the size of the protein core, the size of the heparan sulfate chains varied considerably among cell types. HS chains in cultured cells were considerably longer than their counterparts in the lens capsule (M_r= 24,000 compared to 14,000).

These results point to the high degree of variability between HSPGs isolated from different tissues, and illustrates the difficulty of relating varying proteoglycans to each other.

V. Cytokines and Proteoglycans

All exogenous stimuli cause localized perturbations in cells, resulting in imbalances in cellular metabolism. If not corrected, these may lead to pathological consequences, not only to the receiving cells, but also to neighboring cells and possibly to the whole organism. In most circumstances, cells receiving exogenous stimuli respond rapidly to counteract any subsequent imbalances by internal adjustment of metabolic processes and by the secretion of mediators to communicate the nature of the imbalance to other cells and stimulate such cells to respond accordingly [41]. Proteoglycans at the cell surface and in the ECM play an important role in the cell's response to its environment.

Acute inflammation is the immune system's response to a variety of insults including infection, ischemia, foreign particles, neoplasia, and trauma. Initiation of the inflammatory response following tissue injury occurs within the microvasculature at the level of the capillary and postcapillary venule [42]. Following tissue injury, structural changes occur in the vessel wall, leading to a loss of endothelial cell integrity, leakage of fluid and plasma components from the intravascular compartment, and diapedesis of both red and white blood cells from the intraluminal space into the extravascular tissue, particularly the neuropil when considering the brain.

Specific inflammatory mediators produced at the sites of injury regulate the response of the vasculature to injury. Among these mediators are vasoactive molecules that act directly on the vasculature to increase vascular permeability. In addition, chemotactic factors are generated that recruit white blood cells from the vascular compartment into the injured tissue. Once present in tissue, recruited white blood cells secrete additional inflammatory mediators that either enhance or inhibit the inflammatory response [43].

Lymphokines, cytokines, and several other factors that are produced due to inflammation have direct effects on their target tissues as well as cause the recruitment and stimulation of inflammatory cells which in turn will have additional effects and produce other compounds involved in inflammation. Circulating factors can affect the brain by two routes. They may be produced by cells already existing in the brain parenchyma, such as microglia. Secondly, cells enter the brain during the inflammatory process, such as polymorphonuclear leukocytes, monocytes, basophils and eosinophils, and by direct penetration of the blood-brain barrier (BBB) [42]. The BBB, comprised of of the capillary bed of the brain and the ependymal lining of the choroid plexus, separates the blood from the cerebrospinal and interstitial fluids of the CNS. The BBB can act as a near absolute barrier to blood-borne peptides and proteins, or can regulate their passage by active or passive transport, as exemplified by the enkephalins. Cytokines such as IL-1 have been shown to be transported across the BBB [44], and may be produced by resident microglia in the brain [45].

Heparan sulfate molecules are involved in the adherence of inflammatory cells to the endothelium during the process of margination (the movement of cells from the vessel lumen to the parenchyma), and alterations in the composition of heparan sulfate may be important to the effectiveness as well as to the sequelae of the inflammatory process. As previously mentioned, proteoglycans accumulate in intimal lesions of blood vessels in the early phases of atherosclerosis as well as in other vascular diseases [10]. Both the core proteins as well as the GAG chains are known to have interactions with a number of different macromolecules. These interactions influence such arterial properties as viscoelasticity, permeability, lipid metabolism, hemostasis, and thrombosis. Additionally, evidence has accumulated that HSPG may play a role in the pathogenesis of AD, and the argument for a central role of the vasculature

in the disease continues to be accumulate [46]. Taken in this context, a quantitative and/or qualitative modification of vascular proteoglycans may have profound effects on the function of this tissue.

Numerous factors involved in inflammation have been also been associated with AD. These include complement, cytokines, as well as MHC antigens and others. Given the substantial role that proteoglycans play in several physiologic and pathologic processes we undertook to examine the ways in which proteoglycans may be regulated by several of these factors; IL-1ß, TGF-ß and low molecular weight hyaluronic acid.

IL-1ß beta is a 153-amino acid protein produced by activated monocytes, macrophages, endothelial cells, central nervous system microglia, and B cells, all of which are antigen presenting cells [18,47,48]. Monocytes and macrophages are the major producers in vivo. IL-1ß has a broad spectrum of activities, most of which are stimulatory. IL-1ß induces I-CAM-1 on endothelial cells and thereby increases the ability of endothelial cells to bind to T cells. In acute inflammation IL-1ß activates endothelium to secrete prostaglandins and adhesion molecules. In chronic inflammation it causes endothelial cells to produce growth factors and leads to angiogenesis [43]. The action of IL-1ß in both acute and chronic inflammation promotes the activation of endothelium, which leads to vascular leakage, a condition that may have particular significance in the BBB where maintenance of separate vascular and parenchymal compartments is critical to proper brain metabolism.

IL-1 beta has been shown to increase proteoglycan degradation and inhibit the synthesis of new proteoglycans, without altering the structure of the proteoglycans (Pasternak et al.). IL-1 has been localized to neuritic plaques and has been shown to regulate the synthesis of APP [47]. IL-1 plays a role in the acute phase response in the brain as well as in the pathogenesis of AD [49].

The mature form of TGF-ß is 25 kDa and is composed of two identical 12.5 kd subunits covalently linked by disulfide bonds [18]. The effects of TGF-beta on the immune system are overwhelmingly inhibitory, indicating that it may subserve an important negative feedback role. TGF-beta also acts as an inhibitor of cell proliferation. It has a marked effect on ECM production by a variety of cell types. TGF-ß stimulates the synthesis and secretion of different types of collagen and fibronectin, thrombospondin, as well as PGs [2,18]. It stimulates the synthesis of collagen and PG degrading enzymes in chondrocytes [50]. It is also known to influence the expression of integrins. There is a chemotactic effect on several different cell types. TGF-ß binds to the core protein of several proteoglycans, and modifies PG expression and structure.

Hyaluronic acid (HA) is the simplest of the GAG structures, and consists of alternating polymers of N-acetylglucosamine and glucuronic acid [51-53]. HA is not synthesized covalently bound to a protein core, and is therefore classified simply as a glycosaminoglycan. A single molecule of HA may have a molecular weight up to 10 million (~25,000 repeat disaccharides). Their open, random coil structures occupy large solvent domains which give solutions of high viscosity.

Hyaluronic acid may play a role in several developmental processes [51,54,55]. In early development and before tissue differentiation, HA is often the major structural macromolecule in the extracellular matrix, where it can promote both cell proliferation and migration. HA is the most abundant of the GAGs in the extracellular matrix of the brain and plays a major role in the maintainenance of the structure of the extracellular matrix of the brain [54]. Several proteoglycans, including versican, have been shown to bind to HA and share a common immunolocalization to HA.

Hyaluronic acid oligosaccharides have been shown to be angiogenic [56]. These low molecular weight fractions increase the production of collagen in

bovine endothelial cells in vitro and in vivo as demonstrated in the chorioallantoic membrane of the chick embryo [57]. The enzyme hyaluronidase degrades the high molecular weight HA into smaller fragments and this enzyme is produced by activated macrophages during inflammation and the acute phase response. In additon a variety of wound and mucosal pathogens, such as Streptococcus pyogenes, produce hyaluronidase.

VI.The Role of Heparan Sulfate Proteoglycans in Alzheimer's Disease

A. Background

In addition to the attention HSPG has receiving for its role in modulating growth factor activity and as a structural constituent of the basement membrane, considerable efforts are seeking to determine the role that HSPG plays in Alzheimer's disease (AD) as well as amyloidoses and dementing illnesses. HSPG plays a fundamental role in the formation of amyloid of all types including the beta-amyloidosis of AD. There is also evidence demonstrating this extracellular matrix molecule in the intraneuronal neurofibrillary tangles of AD. In the following pages, I will give a brief survey of some of the important issues in AD, as well as a description of the key findings demonstrating the role of HSPG in amyloidosis.

The impact of AD on public health is truly of large proportions. It is estimated that there will be about 2 million cases of the disease in individuals over 75 by the year 2000.

A minority of cases of AD are thus far thought to be related to genetic factors. An important genetic relationship exists between Down's syndrome and AD. Down's syndrome is caused by duplication of chromosome 21 which contains the gene for beta-amyloid precursor protein (ß-APP). Autosomal dominant AD may be linked to this chromosome as well, and in at least a few rare families, AD seems to be caused by a specific mutation of chromosome 21. Nevertheless, the relative number of cases that may be attributed to genetic factors is very minimal.

The etiology of AD, in the majority of cases remains completely unknown. Although viruses have been demonstrated to cause other dementing illnesses such as Kuru, Creutzfeldt-Jakob disease, and Gerstmann-Strausler-Scheinker syndrome , they have not been demonstrated in AD[45]. Both aluminum and

silicon have been found in senile plaques in AD, and patients with both AD and Down syndrome may have defective aluminum transport proteins in the blood [58]. Still, many researchers feel this is a result of neuronal damage and not a cause.

A marked decrease in choline acetyltransferase is seen in the cerebral cortex as well as a loss of cholinergic neurons of the nucleus basalis of Meynert in Alzheimer's Disease [59,60]. These neurons send afferents to the cerebral cortex, especially the parietal and temporal lobes. These observations resulted in the formulation of the cholinergic model of senile dementia of the Alzheimer Type [61,62]. Since deficits were later observed in the norepinephrine, serotonin, dopamine, glutamate, GABA, neuropeptide Y, corticotropin releasing factor, substance P, and somatostatin circuits, there has been less significance placed on the unitary cholinergic model of AD [59,63-65].

A number of growth factors that may be necessary for the development and ongoing maintenance of neural pathways have been considered as candidates for playing a role in AD [66-68]. NGF is believed to play a role in the function of the basal forebrain cholinergic neurons [68]. Continuous intracerebral infusion of NGF over a period of four weeks has been demonstrated to partly reverse cholinergic cell body atrophy and improve the retention of a spatial memory task in behaviorally impaired aged rats [69]. The FGFs, insulin-like growth factor, BDNF, EGF, and others all appear to play a role in the maintenance of aging and/or injured neurons, but no conclusions can currently be made about their specific role in AD.

Neuritic plaques, neurofibrillary tangles, and congophilic angiopathy constitute the hallmark lesions of AD and may be found widespread in the hippocampus, nucleus basalis, association cortices, and other regions, while the primary sensory and motor areas are relatively spared from neuropathology. A

subset of cortical pyramidal neurons have been shown to be the most vulnerable cell types in AD [70]. These pyramidal neurons stain positively for the non-phosphorylated form of heavy and light neurofilament, and their loss is found within layers III and V of the cerebral cortex. Studies on monkey brain have shown the analogous neurons to be involved in cortico-cortical connections (Jellinger et al., 1991). These findings have resulted in a view of AD as a cortical disconnection syndrome [62,70,71].

In normal aging, hippocampal changes are evident but association area changes are not. There is overall loss of neurons in many regions, resulting in sulcal widening of the hemispheres. As it appears that a subset of neurons may be most involved in AD, it raises the question of selective vulnerability [71]. Although the pyramidal neurons in question only constitute approximately 20% of total neurons within layers III and V, the largest pyramidal neurons experience an 85% reduction in number [70]. These neurons may have specific metabolic requirements which cannot undergo even minimal fluctuations.

Small changes over the course of a lifetime in the vascular supply may be one of the alterations affecting these neurons. The cerebral vasculature has also been shown to display pathogenic alterations in AD. Capillary loss appears to correlate with the degree of pyramidal cell drop-out. Nevertheless, capillaries appear fragmented and irregular and develop thickened and reduplicated basement membranes [72]. The degree of microangiopathy correlates well with the laminar and regional distribution of effected pyramidal cells, with layers III and IV of the association cortices having the highest levels of atrophic vessels and the lowest vascular density [73]. It is not known if the vascular alteration are a primary or secondary factor in the disease process.

The vascular pathology of AD may be compounded by a compromise in the blood-brain barrier (BBB). Increased CSF/serum ratios for IgG and albumin

are consistent with increased permeability of the BBB in some cases [58]. The immunohistochemical localization of serum proteins in senile plaques may only be indirect evidence for these changes because of the confounding effect of the postmortem delay in which serum proteins might be leaking into the parenchyma.

Heparan sulfate proteoglycans play an important role in the function of the normal vascular barrier especially affecting the charge selectivity of the vascular barrier [10]. Alterations in the proteoglycan content of basement membranes severely compromise the functioning of this filtration barrier [39,74]. The presence of both forms of basement membrane HSPG in senile plaques also suggests a role of the vasculature in senile plaque formation.

The increasing amount of attention being directed to the amyloid lesions of AD has given us a better understanding of the amyloid precursor protein, APP, and its aberrant cleavage product, A4 or beta protein, the major protein constituent of amyloid deposits which characterize the neuritic plaques and the congophilic angiopathy seen in AD [65]. A mature senile plaque contains a core of the A4 peptide, surrounded by dystrophic neurites, activated microglia, and fibrillary astrocytes. A4 has a molecular weight of 4 kDa is approximately 40 amino acids and is derived from APP. APP exists in three major forms, derived from alternate transcripts, having 695, 751, and 770 amino acids [75]. The 695 a.a. form is the predominate type in brain, and lacks the Kunitz protease inhibitor which 751 and 770 contain. Cortical and hippocampal neurons, astrocytes, endothelial cells, and microglial cells have been reported to be cortical sites of APP synthesis [76]. Cleavage leading to formation of A4 occurs within the first 14 amino acids of the membrane region of APP and 28 amino acids to the N-terminus of the membrane region. Cleavage by an unknown secretase within the A4 sequence between amino acid 687 and 688 precludes the formation of

A4 [77]. The resulting amino terminal fragment of approximately 100 kDa is secreted and has been identified as protease nexin (PN) II [78]. The amyloid deposits are most commonly seen as senile plaques (SP) but may also be manifested as congophilic angiopathy or diffuse amyloid deposits. All deposits invariably contain A4 peptide [79], but other components of senile plaques have also been described such as a_1-antichymotrypsin [64], complement factors, amyloid P component [80] and glycosaminoglycans and/or proteoglycans [81]. The presence of serum proteins in the senile plaques has led to the idea that the blood-brain barrier may be defective in AD. However, the number of proteins found in senile plaques is large and their apparent origin is quite diverse. The degree to which any one of these constituents is playing a fundamental role in the pathogenesis of AD remains unclear, warranting an understanding of the relative contributions from each of the contributory cellular sources.

Although amyloidosis is a key feature of senile plaques of AD, the actual process of amyloid deposition is common to all forms of amyloidosis. There are many amyloidogenic proteins with very diverse origins, but the process of amyloidosis shares a common element, heparan sulfate proteoglycan.

A. Proteoglycans and amyloidosis

1. GAGs and amyloidoisis

It has been demonstrated that both highly sulfated glycosaminoglycans and amyloid proteins deposited in tissues (spleen, liver, and kidney) at virtually the same time and in the same location using an experimental model of inflammation-associated amyloidosis [82].

Although the sites of GAG synthesis in various systemic organs during amyloid deposition has not yet been identified, light microscopic and ultrastructural [83] studies suggest that endothelial and/or reticuloendothelial

cells may be involved. The initial accumulation of GAGs and amyloid in experimental AA amyloidosis occurs in the perifollicular sinusoids of the spleen and the walls of the central veins in the liver, two sites having a predominance of reticuloendothelial and/or endothelial cells [84]. The first clear evidence for the intimate relation between AA amyloid and highly sulfated PGs (HSPGs) came from an ultrastructural study demonstrating positive Ruthenium red and Cuprolinic blue staining associated with amyloid fibrils in both amyloidotic spleen and liver as well as in isolated fibril preparations. Immunocytochemical evidence has demonstrated that heparan sulfate is specifically localized to sites of amyloid deposition in the mouse model of AA amyloidosis [82].

Neither the nature of the inflammatory inducing agent nor the length of time of the inflammatory reaction influenced the concurrent deposition of amyloid protein and GAGs [85,86]. This initial observation indicated that highly sulfated GAGs such as heparan sulfate, heparin and/or keratan sulfate were present. It was later shown that HS and/or heparin were the only GAGs accumulating in the spleen in association with the amyloid protein [87]. These results indicated that the accumulation of GAGs was not a general reaction to an inflammatory stimulus but was specifically related to amyloid deposition itself.

These and other findings demonstrate that sulfated GAGs and/or PGs are present in close association with all forms of amyloidoses regardless of the nature of the amyloid protein deposited, the tissue or organ involved, or the extent of deposition. This includes the prion amyloids that are associated with the Gerstmann-Straussler Scheinker Syndrome, Creutzfeld-Jakob disease, and experimental scrapie, as well as the amyloid associated with type II diabetes, familial amyloidotic polyneuropathy (FAP), AA amyloidosis, and Beta-amyloidosis. The evidence linking HSPG to AD follows.

B. HSPG and Alzheimer's Disease

AD brain tissue has been shown to contain an increased amount of GAGs as determined by hexuronic acid analysis when compared to normal aging brain. Identification and quantification of GAGs after electrophoresis on polyvinyl chloride determined hyaluronic acid and chondroitin sulfate to be the major GAGs increased in AD brain [88]. While not specifying the identity, others used infrared spectroscopy to identify a carbohydrate as well as a protein component to the neuritic plaques and amyloid cores isolated from AD brain. Histochemical techniques have demonstrated sulfated GAGs and/or PGs present in the characteristic lesions of AD (neuritic plaque, neurofibrillary tangles, and congophilic angiopathy) [73,81,89,90].

Using antibodies to both forms of basement membrane HSPG separate investigators have identified and localized HSPG core protein to the amyloid fibrils present in senile plaques and cerebrovascular amyloid deposits in AD brains [73,81]. Polyclonal and monoclonal antibodies to perlecan core protein stain early or primitive amyloid plaques. Since these plaques are believed to be the precursor form of neuritic plaques containing a central amyloid core, these observations suggest that HSPGs may serve as a nidus for further plaque development to occur. Snow and Kisilevsky have speculated about the source of this HSPG [81,91,92]. Based on immunohistochemical evidence they suggest that HSPG is produced by astrocytes, neurons, and endothelial cells in AD. The same paper also discusses the possibility that reduced immunostaining of HSPG is due to either a loss of HSPGs from blood vessel basement membranes or a change in the HSPG conformation at the sites of reduced staining. These were nonamyloidotic vessels in the vicinity of abundant neuritic plaques, congophilic angiopathy, and/or neurofibrillary tangles [84]. These findings support the

concept that HSPG plays a significant role in the formation of extracellular amyloid.

The major intracytoplasmic lesion of AD, the neurofibrillary tangle (NFT), also associates with HSPG [90,93,94] . Using an assay for HSPG employing basic FGF binding to heparinase sensitive sites, the presence of HSPG in NFTs was established. The binding of HSPG to NFTs requires calcium which may be acting as a bridge between anionic sites on both HSPG and the NFTs [95]. A role for HSPG in the filamentous inclusions of Pick's and Parkinson's diseases has been established using this same assay [90]. Basement membrane HSPG is an unlikely candidate to appear in intranuclear inclusions [93], and the mechanism by which it localizes inside the neuron remains unclear. The evidence does point to a significant dysregulation in the production of basement membrane HSPG which then plays a central role in the neuropathological lesions of various brain disorders. A more precise role for HSPG in the formation of senile plaques may result from experiments aimed at determining the binding affinities of HS/HSPG for APP and A4.

C. High Affinity Interactions Between HS/HSPG and Amyloid Precursor Protein/A4 Peptide.

Several investigators have demonstrated high affinity between HS and HSPG with both APP and the A4 peptide (ABP) [96,97]. Narindrasorasak synthesized recombinant Beta-Amyloid precursor protein in a baculovirus vector and demonstrated high affinity binding with perlecan (Kd=1nM). Heparitinase digestion of the intact proteoglycan displayed very similar binding affinities. This led the authors to conclude that the binding was taking place on the protein core of perlecan. On the other hand, high affinity binding has been demonstrated between the A4 peptide and HS glycosaminoglycan chains [97]. The existence

of high affinity interactions between APP/A4 and HSPG along with the presence of HSPG as a common structural component of all forms of amyloid suggest that HSPG may be exerting an effect on the formation of the A4 beta-pleated sheet or as a nucleating agent enhancing aggregation or fibrillogenesis.

Materials and Methods

Preparation of Proteoglycans

Vascular proteoglycan was obtained by methods previously described from the capillary beds of bovine glomeruli and have been previously characterized with regard to their purity and composition [19]. This method produces a preparation which is approximately 90% heparan sulfate proteoglycan. Briefly, glomeruli were isolated from fresh bovine kidneys by a sieving method. After hypotonic lysis of the glomeruli in distilled water proteoglycans were isolated by stepwise chromatography on DEAE-Sepharose CL-6B by use of increasing concentrations of NaCl in the same buffer. The material eluted by 0.6M NaCl in urea-Tris buffer was dialyzed and lyophilized. Proteoglycans were purified further by chromatography on a Sepharose CL-4B column (Pharmacia). This resulted in two fractions containing hexosamine, referred to as peak A and peak B herein.

snPG were isolated from the supernatants of human neuroblastoma SK-SNY cells using the same chromatographic methods described before [98]. EHS HSPG was isolated from the Engelbret-Holm-Swarm mouse sarcoma, a tumor producing large quantities of basement membrane constituents and provided by Dr. Robert Kisilevsky.

Preparation of Proteoglycans from Cultured Endothelial Cells

The conditioned medium of cultured cells was dialyzed against 7M urea buffer (7 M Urea, 50 mM Na acetate pH 6.4, 150 mM NaCl, 5 mM N-ethyl-maleimide, 1 mM PMSF, 5 mM Na2SO4 and 0.05% CHAPS). The last dialysis was performed without Na2SO4. The dialyzed medium was loaded onto a 50 ml DEAE Sepharose CL-6B equilibrated in the same buffer. The column flow rate was 0.35 ml/minute, and the column diameter was 15 mm. After

washing with the 7M urea buffer, a linear salt gradient were performed from 0.15 to 2 N NaCl. The $^{35}SO4$ positive anionic fractions then concentrated and loaded on Sepharose CL-6B (55 x 0.95 cm) equilibrated in 7M urea buffer for molecular weight determination.

Enzyme Linked Immunosorbent Assay (ELISA).

Nunc immunoplate [Intermed, (Denmark)] were coated with 50 ml of the respective proteoglycan per well at 10 μg/ml concentrations in 0.1 M carbonate buffer pH 8.5 containing 0.3 mM MgCl2 and kept overnight at 4 ^{o}C. After rinsing the plate and blocking the binding sites with phosphate buffered saline-Brij (PBS-Brij) five times, antibodies with or without competitive inhibitors were added and incubated two hours at room temperature with gentle shaking. After washing the immunoplates in 5 changes of PBS-Brij, 100 μl of an alkaline phospatase labelled goat anti-mouse, rat or rabbit whole IgG diluted to the appropriate concentration was added to each well for 1 hour at room temperature. Following washing, the enzyme reaction was developed by addition of 100 μl of substrate solutition per well (1 μg/ml nitrophenyl phosphate [Sigma (St. Louis, MO)] in 0.1M diethanolamine buffer, pH 9.8). The OD was measured at 405 nm in a Titertek ELISA plate reader.

Immunoblotting

Immunoblotting was performed as previously described [99]. Proteoglycans in SDS sample buffer (1 μg/ml) were electrophoresed on a 5-15% SDS-polyacrylamide gel. The material was electroblotted to nitrocellulose paper (Schleicher and Schuell) in methanol buffer in a blotting transfer system. After washing the Immobilon-P in PBS-0.05% Tween 20 (PBST) for washes of 30 minutes each, the particular antibody designated for each blot was incubated (diluted in PBST) overnight with rotation at room temperature. After washing in PBST three times for five minutes each, an alkaline phosphatase conjugated

anti-IgG antibody at appropriate dilution was added for one hour. After several washes in PBST the blot was developed by addition of enzyme substrate solution.

Preparation of Monoclonal Antibodies

Monoclonal antibody 7E12 has been described elsewhere [19]and has been shown to recognize the protein core of glomerular basement membrane heparan sulfate proteoglycan (Mr=110 kDa).

Preparation of rabbit polyclonal antibodies to the vHSPG

Preparation of these antibodies involved standard procedures previously described [100]. Intradermal injections of approximately 100 μg of vHSPG mixed with Complete Freund's Adjuvant and were made in four locations. Three weeks later the antigen was mixed with Incomplete Freund's Adjuvant and reinjected at 50 μg per injection. This was repeated every two weeks for 6 weeks. . Immunoblotting of the intact HSPG using the polyclonal antibody also recognizes the intact vHSPG.

The antibody was used directly as serum or after IgG purification on a Protein A-Sepharose affinity column according to standard procedures. The serum was loaded onto the Protein A-Sepharose column, eluted with sodium citrate buffer (pH 3.0), neutralized with 1N NaOH, and dialyzed into phosophated buffered saline. Rabbit anti-EHS HSPG was a kind gift of Dr. Robert Kisilevsky.

Culture of Mouse hemangioma aortic endothelial cells

A line of mouse hemangioma aortic endothelial cells (a kind gift of Dr. Rifkin, New York University) was maintained in DMEM (Gibco, Grand Park, Long Island) with 10% heat inactivated fetal calf serum. Cells were plated at 5.0 X 10^5 cells/well of each 6-well tissue culture plate (Falcon).

^{35}S Methionine/Cysteine Radiolabelling

Cells were depleted of methionine by preincubation in medium lacking methionine, cysteine, and fetal calf serum for 30 minutes before radiolabelling. Cells were radiolabelled in 1.0 ml of methionine and cysteine-free medium containing 500 μCi of [^{35}S]methionine and cysteine (ICN Biochemicals) for 20 min, and chased for 0.75, 1.5, 2.25 and 24 hours. After each incubation, the medium was removed and the cell layer was rinsed with 0.5 ml culture medium. The rinse was combined with culture medium. The cell layer was solubilized in 0.5 ml of 0.15 M NaCl plus 0.02 M Tris-HCl, pH 7.4, containing 1% sodium deoxycholate, 1% Triton X-100, 1% aprotinin (Sigma), and 0.1% SDS (lysis buffer). The cell lysate was sonicated for 5 seconds and insoluble material was removed by centrifugation in an Eppendorf microfuge at 10,000Xg.

A 4-fold concentrate of the lysis buffer used to lyse the cells was added to the combined medium and rinse. Cell lysate and medium samples were stored at -70^{o}C until use.

The procedure used for immunoprecipitation of proteins from cell lysate and media was adapted from that of Ledbetter et al. [101] Protein A-Sepharose (Sigma) was allowed to swell in saline buffered with 20 mM Tris-HCl, pH 7.4, containing 1% Nonidet P40, 1% Triton X-100, and 0.05% SDS (buffer A). The protein A-Sepharose was diluted 1:10 (v/v) in buffer A and used at this dilution in all experiments. Protein A-Sephrose was stored in 0.5 ml aliquots at -70^{o} C until used.

The lysate or media was pre-adsorbed to reduce background. 50 ul of protein A-Sepharose suspension was incubated with 2.5 μl of preimmune serum (obtained before immunization) with constant agitation at 4 ^{o}C for 1 hour. The IgG-protein A complex was washed as 3 times with 1 ml of buffer A by centrifugation. 100 ml of cell lysate or 500 ml of medium was then incubated

with the Ig-protein A complex with constant agitation for 1 hour at 4 C. The adsorbed lysate was recovered after removal of the IgG-protein A complex by centrifugation, and the complex was discarded.

The immunoprecipitation was then performed on the adsorbed cell lysate or media. 100 μl of protein A Sepharose suspension was incubated with 20 μl of immune serum (or with 20 μl of preimmune serum for controls) for 1 hour with agitation at 4 ^{o}C for 2 hours with agitation. The resulting antigen-antibody-protein A-Sepharose complex was recovered after centrifugation. The complex washed five times with with 1.0 ml aliquots of buffer A to remove nonspecifically bound molecules. The antigen antibody complex was solubilized in 0.01 M phosphate buffer, pH 7.4, containing 2% SDS with 0.1 M β-mercaptoethanol at 100 oC for 3 minutes.

The proteins in the immunoprecipitate were separated by gel electrophoresis according to the procedure of Laemmli [102]. Polyacrylamide (5% SDS-PAGE) and 0.5% agarose/2.5% acrylamide/0.1% SDS, in 0.1 M phosphate buffer, pH 7.0 gels were prepared for flourography with Enhance (NEN-Dupont), according to manufacturer's instructions. Gels were dried and exposed to XAR-1 x-ray film (Kodak) at -70 ^{o}C, for approximately 3 days.

Heparinase digestions

Peak A and Peak B samples from DEAE CL-6B ion-exchange chromatography were each pooled and submitted to enzymatic digestion of glycosaminoglycans using specific glycosidases. To demonstrate the presence of HS in preparations, heparinase I, II, and III and chondroitinase ABC (Sigma) was used to remove heparan sulfate side chains by digestion in 20 mM Tris-HCl, pH 7.4, containing 1 mM CaCl2 at 37 ^{o}C overnight at a concentration of 100 mUnits/ml with PMSF or BSA to inhibit protease activity at 37 ^{o}C overnight, and then enzyme was inactivated by boiling for 5 minutes. Samples were then

analyzed by gel filtration on BioGel P6 (Pharmacia). The column flow rate was 11.6 ml/hr 0.5 ml fractions were collected (2.58 min/fraction) and 0.25 ml of each fraction was counted in a scintillation counter.

Immunohistochemistry

Blocks of tissue were fixed in 4% paraformaldehyde for 24 hours before crypoprotection in a graded series of sucrose solutions (12%, 16%, and 18% in 0.1 M phosphate buffered saline) and subsequent freezing in dry ice. A series of frozen 40 μm-thick sections was cut on a cryostat (Reichert-Jung), and transferred to phosphate buffered saline (pH 7.5). Endogenous peroxidase was quenched by incubating sections in 3% H_2O_2 methanol for 5 minutes. Sections were washed in phosphate buffered saline, incubated with rabbit polyclonal anti-vHSPG at 1:1000 dilution overnight at 4°C with gentle agitation, and processed using the avidin-biotin-peroxidase method with a Vectastain ABC kits (Vector Labs, Inc.), reacted with 3,3'-diaminobenzidine tetrahydrochloride (DAB) and 0.01% hydrogen peroxide, mounted, stepped through a series of alcohol dehydrations, and coverslipped.

RNA analysis

We employed molecular probes to perlecan derived from a cDNA library made with mouse Engelbert-Holm-Swarm (EHS) mRNA (EHS tumor was a kind gift of Dr. John Hassell), and performed northern blot analysis as well as the RNase protection assay using RNA from mouse, bovine, and human sources. The following methods are derived from Sambrook et al. (1989).

In order to obtain the cDNA probes suitable for Northern blots, the following procedures were carried out. The mouse cDNA clones, BPG5 and BPG7, were used to transform *Escherichia* coli, strain JM101, and then amplified in a large scale plasmid preparation, according to Sambrook. A 500 ml overnight culture grown in Terrific Broth was spun down in two 250 ml

polypropylene centrifuge bottles at 4000 rpm for 10 minutes. The supernatant was decanted, and the pellet resuspended in 19 ml of Solution I by vortexing. Twenty ml of Solution II was added, mixed, and placed on ice for 10'. Ten ml Solution II was then added and the solution vortexed, with a white flocculent precipitate forming. Samples were spun at 10,000 rpm for 10 minutes to pellet the precipitate. Supernatant was decanted to a fresh centrifuge bottle (250 ml) through gauze to trap any floating bits of precipitate. Isopropanol (0.6 vol) was added, mixed and spun at 10,000 rpm for 10 minutes. Eight ml of 1X TE were added to the precipitate. Eight grams of $CsCl_2$ and 100 µl of ethidium bromide (10 mg/ml) were added, and the solution put in a Quick Seal tube, and balanced. Purified plasmid DNA was banded after centrifugation at 65,000 rpm for 36 hours. The plasmid band was removed and purified by extraction with propanol. The purified plasmid DNAs containing the BPG5 and BPG7 inserts were digested with the restriction enzyme EcoR1 for 1 hour at 37 °C. Bromophenol blue sample buffer was added to the samples and they were ran on a 1% low-melting agarose gel, along with Lambda Hind III markers. Inserts were purified away from the low melt gel. Using the Random Primer kit from Promega, reactions were carried out incorporating ^{32}P-ATP according to manufacturer's instructions.

Preparation of RNA

Human umbilical vein endothelial cells, bovine aortic endothelial cells, bovine capillary endothelial cells, human neuroblastoma cells, and human glioblastoma cells were grown in culture until 80-90% confluence. Mouse EHS sarcoma was obtained from Dr. Hynda Kleinman. Using a method modified from Glisin we isolated the RNA from approximately 4 X 10^9 cells, or approximately 5 grams of tissue in the case of the EHS tumor. Cells were harvested with Hepes Buffered Saline and 1x trypsin-EDTA, and then pelleted in 50 ml polypropylene

tubes. Guanidinium solution (3.5 ml of 4 M guanidinium isothiocyanate, 20 mM NaOAc, pH 5.5, 1 mM DTT, 0.5% N-lauryl sarcosine) was added per ml of packed cell volume. When cells were visibly lysed by vortexing and the solution appeared clear, we used a 10 ml syringe with a 20 gauge needle to reduce the viscosity of the solution by shearing the DNA. Cesium Chloride solution (1.5 ml of 5.7 M $CsCl_2$, 0.1 mM EDTA) was then added to a siliconized, autoclaved SW50.1 (Beckman Instruments) polyallomer tube using sterile plastic pipet. This solution was then overlayed with 3.5 ml of the cell/guanidinium mixture, and the tubes were carefully balanced. The samples were then centrifuged at 35,000 rpm, 18 ^{o}C, for 12 or more hours. The supernatant was aspirated and the pellet resuspended in 360μl of TES solution (10mM Tris-HCl, pH 7.4, 5 mM EDTA, 1% SDS).

Total RNA obtained by this method was quantitated by spectrophotometry at 280 nm and 260 nm. Ten μg of total RNA was added to an RNase free tube and volume was adjusted to 5 μl with DEPC-treated, autoclaved H_20 and 25 μl electrophoresis sample buffer, denatured at 65 ^{o}C for 15 min. The RNA was ran on an agarose denaturing gel (1% agarose, 1X MOPS, 1.85% formaldehyde).

Northern Blots of total RNAs using BPG5 and BPG7 labelled probes

The denaturing gel was blotted on nylon backed nitrocellulose overnight, and dried for 2 hours under vacuum at 80 ^{o}C.The blots were prehybridized in 6X SSC, 5X Denhardts solution, 0.5% SDS, and 100 μg/ml salmon sperm DNA for 2 hours, and then hybridized overnight with radiolabelled mouse cDNA probes obtained from Dr. John Hassell (Department of Opthamology, University of Pittsburgh).

RNase Solution Hybridization Assay

The application of this technique to the study of HSPG gene expression required the construction of a plasmid containing perlecan specific cDNA sequence flanked by bacteriophage RNA Polymerase promoters..

Subcloning of an EcoR1/Pst1 322 base pair fragment of BPG7 into pBluescript.

Following methods from Sambrook et al. (1989), a restriction digest of the perlecan clone BPG7 was carried out using the restriction enzymes EcoR1 and Pst1. It was calculated that these enzymes would provide a 322 base pair fragment, amongst others, which would be appropriate for production of a riboprobe. The digest was subjected to electrophoresis on a 1.5% low melting agarose gel. The 322 bp fragment, designated BPG7/322 was visualized under ultra violet light and excised. The DNA was purified by phenol extraction, and amonium acetate/ethanol precipitation. pBluescript was used to transform competent XL-1Blue cells and large quantities of this plasmid were prepared as described above.

BPG7/322 was submitted to DNA sequencing according to manufacturer's instructions (USB) in order to confirm its identity. Comparing it to the published cDNA sequence of perlecan, it displayed complete identity to the published sequence.

The purified pBluescript was digested with the same restriction enzymes used to produce the 322 bp fragment (EcoR1 and Pst1) and linearized plasmid was purified on a low melting agarose gel as described above. The 322 bp fragment was then ligated overnight with the digested pBluescript. The ligated recombinant plasmid was used to transform XL-1 Blue cells and the subsequently amplified plasmid was purified as above. *In vitro* transcription was used to synthesize riboprobes according to manufacturer's instructions (Promega Riboprobe Kit) using the vector cut with EcoR1 to generate minus

strand RNA using T7 polymerase, and cut with Pst1 to generate plus strand RNA using T3 polymerase.

Solution hybridizations containing an excess of labelled probe were then set up for a set of standards with known quantities of synthetic sense RNA, or for experimental samples containing a known amount of tissue-derived RNA. Subsequent incubation of the standard and experimental samples with Ribonuclease A and T1 resulted in the degradation of all RNA except the HSPG specific hybrid. Samples were run on polyacrylamide gels (4-5%), dried, exposed to X-ray film, and the protected bands were cut out of the gel. These bands were submitted to scintillation measurements, and by comparison with the standards, a quantitative measure of the amount of perlecan/HSPG transcript in the sample was obtained.

Cloning of cDNA using the polymerase chain reaction and degenerate oligonucleotides

The 110 kD heparan sulfate proteoglycan was purified from bovine kidney as described above, was deglycosylated with heparinase I, and III, and quantitatively electrophoresed on a 6% SDS polyacrylamide gel. Core proteoglycan was transferred onto either Immobilon P or nitrocellulose membranes and excised. Alternatively the proteoglycan band was directly excised from the gel. The identity of the band was confirmed by parallel Western blotting using previously characterized mono or polyclonal antisera to the 110 kD heparan sulfate proteoglycan. Following enzymatic digestion, three initial peptides were sequenced and degenerate oligonucleotides of 17, 20 and 26 nucleotides in length were designed based on bovine codon usage tables. Serine and leucine residues which present a very high degree of degeneracy were omitted from the design of the oligonucleotides. In addition, only the first and second base of the C-terminal glutamic acid codon were used in order to

avoid further introduction of variation into the probes. No highly homologous sequences were found on comparison of the peptide sequences to the protein databases. Pools of 256-fold degenerate oligonucleotides were employed in the polymerase chain reaction (PCR) using standard conditions. First strand cDNA was synthesized from approximately 30 µg of total bovine endothelial RNA using MMLV reverse transcriptase in a 50 µl reaction volume, and 1 µl of cDNA was amplified using 1-10 µg primer and Vent polymerase. Amplification during the polymerase chain reaction was done using a standard program (94^{o}CX1min/55^{o}/cx2min/72^{o}Cx5min).

Screening of a bovine endothelial cell cDNA expression library.

A lambda GT11 bovine endothelial cell cDNA expression library was purchased from Clontech Inc. After having titered the library we proceeded to screen the library at a density of 5 X 104 plaques per 150mm plate. The infected plates were incubated for 3.5 hours at 42 C. During this time, 150mm nitrocellulose filters were soaked in a solution of isopropalthio-b-D-galactoside (IPTG) (10 mM in distilled water) for a minutes. Filters were dried at room temperature on Whatman paper and quickly overlaid on to the plates. The plates were incubated for at least 4 hours at 37 ^{o}C, and for 30 minutes at 37 ^{o}C. Filters were marked for orientation purposes and removed from the plates. The filters were washed in TBS-Tween and then placed in dishes containing the monoclonal antibodies, 4F2 and 7E12 to vHSPG protein core diluted 1:10 in TBS-Tween, and the polyclonal antibody to vHSPG (EP01), diluted 1:500, with 20% fetal calf serum (7.5 ml for each 82-mm filter) and incubated overnight. After washing, the secondary antibody (goat anti-mouse alkaline phosphatase conjugated IgG) was added for 1 hour. Detection of the antigen-antibody complexes was then performed with 5-bromo-4-chloro-3-indoyl phosphate in the presence of nitro-blue tetrazolium.

Immunological Screening of Expression Libraries

Using a single colony of Y1090 R- grown in the presence of ampicillin (100 ug/ml) a plating culture was prepared as follows. Ten ml of sterile Luria Broth supplemented with 0.2% maltose in a sterile 50-ml conical tube was inoculated with a single bacterial colony. The culture was grown overnight at 37 ^{o}C with moderate agitation (250 cycles/minute in a rotary shaker). Tenfold serial dilutions of bacteriophage stocks were prepared in SM (0.1 M NaCl, 0.01M $MgSO_4$, 0.035 M Tris-HCl pH (7.5). Phage were then placed into a sterile tube (0.1 ml each dilution). 0.1 ml of plating bacteria was added to each tube and incubated for 20 minutes at 37 ^{o}C to allow the bacteriophage particles to adsorb to the bacteria. Three ml of molten (47 ^{o}C) agar (0.7%) was added to each tube, vortexed gently, and immediately poured onto the center of a plate containing 30-35 ml of hardened bottom LB agar medium. After five minutes the plates were inverted and incubated at 37 ^{o}C for 16 hours.

Having titered the library in this manner, we then proceeded to screen the library at a density of 5 X 104 plaques per 150-mm plate, following the procedure stated above. The infected plates were incubated for 3.5 hours at 42 C. In the mean time, 90-mm nitrocellulose filters were soaked in a solution of IPTG (10 mM in distilled H_2O) for a few minutes. Filters were dried at room temperature on a Whatman paper and quickly overlaid on to the plates. The plates were incubated for at least 4 hours at 37 ^{o}C, and for 30 minutes at 37 ^{o}C. Filters were marked for orientation purposes and removed from the plates. The filters were washed in TBS-Tween and then placed in dishes containing the monoclonal or polyclonal antibodies to the 110 kDa HSPG diluted 1:10 in TBS-Tween with 20% fetal calf serum (7.5 ml for each 82-mm filter) and incubated overnight. After washing, 3 X 10 minutes, the secondary antibody (goat anti-mouse alkaline phosphatase conjugate IgG) was added and allowed to incubate

for 1 hour. Detection of the antigen-antibogy complexes was then performed with 5-bromo-4-chlor-3-indoyl phosphate in the presence of nitro-blue tetrazolium.

Phage Propagation and Purification

As putative vHSPG clones were identified, the phage DNA from these clones was isolated. This requires the addition of 1-3 ml of phage stock to 1 liter of Y1090R$^-$. The phage was preabsorbed in the following ratio at 37 ^oC for 15-20 minutes, 5ml overnight/500ml media. The phage/bacteria mixture was shaken at 37 ^oC overnight. Chloroform was added to lyse remaining cells, with an additional 15 minutes of shaking. The lysate was made 1 M NaCl while being shaken. The material was chilled on ice and then spun at 8,000 rpm for 10 minutes. Carbowax PEG 6000 was added to the supernatant to 7% (polyethylene glycol, MW 6000-7000, Sigma). After the PEG was dissolved, the solution was incubated on ice for at least two hours. This material was spun at 10K for 10 min and the supernatant was discarded. The pellet was resuspended by swirling in 8-10 ml SM/500 ml culture. To this DNase was added to a concentration of 15mg/ml (Bovine pancreas) and RNase to a concentration of 30 mg/ml (bovine pancreas) and incubated for 20 min. at room temperature. This digestion was centrifuged at 8-10K for 10 min. The supernatant was adjusted to 10 ml with phage SM and 7.5 grams of cesium chloride was added. This was spun at 40 K for 24 hours in a fixed angle rotor (Beckman 20TI) with polyallomer tubes.

The phage DNA was isolated with a syringe needle from the center of the gradient. The cesium chloride was removed by dialysis against 0.1M NaCl, 20mMTris, pH 7.5, 10mM $MgSO_4$ overnight at 4 ^oC. The phage DNA was further purified by phenol/chloroform extraction and ethanol precipitated using 2 vol. 95% ETOH and 100 micro liters/ milliliter. The DNA pellet was washed with 70%

ETOH, respun and dried. The pellet was carefully dissolved in TE pH8.0 (10 mMTris-HCl,1mM EDTA) and saved for further analysis.

Restriction enzyme analysis

Restriction enzyme digests were performed on the isloated phage DNA to determine the insert size. This was done with EcoRI (1-5 units/μg DNA) or other enzymes found on either side of the lambda phage cloning site. Digestions were performed at 37 ^{o}C for 1 h, and analyzed on agarose gels (0.7-1%).

Subcloning cDNA into the pBlueScript vector

The cDNA of putative positive vHPSG clones were cut with restriction enzymes from the flanking lambda phage DNA in the case of expression screening or used directly as a product of polymerase chain reaction. These DNA fragments were made blunt-ended with Klenow Large fragment DNApolymerase (1 unit enzyme/μg DNA at 37 ^{o}C for 1 h) and ligated into EcoRV digested pBlueScript that had been subjected to an alkaline phosphatase reaction to minimize self-ligation (1 U calf intestinal phosphatase (CIP) in CIP buffer for30 min at 37 ^{o}C). Ligations were done using T4 DNA ligase at 15^{o}C overnight. Ligated DNA was used to transform competent Escherichia *coli* strain JM109. Log phase E. *coli* were made competent by suspending in 0.1 M rubidium chloride, 1 M MOPS (pH 7.0), followed by suspension in 0.1 M rubidium chloride, 1 M MOPS (pH 6.5) and 0.5 M calcium chloride. The ligated DNA was added to the competent cells and the mixture is placed on ice for 1 hour followed by a 43^{o}C heat shock for 2 minutes. Cells were grown for 90 minutes with shaking at 37^{o}C for 90 minutes and plated on LB-amp. Viable colonies were selected and the plasmid DNA was prepared for use in restriction enzyme analysis, DNA sequencing, and for library sceening.

Computer Analysis of Protein Homologies and Motifs

The computer analysis of sequenced peptide fragments for possible homology to pre-existing protein sequences was performed using the FastA application of the GCG program (U.S. Department of Health and Human Services). Glycosaminoglycan motifs of agrin were determined by the "motif" function of this program.

Chapter 3. Results

I. Localization of Vascular Heparan Sulfate Proteoglycan in Alzheimer's Disease and Aged Squirrel Monkey Brain

Polyclonal antibodies produced to bovine glomerular basement membrane HSPG reacted with a number of species; human, monkey, bovine, dog, rat and mouse. The immunohistochemistry of vHSPG in Alzheimer's Disease brain and aged monkey is discussed here.

Human brain hemispheres from two control cases (73, and 80 y.o. females) and two Alzheimer's Disease cases (77, and 71 y.o. males) were fixed in 4% paraformaldehyde, and then segmented into blocks, after which they were further fixed in 4% paraformaldehyde for up to 24 hours. The tissue was then cryoprotected in a series of sucrose solutions (14%, 16%, and 18%) frozen and cut at 40 μm thickness using a cryostat (Reichert-Jung). Sections were then treated with H_2O_2 to eliminate endogenous peroxidase activity that may have been present due to red blood cells remaining in the vascular bed. Immune serum was passed over a protein A-Sepharose column to specifically isolate immunoglobulins. The protein-A purified anti-vHSPG polyclonal rabbit antibody was used at a dilution of 1:1000 on human brain AD tissue. Using horseradish peroxidase conjugated goat anti-rabbit IgG as the secondary antibody, and processing according to the ABC kit (VectaStain), anti-vHSPG polyclonal antibodies were localized to the capillaries and larger blood vessels in all brain sections examined as observed by light microscopy. No reaction product was seen on sections in which preimmune sera was used (not shown). Staining generally appeared localized in a linear pattern throughout the extent of the blood vessels present in the section (Figure 1a-f). This localization corresponds to the basement membrane of the endothelial cells and pericytes comprising the

blood vessels. The pattern observed with anti-vHSPG antibodies parallels the patterns seen with other anti-vHSPG antibodies [73,103,104] . Immunostaining of brain tissue gives a dramatic profile of the extent of vascularization in the brain. Immunostaining of a section of AD brain from the hippocampal region (Figure 1a) demonstrates the presence of vHSPG in blood vessels as well as in what appears to be a diffuse plaque. Also noteworthy in this section is the generally increased density of vessels in this region as well as the particularly high density in the inner molecular layer of the CA1 region of the hippocampus This may be due to the overall shrinkage of the AD brain. A vessel in this layer appears to have accumulated a large amount of vHSPG, which may be due to congophilic angiopathy. Congophilic angiopathy is one of the hallmarks of AD and involves the accumulation of both amyloid and HSPG in the basement membrane of blood vessels [79,105]. Although we have not stained these sections with Congo Red, it is likely that this type of lesion would prove to be congophilic angiopathy.

In figure 1e, "string vessels" are present. This is a form of microangiopathy present in AD as well as aged brain. This structure probably represents a blood vessel that has atrophied for various reasons, and its lumen is occluded.

The section in figure 1b exemplifies the pathologic hallmarks of advanced stage AD. All six cortical layers may be seen in this entorhinal section, a testament to the high degree of cortical atrophy that has taken place. The diffuse staining pattern in layer II corresponds to the presence of islands widespread neurofibrillary tangles (NFT). In normal brain, neurons in this region are clumped together in these "islands". Neuronal perikarya in this layer convey cortical input to the hippocampus, providing the axons that traverse the perforant pathway and form synapses in the outer molecular layer of the hippocampal dentate gyrus. It

is now known that these are some of the most vulnerable neurons in AD. The NFTs in this layer are immunopositive for HSPG, and have been described as being of the "extraneuronal or tombstone" variety (figure 1b) [106]. A similar banding pattern of NFTs occurs directly below the larger accumulation of NFTs, and may still be considered to be in layer II of the cortex. It is known that layer II of the entorhinal cortex (ERC) is one of the brain areas that is most vulnerable to neuronal dropout [107]. This finding is consistent with the observation of widespread NFTs in this layer [106,108,109]. The presence of HSPG in both diffuse and primitive plaques may also be observed in this section, with higher magnification in figures 1e and f. It has been suggested (Yamaguchi et al., 1989) that diffuse plaques may represent a class of plaques that may remain as mature diffuse plaques, while immature plaques presumably transform into mature (compact or "burned-out") plaques. In comparison to the previous two sections, figure 1c is representative of normal aged cerebral cortex, in which HSPG immunopositive localization is confined to the cerebrovasculature. This section is from inferior temporal cerebral cortex. The intense immunoreactivity of the perforating arteries originating at the pial surface is notable.These arteries are the predominant blood supply to the cortex, where they branch off into capillaries.

There is a well known correlation between the metabolic demands of specific poplulations neurons and the degree of vascularization required to supply these requirements. This correlation is evidenced in layer IVc of the visual cortex (Figure 1d). Layer IVc of the visual cortex is the most highly vascularized of all the cortical layers, as well as being the most metabolically active layer, receiving inputs from the lateral geniculate nucleus. A band-like formation composed of the blood vessels supplying this layer is evident in this light micrograph. In addition, qualitatively, the overall degree of vascularization

in the visual cortex is considerably greater than that found in the inferior temporal cortex.

In summary, the immunohistochemistry of anti-vHSPG antibodies in control and AD brain demonstrates several points concerning the role of HSPG in the cerebrovasculature as well as in AD. First, HSPG is present in the full spectrum of senile plaques, from immature, and diffuse plaques to mature senile plaques. Second, the other neuropathologic hallmark of AD, the neurofibrillary tangle is also closely associated with positive HSPG immunoreactivity.

An examination of the immunohistochemical profile of basement membrane HSPG in the squirrel monkey brain reveals several interesting observations concerning the relationship between HSPG and vascular amyloid.

Aged squirrel monkey (18 year old female) brain sections displayed many of the angiopathic lesions preseent in the AD brain. In figure 2a widespread staining of both large and small blood vessels and a large number of senile plaques is observed. It appears many of these vessels have atrophied extensively, appearing as "string vessels", making it unlikely that the lumen of these vessels has remained patent. What is most striking about this section is the large number of plaque-like structures with very intense anti-vHSPG immunoreactivity. Many of these plaques in this field appear intimately associated with a blood vessel (figure 2a), as if it were occluding this vessel. The level of immunoreactivity in this plaque is relatively homogeneous, whereas the degree of staining in some of the other plaques shows areas of higher intensity, suggesting that various stages of these plaques are present. In one particular plaque, it appears that a vessel observed in cross-section has undergone basement membrane thickening and the lumen appeared partially occluded. Figure 2b shows a higher magnification of the association of a plaque with a blood vessel. In this section, there are three plaques in close proximity

with each appearing to be encircled by vessels, or a vessel terninating in a plaque. Basement membrane thickening previously ascribed to aging can be observed in Figure 3a. along with dense mature plaque-like accumulations. A clear association between the vascular plaque and a "string" vessel was observed (Figure 3b). Another example of a vessel with a large accumulation of HSPG immunoreactivity was observed in figure 3d.

Double labelling of anti-vHSPG and anti-A4 antibody (10D5 to amino acids 1-16 of A4 peptide, from Athena Neuroscience) was performed. The rabbit polyclonal to the 110 kDa HSPG was visualized with a goat anit-rabbit IgG antibody conjugated to biotin, and developed with the ABC Vectastain kit using diaminobenzidine as substrate. The anti-A4 monoclonal antibody was visualized after complete visualization of HSPG had ocurred using a goat anti mouse followed by BDCK as the substrate for horse radish peroxidase.

Colocalization of HSPG and A4 peptide was observed in a number of vessels and senile plaques (Figure 3e and f). A4 immunoreactivity was observed closely adherent to the vessel wall in some instances, as if forming a complete covering of the microvessel (Figiure 3f). Although the A4 was closely adherent to the vessel wall its localization was more likely to be in the basement membrane surrounding the vessel, as HSPG immunoreactivity was noticed underlying that of A4 immunoreactivity. The acumulation of these cellular products was quite marked in comparison to the diameter of the vessel. Both dense and diffuse plaques stained positively for A4 antibodies. HSPG immunoreactivity was more widespread than A4 staining, and was always co-localized with A4 immunoreactivity, but not vice versa.

II. Biochemical and immunological characterization of heparan sulfate proteoglycan

As evidenced by the immunohistochemical findings presented here, and by others, heparan sulfate proteoglylcan is intimately associated with the hallmark lesions of AD. Since HSPG represents a family of molecules and vHSPG represents a specific species of BM HSPG, a better understanding of the exact relationship of vHSPG to other HSPGs was sought. Specifically, the immunologic and molecular relationship between bovine glomerular heparan sulfate proteoglycan (vHSPG) and the large heparan sulfate proteoglycan derived from the Engelbreth-Holm-Swarm mouse sarcoma, known as perlecan, was investigated. We employed a variety of immunologic, biochemical and molecular biological techniques for these experiments

. These techniques included the enzyme linked immunosorbent assay (ELISA), SDS-PAGE in conjunction with immunoblotting, amino acid sequencing, pulse-chase studies, and immunoprecipitation, as well as cDNA cloning methodologies using the polymerase chain reaction and expression screening. Central to these studies was the development of a polyclonal antibody to vHSPG capable of recognizing antigen from different species. The preparation of the anti-vHSPG polyclonal antibodies was described in the Materials and Methods section and their characterization is discussed below.

Preparation of Proteoglycans

Glomerular basement membrane heparan sulfate proteoglycan was obtained by methods previously described from the capillary beds of bovine glomeruli (see Materials and Methods). Briefly, glomeruli were isolated from fresh bovine kidneys by a sieving method, hypotonically lysed in distilled water, afer which proteoglycans were isolated by stepwise chromatography on DEAE-Sepharose CL-6B by use of increasing concentrations of NaCl in 7M Urea-Tris

buffer (pH 6.0). The material eluted by 0.6M NaCl in Urea-Tris buffer was dialyzed and lyophilized. Proteoglycans were purified further by chromatography on a Sepharose CL-4B column. This resulted in two proteoglycan fractions, each containing hexosamine, and referred to as peak A and peak B herein.

snPG were isolated from the supernatants of human neuroblastoma SK-NSY cells using the same chromatographic methods described above. Approximately 1 μg of snPG was obtained from 1 X 10^7 cells. This material was determined to be approximately 95% heparan sulfate proteoglycan as determined by uronic acid content.

Perlecan, a kind gift of Dr. Robert Kisilevsky, was isolated from the Engelbret-Holm-Swarm mouse sarcoma, a tumor producing large quantities of basement membrane constituents. Preparations of perlecan from other tissues have demonstrated close homology between species at the immunological as well as molecular level.

Characteristization of heparan sulfate proteoglycan employing antibodies.

Rabbits were immunized with vHSPG as described above, and bleeds were performed at regular intervals after each boost. The blood was allowed to clot overnight at room temperature, centrifuged and the sera was taken off. IgG was purified from this sera with a Protein A-Sepharose CL-4B affinity column. After extensive washing, the IgG component was eluted with 100 mM glycine (pH 3.0), and neutralized. The immunoglobulin-containing fractions were identified by reading the absorbance at 280 nm.

As seen in figure 4a anti-vHSPG antibodies recognize vHSPG with high affinity. In this ELISA, vHSPG was bound to the microtiter plate at a

concentration of 10 µg/ml. The E_{50} for this antibody is attained with a dilution of 1:2000. Monoclonal antibody 4F2 supernatant recognizes vHSPG at a comparable level with a dilution of 1:200. Monoclonal. Polyclonal antibodies to perlecan demonstrate cross-reactivity with vHSPG, producing an $O.D._{405nm}$ of approximately 0.5 at a dilution of 1:160 when monitored 1 hour after the beginning of the colorimetric development process.

As expected, perlecan antibodies demonstrate relatively high affinity for perlecan (Figure 4b). However, both monoclonal and polyclonal antibodies to vHSPG do not exhibit significant cross-reactivity with perlecan as the antigen, especially in comparison to the level of cross-reactivity obtained with perlecan antibodies for vHSPG as antigen.

The titration curve of anti-vHSPG reveals that these antibodies bind to snPG with a titer of approximately a 1:500 dilution (Figure 4c), suggesting that vHSPG and snPG are imunologically homologous molecules. The immunoreactivity of anti-vHSPG for snPG is not inhibited by free HS chains, supporting the hypothesis that snPG and vHSPG share common protein core epitopes. However, the decreased affinity of anti-vHSPG for snPG as compared to vHSPG suggests that antigenic differences do indeed exist between these protein cores.

To confirm that anti-vHSPG antibodies do not cross react with perlecan we performed a competitive inhibition immunoassay using vHSPG and perlecan as inhibitors (Figure 4d). Varying concentrations of inhibitors were incubated with anti-vHSPG at the E_{50} (1:2000) following procedures described above, and these mixtures were then used in the immunoassay to detect vHSPG coated on microtiter wells. As expected, soluble vHSPG inhibited anti-vHSPG antibodies. Perlecan, on the other hand, displayed very limited ability to inhibit anti-vHSPG.

To further elucidate the nature of the cross-reactivity between perlecan antibodies and vHSPG, the antigenicity of the heparan sulfate side chains attached to the protein cores of both molecules was investigated. Competitve inhibitions with heparan sulfate glycosaminoglycans as inhibitor were performed.

In the presence of HS the binding of perlecan antibodies to vHSPG is inhibited by almost 50% (Figure 4e), suggesting that the cross-reactivity observed in the recognition of vHSPG by anti-perlecan antibodies was in part due to the recognition of heparan sulfate chains which both proteoglycans have in common. Thus, common heparan sulfate epitopes may explain a significant portion of the cross-reactivity between anti-perlecan and anti-vHSPG antibodies. As expected, perlecan antibodies were also inhibited by HS when perlecan antibodies were used as the antigen in the immunoassay (Figure 4f). The affinity of vHSPG antibdodies for snPG was not significantly inhibited in the presence of free HS, suggesting that the protein core epitopes on snPG are the primary epitopes recognized by anti-vHSPG (Figure 4g). HS also inhibited the affinity of EP01 antibodies for vHSPG by approximately 10%, suggesting a limited level of the immunoreactivity was directed to the HS side chains.

Size characteristics of heparan sulfate proteoglycans

Immunoblots of vHSPG and perlecan reveal molecular weights of these molecules in the expected ranges when immunoreacted with the respective antibody. vHSPG migrates as a smear at about 200 kDa. (Figure 5a, lane 1), and perlecan (expected MW 600,000) migrates as a larger smear beginning at the top of the separating gel (Figure5b, lane 3). In fact, much of the perlecan remains trapped in the stacking gel, and does not enter the separating gel.

These results agree with previous reports regarding the molecular weights of these molecules *[19,36]*. There was no significant immunoreactivity observed in lane 3 (Figure 5a) of anti-vHSPG antibody for perlecan, yet partial cross-reaction of anti-perlecan antibodies for vHSPG was observed (Figure 5b, lane 1). Anti-vHSPG antibodies detected a high molecular weight smear in figure 5c, lane 4 that was reduced to a lower molecular weight band of ~110 kDa when treated with heparitinase, that represented neuroblastoma peak B proteoglycans. These patterns were similar to that seen for vHSPG (Figure 5c, lane 6, and 5d, lane 2 respectively).

A more direct approach in considering the immunologic cross-reactivity and the nature of the relationship between perlecan and vHPSG is to combine the techniques of immunoprecipitation with immunoblotting. Immunoprecipitates of radiolabelled mouse aortic endothelial cells were combined with immunoprecipitates of unlabelled conditioned media (Serum Free Media) that had been concentrated ten-fold by ultrafiltration with an Amicon concentration device (30,000 molecular weight cut off). The immunoprecipitates employed anti-vHSPG antibodies. Three lanes of a 3-10% polyacrylamide gradient gel were loaded with this immunoprecipitate. After electrophoresis, the blots were blocked with 3% non-fat dry milk in phosphate buffered saline with 0.01% Tween-20. The membrane was cut into strips corresponding to the original lanes on the gel. Individual strips were incubated with anti-vHSPG antibodies (1:2000), anti-perlecan antibodies (1:100), or no primary antibody for 1 hour at room temperature, washed and incubated with goat anti-rabbit IgG conjugated alkaline phosphatase, followed by development with 5-bromo-4-chloro-3-indoyl phosphate in the presence of nitro-blue tetrazolium. The blot was autoradiographed, so that the radiolabelled material could be correlated with the protein detected by the conjugated secondary antibody with regard to molecular

weight. Protein that immunoprecipitated with anti-vHSPG antibodies was visualized on the immunoblot and the molecular sizes coincided (Figure 6). Normal sera failed to precipitate any detectable material (Figure 6, lane 3, and lane B). The presence of denatured IgG heavy chains from the immunoprecipitation was observed on the blot at approximately 55 kDa, and a band representing BSA was present at 69 kDa. Detection of the immunoblotted material with anti-perlecan antibodies failed to resolve any protein bands, supporting the lack of immunologic homology between the molecules recognized by anti-vHSPG and anti-perlecan antibodies. The immunoblotted material detected by EP01 (anti-vHSPG antibodies) appeared as a wide doublet. Upon close examination, the radiolabelled material also migrates on electrophoresis as a doublet.

Precursor product relationships amongst the basement membrane heparan sulfate proteoglycans

The data strongly suggest unique antigenic identities for perlecan and vHSPG, with some similarity arising from either common heparan sulfate moeities, or from similar protein structure motifs. The question of a high molecular weight precursor for vHSPG becomes relevant if we can no longer assume that perlecan and vHSPG share a precursor-product relationship. This question was addressed with a pulse-chase experiment. Subconfluent mouse aortic endothelial cells grown in six-well plates (~750,000 cells/well) were starved of methionine, and cysteine for 20 minutes by incubation in serum free media lacking these amino acids at 37^{o}C. Cells were then radiolabelled with [^{35}S] methionine/cysteine (500 μCi/ml) for twenty minutes, and used to investigate a possible precursor to vHSPG. Sera taken from rabbits before immunization (preimmune sera) were used to immunoprecipitate proteins from

adsorbed lysate. Preimmune serum did not precipitate any proteins from the adsorbed lysate (Figure 7, lane 2). Antibodies against vHSPG immunoprecipitated a single protein of approximately M_r 250 kDa (Figure 7, lane 1) as estimated by extrapolation of proteins of known size (Bio-Rad Kaleidoscope prestained markers). Since these samples were reduced before electrophoresis, this high molecular weight protein is a single chain. Immunoprecipitation of protein precursors with anti-perlecan antibodies revealed a range of proteins with high molecular weights (Figure 7, lane 4). In addition to proteins of ~400 kDa, smaller proteins were also visible, and one protein band coincided almost exactly with the protein precipitated by anti-vHSPG. These results are surprising, and suggest that perlecan antibodies may be recognizing more than one unique precursor protein.

Northern analysis with a cDNA probe to perlecan demonstrated the presence of a 12 kb perlecan transcript in RNA extracted from mouse aortic endothelial cells, bovine capillary endothelial cells, and EHS tumor, but not from RNA extracted from neuroblastoma cells (Figure 7b). The fact that neuroblastoma cells do not make a perlecan transcript but do make make a basement membrane HSPG that cross reacts with vHSPG suggests that this molecule probably has a transcript distinct from the 12 kb transcript of perlecan.

Attempted cloning of the cDNA that codes for vHSPG using the polymerase chain reaction and degenerate oligonucleotides

The 110 kD heparan sulfate proteoglycan was purified from bovine kidney as described above, deglycosylated with heparinase I, and III, and electrophoresed on a 6% SDS polyacrylamide gel. Core proteoglycan was transferred onto Immobilon P membranes and excised. Alternatively the proteoglycan band was directly excised from the gel. The identity of the band was confirmed by parallel Western blotting using previously characterized mono or polyclonal antisera to the 110 kD heparan sulfate proteoglycan. Following enzymatic digestion, three initial peptides were sequenced and degenerate oligonucleotides of 17, 20 and 26 nucleotides in length were designed based on bovine codon usage tables. Serine and leucine residues which present a very high degree of degeneracy were omited from the design of the oligonucleotides. In addition,only the first and second base of the C-terminal glutamic acid codon were used in order to avoid further introduction of variation into the probes. For example, the 1st peptide sequence was Asp Val Val Ala Gln Glu Ser Leu Leu and the oligomers were GA(T or C) GTN GTN GCN CA(G or A) GA. No highly homologous sequences were found on comparison of the peptide sequences to the protein databases (GenBank, Swiss-Prot, etc.) using the GCG program.

Pools of 256-fold degenerate oligonucleotides were employed in the polymerase chain reaction (PCR) using standard conditions. A heat denatured (95^{o}C for 3 minutes) aliquot of the lambda GT11 bovine aortic endothelial cell library was used as the DNA template. Amplification during the polymerase chain reaction was done using a standard program (94^{o}CX1min/55^{o}/cx2min/72^{o}Cx5min). An aliquot of the amplification products was ran on a 1.0% agarose gel containing ethidium bromide (0.5 ug/ml). Several amplified bands were visualized, and the PCR reaction was repeated with a 1 ul

aliquot of the previous amplification reaction. An aliquot of this reaction was in turn ran on a 1% agarose gel and visualized as before. A prominent amplification product of approximately 500 base pairs was observed. In order to subclone this fragment the remaining PCR reaction mix was loaded onto a 3% NuSieve GTG agarose gel, visualized and excised. The excised DNA fragment was excised and blunt ends were made by filling in the overhanging ends with 1 unit Klenow DNA polymerase I and 20 uM dNTPs. The fragment ends were then phosphorylated with T4 polynucleotide kinase and 10 uMATP (for 1 hour at 37^{o}C) to enhance the ligation efficiency.

The blunt ended DNA fragment was ligated into EcoRv digested pBlueScript that had been subjected to an alkaline phosphatase reaction to minimize self-ligation (1 unit of calf intestine phosphatase at 37^{o}C for 60 minutes). Ligations were done using 100 units T4 DNA ligase at 4^{o}C overnight. Ligated DNA was used to transform competent Escherichia *coli* strain JM109. Log phase E. *coli* are made competent by suspending in 0.1 M rubidium chloride, 1 M MOPS (pH 7.0), followed by suspension in 0.1 M rubidium chloride, 1 M MOPS (pH 6.5) and 0.5 M calcium chloride. The ligated DNA is added to the competent cells and the mixture is placed on ice for 1 hour followed by a 43^{o}C heat shock for 2 minutes. Cells are grown for 90 minutes with shaking at 37^{o}C for 90 minutes and plated on LB-amp. Viable colonies are selected and the plasmid DNA is prepared for use in restriction enzyme analysis, DNA sequencing, and for library sceening.

Plasmid DNA was prepared using the alkaline lysis method essentially according to Sambrook et al. [110], and the DNA sequence was determined using the dideoxy sequencing strategy employing Sequenase enzyme, T3 and T7 oligonucleotide primers, Sequenase termination mixes, Sequenase pyro

phosphatase mix, and 10 mCi/ml [alpha-^{35}S]dATP, according to manufacturer's instructions (USB). After the reactions were completed they were stopped with 10 mM EDTA and formamide loading buffer, loaded on a 6% acrylamide/urea denaturing gel, and ran for 4 hours at 50 W, constant power. The gel was then processed in 5% glacial acetic acid/5% methanol, dried and exposed to XAR-5 film.

The DNA sequence was ascertained by reading the bands corresponding to the individual nucleotides in a sequential manner. This sequence was subjected to DNA sequence homology searching using the FastA and Blast programs on the GenBank database. The outcome of this comparison demonstrated a high degree of homology (94.5% identity in 218 base pairs of overlap) to Bacteriophage lambda. Apparently, one of the oligonucleotides used in the PCR reaction was used as a primer for the Vent polymerase in the 5' as well as 3' directions, with respect to the intended directionality of the oligonucleotide primer. This lead to the amplification of an erroneous DNA sequence.

To minimize the likelihood of amplifying irrelevant sequence, it was decided to use cDNA produced from the RNA of bovine aortic endothelial cells, thus avoiding the likelihood of amplifying vector (bacteriophage lambda GT11) sequence. In addition the oligonucleotide primer that had the property of priming Vent polymerase in both directions was eliminated from the pool of oligonucleotides. First strand cDNA was synthesized from approximately 30µg of total bovine endothelial RNA using MMLV reverse transcriptase in a 50µl reaction volume, and 1 µl of cDNA was amplified using 1-10µg primer and Vent polymerase. Amplification during the polymerase chain reaction was done using

a standard program (94°CX1min/55°/cx2min/72°Cx5min) using pools of 256-fold degenerate oligonucleotides as primers.

An aliquot of the amplification products was ran on a 1.0% agarose gel containing ethidium bromide (0.5 ug/ml). Several amplified bands were visualized, and the PCR reaction was repeated with a 1 ul aliquot of the previous amplification reaction. This process was repeated a second time using 1 ul of this reaction as a template for the polymerase chain reaction.

The amplified product was isolated, made blunt ended, and subcloned into pBlueScript, and used to transform JM109 cells as stated above. Plasmid DNA prepared from these cells was sequenced and searched against the molecular sequence databases(GenBank, EMBL) as stated above. The result of this search demonstrated 86.4% identity in 367 base pairs of overlap with human MHC protein.

Screening of a bovine endothelial cell cDNA expression library.

Previous attempts at amplifying a putative sequence of vHSPG using degenerate oligonucleotides as primers for the polymerase chain reaction proved unsuccessful, yet the polyclonal antibodies produced to vHSPG demonstrate high affinity for the protein core of the antigen, and so we chose the expression screening method of cDNA cloning as the next approach.

A lambda GT11 bovine endothelial cell cDNA expression library was purchased from Clontech Inc. Using a single colony of Y1090 R- grown in the presence of ampicillin (100 μg/ml) a plating culture was prepared as follows. Ten ml of sterile Luria Broth supplemented with 0.2% maltose in a sterile 50-ml conical tube was inoculated with a single bacterial colony. The culture was grown overnight at 37 C with moderate agitation (250 cycles/minute in a rotatary shaker). Ten-fold serial dilutions of bacteriophage stocks were prepared in SM.

Phage (0.1 ml of each dilution) were placed into a sterile tube, with 0.1 ml of plating bacteria, and the tube was incubated for 20 minutes at 37 ^{o}C to allow the bacteriophage particles to adsorb to the bacteria. Three ml of molten (47 ^{o}C) agar (0.7%) was added to each tube, vortexed gently, and immediately poured onto the center of a plate containing 30-35 ml. of hardened bottom LB agar medium. After five minutes the plates were inverted and incubated at 37 C for 16 hours.

After having titered the library we proceeded to screen the library at a density of 5 X 104 plaques per 150mm plate. The infected plates were incubated for 3.5 hours at 42^{o} C. Simultaneously, 150mm nitrocellulose filters were soaked in a solution of isopropalthio-b-D-galactoside (IPTG) (10 mM in distilled water) for a few minutes. Filters were dried at room temperature on Whatman paper and quickly overlaid on to the plates. The plates were incubated for at least 4 hours at 37 ^{o}C, and for 30 minutes at 37 ^{o}C. Filters were marked for orientation purposes and removed from the plates. The filters were washed in TBS-Tween and then placed in dishes containing the monoclonal antibodies, 4F2 and 7E12 to the 110 kDaHSPG diluted 1:10 in TBS-Tween , and the polyclonal antibody to 110 kD HSPG, diluted 1:500, with 20% fetal calf serum (7.5 ml for each 82-mm filter) and incubated overnight. After washing, the secondary antibody (goat anti-mouse alkaline phosphatase conjugated IgG) was added for 1 hour. Detection of the antigen-antibody complexes was then performed with 5-bromo-4-chloro-3-indoyl phosphate in the presence of nitro-blue tetrazolium.

Upon primary screening, six immuno-positive plaques were identified. The area on the agarose plate corresponding to the position on the nitrocellulose filter was removed with a 1 ml pipette tip and placed in storage media (SM) to elute the bacteriophage. These phage were replated at a dilution that would yield between 10 to 100 plaques for a secondary screening process, and

processed according to the same procedure as for the primary screening. The plaques on one of the plates were clearly the most immunopositive of all those examined and the plaques were removed from the appropriate position on the plate.

Phage Propagation and Purification

As the putative vHSPG clone was identified, the phage DNA from these clones was isolated, as described in the chapter on methods.

Restriction enzyme digests were performed on the isolated phage DNA to determine the insert size. This was done with EcoRI and other enzymes found on either side of the lambda phage cloning site. The insert size was approximately 700 base pairs as assessed by comparison with the sizes of molecular markers.

The cDNA of putative positive bbm HPSG clones was cut with restriction enzymes from the flanking lambda phage DNA. These DNA fragments were made blunt-ended with Klenow Large fragment DNA polymerase and ligated into EcoRV digested pBlueScript that had been subjected to an alkaline phosphatase reaction to minimize self-ligation. Ligations were done using T4 DNA ligase at 4^{o}C overnight. Ligated DNA was used to transform competent Escherichia *coli* strain JM109.

The purified DNA of the putative vHSPG clone was sequenced by the DNA sequencing core at Mount Sinai, and analyzed as described above for DNA sequence homology. The results of this search showed a near complete homology with bovine 28S ribosomal RNA. This sequence is erroneous as it applies to our attempts to obtain a cDNA clone for vHSPG, and further attempts are awaiting better amino acid sequence information.

IV.Regulation of Endothelial Cell Proteoglycans by IL-1ß, TGF-ß, and Low Molecular Weight Hyaluronic Acid

The ability of several factors to regulate the metabolism of proteoglycans derived from mouse endothelial cells in *vitro* was examined. Proteoglycans isolated from the cell lysate, the cell surface and those proteoglycans secreted into the cell culture media were investigated. Interleukin-1 beta (IL-1ß) was examined because of its ability to produce neovascularization of cerebral blood vessels [111,112], and its well known role in the acute phase response, an inflammatory reaction that may alter the permeability of the BBB, thereby diminishing its protective nature. TGF-ß has been shown to alter the regulation of several proteoglycans by a number of different mechanisms [18]. TGF-ß is elaborated after neuronal injury and is very important in tissue repair. Hyaluronic acid is the most abundant glycosaminoglycan in the brain [25,113] and the angiogenic low molecular weight degradation products produced by macrophages have been shown to increase the production of some extracellular matrix molecules [57].

The analysis of the effects of these factors on the regulation of proteoglycans was performed on two levels. The first was to examine the regulation of a specific proteoglycan called perlecan. We performed RNA solution hybridization (RNase protection assays) to determine the steady state level of the RNA that codes for perlecan.

The second level of analysis examined proteoglycan metabolism of endothelial cells in culture. The degree of sulfation of the GAG component of a proteoglycan can be highly regulated by the activity of sulfotransferases [51] and alterations in the net charge of a given proteoglycan may have profound effects on the functioning of the molecule in normal physiologic processes as well as diseased states [2,51]. The sulfate residues of heparan sulfate make it one of

the most highly negatively charged molecules, and are responsible for the establishment of a charge-barrier in many cell types, including endothelium, [9], as well as a variety of other functions.

We examined the level of sulfation conferred upon the PGs as determined by their elution with an increasing linear salt gradient from an anion exchange chromatograph column. Proteoglycans bind much more tightly to an anion-exchange matrix than do proteins and glycoproteins because of the polyanionic glycosaminoglycan chains, thereby providing a unique characteristic that can be utilized for purification and analysis of proteoglycans. The proteoglycans contained in the major peaks obtained from ion-exchange chromatography were subjected to enzymatic digestion with heparitinase III and chondroitinase ABC which cleave heparan sulfate and chondroitin sulfate/dermatan sulfate, respectively, in order to determine the types of proteoglycans being analyzed.

We next analyzed the size of the intact proteoglycans and the glycosaminoglycan chains after removal of the protein core by beta-elimination, a reaction which cleaves the glycosaminoglycan chains at their attachments to the protein core [114]. Modulation of the length of the the GAG chains attached to the proteoglycans may be altered depending on the physiologic state of a given cell type [115,116]. Alterations in chain length may lead to changes in the net charge of the proteoglycans, or to their affinity for various substrates. Since heparan sulfate proteoglycans bind to the A4 peptide [117], and may play an important role in the deposition of Aβ or A4-amyloid [118], we examined the binding affinity of the endothelial cell derived GAGs for the A4 peptide of AD using A4 affinity chromatography after cell stimulation.

The presence and total level of perlecan mRNA was determined by solution hybridization/ribonuclease protection assay (RNase protection assay) using an exon probe that identifies the perlecan mRNA. We subcloned a 322

base pair fragment from a perlecan cDNA construct into the bluescript (SK) vector as a template for *in vitro* transcription of RNA probes (Figure 8a and b). A single protected band representing the 322 base pair region of the perlecan mRNA was detected and identified as being the appropriate size after electrophoresis through a 5% acrylamide gel, (Figure10b,c). Endothelial cells treated with the appropriate factor were grown in six well plates, and each determination was performed in quadruplicates. The experiment was performed twice. A c-fos construct was used to determine whether the cells were being activated to turn on Fos gene transcription, and thereby serving as as positive control of the ability of the factors to activate the cells. c-fos is an immediate early gene and its expression is induced within 30 minutes of the initial activation of second messenger pathways in a cell. We also included a cyclophilin probe as an internal standard as a way of determining if similar amounts of total RNA were used in each sample (Figure 10 b and c). By using plus strand RNA for both cyclophilin and perlecan we were able to construct standard curves that enabled us to quantify the total amount of specific transcript present in each sample (Figure 9b and c).

We found that c-fos mRNA is present 30 minutes after the addition of IL-1 β and TGF-β, and LMW HA but is no longer detectable after 2 hours (Figure 10a). Our results indicate that the total amount of perlecan transcript is not affected by the exposure of endothelial cells to interleukin-1β , transforming growth factor-β , or low molecular weight hyaluronic acid (Figure 10d).

Biochemical analysis of total cellular, and secreted proteoglycan species from mouse aortic endothelial cells after stimulation with IL-1ß, TGF-ß, and Low Molecular Weight Hyaluronic Acid.

Preparation of Proteoglycans

Mouse aortic endothelial cells were metabolically radiolabelled with ^{14}C glucosamine and ^{3}H-glucosamine for control cultures and experimentally treated cultures, respectively. Cells were grown at approximately 90% confluence in the presence of radiolabel and factors, where applicable. After 24 hours the cells were harvested.

The culture media was removed and saved for analysis as "secreted" material. The cells were washed with phosphate buffered saline and this wash was combined with the labelled culture media that had already been removed. In order to remove molecules on the surface of the cells, they were treated with a dilute solution of trypsin-EDTA for 5 minutes at 37°C. This solution was removed and saved for analysis as the "pericellular" material. The "cellular" material was prepared by lysis of the remaining cell pellet in the presence of 8M urea buffer. This material was centrifuged and applied to a DEAE-CL6B ion exchange column. The cell surface and secreted material was dialyzed in 7M urea buffer and applied in this buffer to the DEAE column. Ion-exchange chromatography allowed us to determine if the added factors had influenced the net charge of the proteoglycans isolated from each of the cellular fractions.

Each application of sample onto the column was in a volume of 1 ml of 7M urea buffer and consisted of a mixture of control material from untreated cells that had been labelled with ^{14}C-glucosamine and material from treated cells that had been labelled with ^{3}H-glucosamine. The column flow rate was 10 ml/hr. After application of the sample the column was washed with three column

volumes of 7M urea buffer. Elution of the bound material was accomplished with a linear salt gradient of 0.15 M NaCl to 1.0 M NaCl. Approximately eighty fractions were collected for each sample application. These fractions contained both ^{3}H and ^{14}C glucosamine and could be analyzed using dual label counting with the automatic quench control feature of the scintillation counter. The automatic quench control feature of the scintillation counter eliminates of the overlap of signals between the ^{3}H and ^{14}C windows alowing the user to attribute counts to either isotope that had been used together in the same sample. By comparing the treated sample to the control sample on the same chromatograph, this experimental design eliminates variations that may occur between two separate chromatographs enabling us to observe subtle alterations in the chromatography profiles. Disintegrations per minute (dpm) for channel one correspond to the ^{3}H-glucosamine labelled treated material, and the dpm in channel two correspond to the 14C-glucosamine labelled control (untreated) material.

DEAE-CL6B ion exchange chromatography

The influence of IL-1beta on mouse endothelial cell proteoglycans

The cellular proteoglycans derived from the cytoplasm of mouse endothelial cells displayed a considerable degree of heterogeneity with three major peaks eluting at ~0.40 M NaCl, 0.62 M NaCl, and 0.75 M NaCl (figure 11a). These peaks were confirmed by absorbances at 280 nm for the detection of protein.. Both pools of control and stimulated proteoglycans displayed the same elution patterns with respect to the sodium chloride molarity at which they eluted and the relative profile of the proteoglycan peaks. From these observations it is concluded that IL-1β does not alter the net charge of

proteoglycans isolated from the cell lysates of endothelial cells under the conditions of our experiment as determined by the elution profile of ion-exchange chromatography .

The population of proteoglycans isolated from the culture media of mouse endothelial cells treated with interleukin-1 beta displayed two major peaks on DEAE ion-exchange chromatography (figure 11b). The first peak eluted at a sodium chloride concentration of 0.52M. This was the smallest peak as well as the peak representing proteoglycans with the least net negative charge in comparison to the other peaks. The second peak to elute from the ion exchange matrix was intermediate to the other two peaks in charge and total quantity as determined by disintegrations per minute (dpm). This peak eluted at 0.63 M NaCl. The third and final group of proteoglycans eluted at approximately 0.77 M NaCl. This was clearly the largest group of proteoglycans in this sample and displayed significant alterations in its elution profile derived from endothelial cells grown in the presence of IL-1β. Subsequent enzymatic digestion of this proteoglycan with heparinases and chondroitinases followed by gel filtration chromatography revealed a smalller digested peak in the heparinase treated material but not the chondroitinase ABC treated material. This suggested that these molecules were composed of heparan sulfate proteoglycans.

IL-1β lead to a stimulation of glucosamine incorporation into these specific proteoglycan species in relation to the other proteoglycan species that are secreted into the cell culture media (figure 11b). Interestingly, both the control and IL-1 beta peaks eluted at the same sodium chloride concentration, suggesting that IL-1 beta did not cause a change in the net negative charge of the proteoglycans but did lead to an increase in the total amount of synthesized product. In order for the net charge to remain the same the charge density on the GAGs would likely remain the same, suggesting an increase in the total

amount of proteoglycan synthesized or that the length of the GAG chains was altered. An increase in the relative amount of glucosamine into the glycosaminoglycan chains with no net change in charge density would suggest the presence of longer GAG chains with a decreased density of sulfation, with the total level of sulfation remaining constant. This possibility was addressed by preparing GAG chains free of protein core and performing gel filtration on Sephadex G-150 (see pp 69-72).

The influence fo TGF-β on mouse endothelial cell proteoglycans

The elution profile of control cellular proteoglycans on DEAE ion exchange chromatography in this experiment was similar to that seen in the interleukin-1 beta experiment (figure 12b). Three major peaks were obtained. The first peak eluted at a sodium chloride concentration of approximately 0.45 M. This represented the major peak with regards to quantity of proteoglycans. The second peak contained fewer incorporated counts of radio-labelled glucosamine than the first peak. The sample treated with TGF-β contained approximately 25% more proteoglycans than the corresponding control peak. This represents a significant alteration in the total amount of proteoglycans eluting at this NaCl concentration relative to control. As the total amount of protein as determined by Bradford assay was the same in both control and TGF-β treated cells, this alteration is not related to total protein content. In addition, cell counts performed on parallel samples revealed similar numbers of total cells.

Treatment of endothelial cells with TGF-β lead to subtle alterations of the elution profile of secreted proteoglycans on DEAE-ion exchange chromatography (figure 12 b). In this case the control proteoglycans in peak II appear to be produced in excess of those from TGF-β treated cells, but only marginally.

The influence of low molecular weight hyaluronic acid on endothelial cell proteoglycans

The first peak of the cytoplasmic proteoglycans elutes at ~0.55 M NaCl and is the largest peak but is not altered by treatment with low molecular weight hyaluronic acid (figure 13a). Low molecular weight hyaluronic acid had a dramatic effect in decreasing the relative amount of proteoglycans eluting in the second peak of the DEAE-IEC. This peak elutes at ~0.75 M NaCl. HA appears to decrease the amount of material in the second peak by about 60%. This represents a considerable move towards a decreased proportion of proteoglycans with a high net negative charge.

The secreted proteoglycans of cells treated with hyaluronic acid demonstrate no alterations from control cells (figure 13b). The elution profile was quite similar to that seen for TGF-β with two major peaks eluting at ~0.75 and 0.85 M NaCl.

Gel Filtration (Sephadex G-150) of Glycosaminoglycan Chains

As demonstrated by DEAE ion exchange chromatography, specific alterations in proteoglycan metabolism were observed upon treatment of endothelial cells with specific factors. IL-1β treatment lead to an increase in the relative amount of proteoglycan compared to control that eluted at higher sodium chloride concentrations on DEAE ion exchange chromatography. The elution of this material at higher salt concentrations suggest that this material contains a higher net negative charge. IL-1β treatment did not alter the elution profile of cellular proteoglycans as determined by ion exchange chromatography. TGF-β treatment lead to an increase in the relative amount of material eluting at lower sodium chloride concentrations compared to control, and had very subtle effects

on secreted material. LMW HA treatment of mouse endothelial cells resulted in the relative decrease of material eluting at lower salt concentrations on ion exchange chromatography compared to control. This was opposite to the effect of TGF-β. LMW HA did not influence the elution profile of secreted proteoglycans.

In order to gain further insight into these changes we analyzed the protein-free glycosaminoglycan components of the PGs with regard to their size distribution using gel filtration chromatography. Most GAG chains fall within the range of 10-50 kDa. Sephadex G-150 can separate molecules in the range of ~4,000-150,000 making it appropriate for the separation of GAG chains.

The individual fractions of proteoglycan peaks I and II, containing treated (^{14}C-glucosamine) and untreated (^{3}H-glucosamine) material were pooled. Half the sample was dialyzed in water, lyophilized and used for gel filtration of intact proteoglycans. The other half was chemically treated with 1 M sodium borohydride for the preparation of free glycosaminoglycans. These samples were dialyzed in water and lyophilized. The lyophilized sample was solubilized in 0.5 ml phosphate buffered saline. One half of the sample was used for gel filtration on Sephadex G 150 and the other was used for A4 affinity chromatography.

The Sepharose G 150 gel filtration column (0.7 X 50 cm) had a Vo of 6 ml and a Vt of 18 ml, and was used for the separation of GAG chains. The sodium borohydride generated glycosaminoglycan chains from peak I of HA/control proteoglycans displayed a wide range of sizes (Figure 15a), with some molecules eluting at the void volume (Vo) while others eluted at close to the total volume of the column, as well as throughout the entire elution volume. There was a considerable amount of glucosamine labelled material corresponding to high molecular weight species.These molecules eluted as

three distinct peaks with Vo/Vt ratios of 0.92, 0.86, and 0.79. The molecular weights lie in the range of 20 to 50 kDa as determined by calibration according to protein standards. These molecules may represent both incompletely digested high molecular weight proteoglycans as well as high molecular weight GAGs. There was a smaller amount of mid range GAGs as judged by the total amount of dpm obtained in the middle of the elution profile. Lower molecular weight GAGs represented the largest pool of molecules isolated from peak proteoglycans after sodium borohydride treatment. Six distinct peaks may be identified in this range. These GAGs may represent species of small GAGs that have been synthesized to their full length. The other explanation for these GAGs takes into consideration the method with which they were isolated. They were radiolabelled with ^{3}H and ^{14}C glucosamine for 24 hours and isolated from the cellular fractions. This isolation would therefore result in GAGs that have been incompletely elongated and have been isolated during their synthesis in the Golgi.

Gel filtration of the sodium borohydride generated GAGs derived from peak B proteoglycans revealed a substantial amount of larger GAGs represented by three distinct peaks (Figure 15b).These GAGs were derived from proteoglycans in peak B of the ion-exchange chromatography and therefore carry a higher net negative charge than peak A proteoglycans.

The GAGs eluting in the middle range of molecular weights are the widest peaks of all those collected (figure 15c). This peak is substantially larger in relation to the other peaks of this chromatography. The lower molecular weight peaks make up the majority of GAGs obtained by this method probably for the same reasons stated above.

It is noteworthy that the GAGs from peak B are found at a relatively lower amount when derived from HA treated endothelial cells as compared

to control GAGs. The decrease in relative amounts appears to exist almost over the entire range of sizes of GAGs. This depression in GAG synthesis was also notable in the DEAE ion exchange chromatography of the proteoglycans which served as the source of these GAGs (figure 13a). The decrease in relative amounts was most noticable at the high and mid-range sized GAGs with less difference existing for the smaller GAGs.

A4-affinity chromatography

Affinity chromatography was performed using the A4 peptide (amino acids 1-28), the cleavage product of the β-APP molecule, as previously described (Buee et al., 1993). Using FPLC, the retention of the proteoglycans on the column was monitored, and binding of GAGs to the A4 peptide was examined.

Cellular GAGs which eluted in peak A of DEAE-IEC from the IL-1β experiment displayed specific binding for A4 yet this appears to be of a relatively moderate affinity (Figure 16a). The interaction between GAGs and A4 could be disrupted at a salt concentration of ~0.55 M NaCl. This was slightly lower affinity than the binding of intact proteoglycans for A4, which was disrupted at an NaCl concentration of ~0.65 M. None of the treatment modalities examined here (IL-1β, TGF-β or LMW HA treatment) altered the binding of the corresponding GAGs to A4 peptide as determined by A4-affinity chromatography.

Chapter 5. Discussion

A. Localization of vascular Heparan Sulfate Proteoglycan in Alzheimer's Disease and Squirrel Monkey Brain.

Heparan sulfate and HSPG are both known to have strong binding affinities for some of the molecules which are found in plaques, particularly the A4 peptide and bFGF [97,117,119-121]. HSPG has also been been associated with the neurofibrillary tangles of AD [90]. We have observed the association of HSPG with the pathologic lesions of AD and cerebral amyloidopathy at the morphologic level by immunoreactivity to polyclonal antibodies vHSPG in AD and aged squirrel monkey brain. The diffuse senile plaques immunoreactive for vHSPG displayed a fainter staining pattern than the blood vessels, presumably due to the fact that HSPG is present in a greater proportion in the basement membrane of blood vessels than in the senile plaques. The actual cellular source of both HSPG and A4 in plaques is unknown. If we assume that bmHSPG reactivity originates from HSPG produced by blood vessels, then the greater density of HSPG in the blood vessel than in the surrounding tissue suggests that the HSPG may first accumulate in the basement membrane and then diffuse into the surrounding parenchyma. The amyloid of neuritic plaques and cerebrovascular amyloid has been found to be antigenically related [122] and the presence of A4(1-42) in both vascular tissues and neuritic plaques suggest that these deposits might arise from a common source [123]. Co-localization of A4 with vHSPG in squirrel monkey demonstrates a very close association with the cerebrovasculature, and the tight interaction of A4 with the capillary basement membrane suggests that the vessel may be the source of vascular amyloid, and potentially the source of parenchymal A4. We observed areas of intense HSPG immunoreactivity in vessels as well as in plaques often adjacent to areas were the blood vessel appeared narrowed.

Recently, it was found that the major form of the A4 peptide in the cores of neuritic plaques is a modified A4(1-42), and that this form, though with fewer modifications, is the major form in the vascular tissue of the brain [123]. The modifications on the A4 peptide include N-terminal degradation and the isomerization and racemization of aspartyl residues 1 and 7. These modifications arise spontaneously in proteins, and so the abundance of these residues might be an indication of the relative age of the protein [123]. Plaque A4 has also been found to have greater N-terminal degradation compared with vascular A4. These results suggest that the A4 found in the cores of plaques is "older" than the A4 associated with vascular tissues. These findings suggest that at least a portion of the A4 found in senile plaques in the brain parenchyma may be derived from the vasculature. This hypothesis confers an important role of the vasculature in the pathogenesis of AD.

The clustering of the angiopathic alterations observed in both AD and aged squirrel monkey brain suggests that the endothelial cells of the blood-brain barrier may be triggering a reparative process. As evidenced by the immunohistochemical data, HSPG is a fundamental constituent of the brain vasculature, found in both microvessels and larger vessels. Its role as a structural organizer of the cerebrovasculature basement membrane and the ability of HSPG to bind several growth factors which have effects on both neurons and endothelial cells suggest an important relationship between the endothelium and the parenchyma of the brain that extends beyond simply functioning as a provider of basic nutritional demands. This role may be an active one, and subtle alterations in brain hemostasis may lead to significant alterations in HSPG metabolism. This in turn may have profound effects on the process of amyloidogenesis in normal and diseased states. The immunohistochemical evidence presented here may be interpreted in this

context. While HSPG is found throughout the normal cerebrovasculature in squirrel monkey brain, it appears that HSPG is significantly altered at sites where blood vessels have an angiopathic morphology. HSPG appears overexpressed in these instances and co-localizes with A4 in squirrel monkey. In addition, the vHSPG produced by these cells is co-localized with the A4 peptide. This finding as well as evidence pointing to the the importance of HSPG in all forms of amyloidosis, and binding studies showing high affinity interactions between HSPG and both A4 and its precursor strongly suggest that HSPG is playing a role in amyloidogenesis in both normal aging and AD. The process of amyloidogenesis is central to AD, therefore any molecule that contributes to this process deserves consideration at least as an important accessory molecule in the disease. The presence of serum protein in the neuropil as well as in neuritic plaques is indirect evidence for a change in BBB permeability of microvessels in AD [124]. Blood-brain barrier compromise has been implicated in the pathogenesis of AD [125,126] suggesting the possibility that a compensatory effort to repair the BBB might be playing a role in the pathogenesis of AD. Endothelial cells may attempt to repair "leaks" in the BBB by increasing the production of HSPG and A4. HSPG has well known properties of charge selectivity in the glomerular basement membrane [127-129], and these properties may be playing a role in the BBB. Likewise, it has been speculated that A4 may be acting as a hydrophobic patch to seal defects in the blood-brain barrier [123]. A reparative process involving these molecules may prove beneficial at first, but then eventually lead to the occlusion of the capillary lumen, leading to severely compromised oxygen and nutrient delivery to a population of neurons. Several factors may be causing the initial compromise to the BBB, including the acute-phase reaction which leads to the elaboration of cytokines. These cytokines, namely IL-1, may lead in turn to the production of more B-APP

[44]. Neuronal populations with high metabolic demands, such as pyramidal neurons in layers III and V of neocortical association areas may straining the transport limits of the BBB, thereby exacerbating the already existing defect beyond the point where proper re-establishment of the BBB is possible.

Our findings confirm the presence of vHSPG in senile plaques in AD as well as demonstrate the presence of vHSPG in the plaques of aged squirrel monkey brain. Perlecan has also been localized to the senile plaques of AD. Several questions arise from the presence of both of these proteoglycans in the neuropathologic lesions of AD. Not only is the physiologic function of these HSPGs unknown, but the cellular source of the basement membrane HSPGs found in the senile plaques has not been determined, nor has the exact relationship between these molecules been determined.

B. Biochemical and Immunological Characterization of vascular Heparan Sulfate Proteoglycan

The view that basement membrane is composed of a homogeneous group of heparan sulfate proteoglycans (HSPG) is currently replaced by one that recognizes basement membrane HSPGs (bmHSPG) as a diverse population of molecules. Despite the significance of basement membrane HSPGs in the normal functioning of cells as well as their possible role in disease, there are conflicting reports as to the exact nature of the processing of basement membrane HSPGs from their precursor to the final cleavage products.

A large degree of structural diversity of PGs stems from the proteolytic cleavage of the core proteins thereby removing peptides and attached glycosaminoglycan (GAG) chains. Structural differences among bmHSPGs may also arise from the synthesis of unique HSPG cores that are distinct products of separate genes, or from differential splicing of mRNA from the same gene. In the case of perlecan, it has been suggested that proteolytic cleavage is responsible for the generation of a small high density HSPG with a heterodisperse core protein of M_r= 95-130 kDa from an intact proteoglycan with a core of M_r=350-400 kDa [21]

As the protein core of the bovine glomerular basement membrane HSPG (vHSPG) falls within the range of the high density form of perlecan, an important question is whether perlecan and vHSPG are immunologically and biochemically related as a result of a precursor-product relationship, particularly since both are found in AD plaques, or whether the two forms represent two different species each derived from a unique gene product. A variety of approaches have been taken in this study to examine the relationship between perlecan and vHSPG, including immunoassay, immunoblotting, immunoprecipitation, and pulse chase methodologies. The present results give convincing evidence that perlecan and

vHSPG are not related immunologically, and that vHSPG is produced from a different precursor protein than the precursor of perlecan.

Having produced a polyclonal antibody to vHSPG that recognizes bovine and murine species, as well as canine, monkey, and human, we performed immunoassays (ELISA) to determine possible cross-reactivity of antibodies to perlecan and to vHSPG. Minimal cross-reactivity was seen when anti-vHSPG was reacted with perlecan. These antibodies were inhibited by purified vHSPG, but not by perlecan. On the other hand, perlecan antibodies showed some reactivity with vHSPG. However, perlecan antibodies were inhibitable by heparan sulfate as determined by competitive inhibition ELISA studies, and a considerable degree of the cross-reactivity for vHSPG was also diminished in the presence of heparan sulfate, therefore the cross-reactivity we observed was attributable to common HS side chains rather than common protein cores.

The results of immunoblots of perlecan and vHSPG reacted with anti-vHSPG antibodies supported the immunoassay data in that almost no cross-reactivity for perlecan was observed. As in the immunoassay, perlecan antibodies did recognize purified vHSPG to some degree. Again, a considerable amount of this cross-reactivity may be explained by the recognition of common heparan sulfate determinants. In addition, shape motifs that the two molecules share may be preserved even when the proteoglycans are bound to nitrocellulose. Another explanation can be found in a report that suggests the immunogen used to produce perlecan antibodies does not represent a single proteoglycan species but a mixture of different proteoglycan species because the extraction procedures used to purify the proteoglycans were overly stringent [24]. As the homologous protein to vHSPG may be present in the EHS proteoglycan preparations, rabbit polyclonal antibodies made to this preparation would in fact contain antibodies to vHSPG. This could account for the cross-

reactivity observed between perlecan antibodies for vHSPG in immunoassays and immunoblots.

An important consideration in examining immunologic relatedness between perlecan and vHSPG is the species variations of these two molecules and the species specificity of antibodies to these molecules. For instance, differences in the amino acid sequence of a protein from one species to another may prevent antibodies from recognizing both proteins. We have had several peptides from bovine vHSPG sequenced, and although no significant homology was found to other proteins in the protein databases, the possibility exists that species differences would obscure these homologies. To eliminate some of the difficulties in our analysis we chose a cell type, mouse aortic endothelial cells that produce the homologues of perlecan and vHSPG as determined by preliminary experiments. As rabbit polyclonals to bovine vHSPG recognize murine basement membrane HSPG and MAE cells have been shown to produce perlecan transcript, and by inference the perlecan protein, mouse endothelial cells are an appropriate cell type for identifying the precursors to basement membrane heparan sulfate proteoglycan. As amino acid sequence to vHSPG derived from mouse endothelial becomes available we will be able to make a direct comparison to the published sequence for mouse perlecan [32].

Both conditioned media and cellular lysates of mouse aortic endothelial cells were used for the immunoprecipitation of vHSPG and perlecan. By combining conditioned media with media from radiolabelled cells we were able to show that the material that anti-vHSPG immunoprecipitated could be visualized on immunoblots with anti-vHSPG. A certain level of variability in post-translational modifications may have occurred. The formation of disulfide bonded aggregates could be one of these modifications [10]. The molecular weight of this material appears larger than the material isolated from bovine glomeruli.

There may be several reasons for this. The strong molecular associations that occur in the basement membrane between distinct matrix molecules may lead to difficulties in purifying intact molecules, and although the preparation of vHSPG from bovine glomeruli is done in denaturing conditions and in the presence of protease inhibitors, the harsh extraction conditions may result in a limited degree of proteolytic cleavage yielding a smaller protein than that found using immunoprecipitation from conditioned media. In addition, differences in molecular weight of vHSPG from mouse and bovine species could be due to species differences in post-translational processing.

Our immunologic data strongly suggest that perlecan and vHSPG are unique proteins not derived from a common gene product. In all likelihood, this would imply that different precursor proteins exist for these molecules. Although the molecular weights of perlecan and its metabolic products have ranged from 10 to 700 kDa [130], the perlecan precursor protein has consistently been found be a protein of ~400 kDa in murine, rat, porcine, and human tissues [24,101,115,131]. Previous attempts at determining the precursor size of the small bm HSPG have used either tumorigenic cells or glomeruli [101,130,132]. As mentioned earlier, the finding that perlecan is processed to the smaller bmHSPG [22] must be qualified by the possibility that the immunogen used in these studies was a mixture of bmHSPGs as a result of technical issues in the purification procedure. In rat glomeruli, endothelial, mesangial, and epithelial cells contribute molecules to the basement membrane. These mixed cell types may producing the various proteoglycans with different kinetics, possibly favoring the production of perlecan over the smaller bmHSPG. This in turn might cause the precursor to vHSPG to be obscured by the large amount of perlecan precursor. Indeed, in the data of Klein et al. [22] a smaller protein of ~250 kDa can be seen in the pulse-labelled lysates of rat glomeruli. The potential also

exists that both large and small bmHSPGs were used as the immunogen in the production of antibodies to rat glomerular HSPG.

To eliminate some of the potentially confounding factors encountered when pulse-labelling mixed cell types we pulse-labelled mouse endothelial cells. We confirmed the precursor size of perlecan, and determined that the precursor of vHSPG has a molecular weight ~250 kDa that is not related to the precursor of perlecan. This molecular weight is clearly below the expected precursor size of perlecan, and considering the short labelling time, it is highly unlikely that this protein size was the result of proteolytic cleavage. In fact, the conversion of high molecular weight perlecan to the low molecular weight form appears to occur within 1-2 hours after the synthesis of the precursor protein. While this may be a rapid conversion rate, we are seeing a 250 kDa precursor to vHSPG in a significantly shorter time period. In addition, while a 400 kDa protein could enter the 3-10% acrylamide gel as determined by extrapolation of molecular weight standards, we do not observe any other precursor besides the one at 250 kDa.

Attempts to isolate the cDNA for vHSPG provided a good foundation for future attempts at this project. The degenerate oligonucleotides proved in adequate for use in both PCR cloning as well as hybridization screening. Using the degenerate oligonucleotides we isolated a lambda GT11 bacteriophage DNA sequence, and an MHC antigen DNA sequence. Until vHSPG amino acid sequence is obtained that with a higher level of certainty, we should use the polyclonal antibody EP01 for continued efforts at expression screening of various cDNA libraries. Using a commercial bovine capillary endothelial cell library we superfluously cloned a 28S ribosomal RNA sequence. Repeated attempts to screen from this library and other libraries made from cells that produce large amounts of vHSPG should be performed and a larger number of immunopositive plaques should be processed for the potential that they contain

vHSPG DNA sequence. Our results suggest distinct precursors for the two major forms of basement membrane heparan sulfate proteoglycan which may be post-translationally modified with great diversity in various tissues and cell types. In addition, species differences clearly exist amongst these molecules. As we begin to understand the similarities and differences amongst heparan sulfate proteoglycan components we will be able to dissect out the subtle alterations in processing and post-translational modification that give these molecules particular functions. In addition, a knowledge of the types of modifications in these molecules and the factors regulating these changes will enable us to understand HSPGs role in the basement membrane in normal processes such as angiogenesis, and may help us gain insight into the pathological conditions such as glomerulonephritis, AD, and the angiogenic process in tumor development.

At present, we only have an incomplete knowledge of the extent of homology of the protein cores between different populations of basement membrane HSPGs. It is clear from several studies that there are antigenically distinct populations of basement membrane-associated and membrane associated HSPGs. However, within the population of basement membrane HSPGs the extent of diversity awaits elucidation. In fact, there may be as yet unidentified forms. Farquhar and Couchman (personal communications) have each identified a distinct heparan sulfate proteoglycan of ~50 kDa which appears to be the product of a different gene than that of perlecan. This may be derived from a unique gene product or be a proteolytic product of vHSPG. Willi Halfter (personal communication) has determined that a basement membrane HSPG isolated from embryonic chick retinal ganglion is homologous has a cDNA identical to agrin, a protein originally isolated from the neuromuscular junction of chick and the *Torpedo californicus*. Others have determined that agrin is in fact a

basement membrane HSPG [133,134]. The final resolution to the issue of the relationship between vHSPG and perlecan will come with the cloning of the cDNA for vHSPG, a project that deserves much attention.

C. Regulation of endothelial cell proteoglycans by factors that may play a role in the pathogenesis of Alzheimer's Disease

Molecules found in the extracellular matrix (ECM) have been shown to play critical roles in development, tissue injury, repair and disease [135]. Changes in ECM synthesis, accumulation and catabolism play major roles not only in wound healing and fibrosis, but also in the initiation and progression of many acquired disease, such as atherosclerosis, liver fibrosis, the secondary consequences of diabetes and Alzheimer's Disease [10,136]. HSPG is closely associated with the accumulation of amyloid in various forms of amyloidosis [89,119,137-140]. Evidence continues to accumulate that proteoglycans may be playing a central role in the pathogenesis of the hallmark lesions of AD brain; amyloid deposits in neuritic plaques and along the walls of the cerebral vasculature, and in the formation of the neurofibrillary tangle [90]. Although the initiating factor that may cause HSPG to be involved in the pathogenesis of AD is unknown, a likely candidate may be the influence of the immune system on the regulation of HSPG. The causal link between the involvement of HSPG in AD and the pathogenesis of this disease may lie in the role that the immune system plays in the regulation of HSPGs. The involvement of the immune system, in the form of chronic inflammation and the acute phase response, in the pathogenesis of AD has been well established [45,141,142]. Activated microglial are highly colocalized with senile plaques and other submicroscopic amyloid deposits, and have a highly reactive morphology [143]. Cytokines such as IL-1α, IL-1β, and IL-6, are found to be elevated in AD brain [144].

In an attempt to better understand the regulation of HSPGs by immune system factors we examined the influence of several immune system products on the production of proteoglycans by endothelial cells. We chose mouse aortic endothelial cells for use in our studies because our examination of the regulation

of the perlecan gene transcript required mouse RNA, and they are also easily maintained in culture.

The regulation of endothelial cell proteoglycans was examined at a number of levels; 1. the steady state level of a specific RNA (perlecan), 2. the net charge as determined by ion-exchange chromatography of the population of proteoglycans from the cell lysate, cell surface, and cell media, 3. the length of these proteoglycans and their attached glycosaminoglycan (GAG) chains as determined by gel filtration chromatography, and 4. the ability of these GAGs to bind to the A4 peptide of AD.

From RNA solution hybridization experiments we determined that the steady state level of perlecan RNA was not significantly altered by the addition of either IL-1β, TGF-β or low molecular weight hyaluronic acid to the culture media of mouse endothelial cells from which the RNA was prepared. Our experiments incorporated a c-fos probe that enabled us to conclude that the endothelial cells were indeed activated by IL-1β and TGF-β but we did not see the presence of the c-fos transcript in cells treated with high molecular weight hyaluronic acid.

We determined that mouse aortic endothelial cells produce a mixture of chondroitin sulfate and heparan sulfate proteoglycans, with the HSPGs possessing a higher negative charge than the CSPGs (figures 14a and 14b). Significant alterations were observed in the ion-exchange profile of specific proteoglycan preparations. IL-1β did not affect cellular proteoglycans but led to a large increase in the relative amount of secreted proteoglycans incorporated into peak II compared to peak I of control proteoglycans. Peak II represents predominantly heparan sulfate proteoglycans, and these proteoglycans are more negatively charged than the proteoglycans represented in peak I of ion-exchange chromatography. Our dual labelling analysis allowed us to submit our

samples to the same chromatograph, thereby eliminating differences introduced by experimental errors inherent in chromatography. This analysis required the comparison of dpm values for ^{14}C and ^{3}H-glucosamine by normalization of each data set to its maximal value. While this does not allow us to compare absolute values, we can nevertheless compare relative values between samples. The overall effect can be considered to be an increase in the ratio of more highly charged proteoglycans HSPGs compared to proteoglycans of lower charge in the culture media due to IL-1β stimulation.

TGF-β treatment of endothelial cells also led to a relative increase in the amount of more highly charged proteoglycans isolated from the cell lysates of endothelial cells but did not affect the profile of pericellular nor secreted proteoglycans compared to control. Hyaluronic Acid produced the opposite effect as TFG-β on cellular proteoglycans leading to a relative decrease in the level of more highly charged proteoglycans. These findings suggest that endothelial cell proteoglycans *in vitro* are subject to specific regulation depending on which factor they are exposed to. The *in vivo* effects of these factors would be complicated due by the complexity of influences on the endothelial cells, such as the cell growth state and the other factors present in the cellular micro-environment.

Using ion exchange chromatography we were able to analyze proteoglycans according to their net charge and alterations in the elution profile were detected in specific experimental treatments. The ion exchange methodology examines the net charge of the proteoglycans and so we may be missing significant alterations in the composition of the glycosaminoglycans attached to these proteoglycans. For instance, an alteration in the composition of the actual disaccharide subunits that compose the full length GAG may be occuring but cannot be detected using ion exchange chromatography. To

analyze alterations in the disaccharide composition of the GAGs would require the use of HPLC.

Proteoglycans contain a large number of post-translational modifications. In fact, a specific CSPG was estimated to contain over 200 of these modifications [10]. This clearly influences the rate of processing of these molecules by enzymes in the Golgi network and leads to long trafficking times. In our study we looked at alterations in proteoglycan metabolism after 24 hours from the introduction of the specified factors. While proteoglycans do reside in the cytoplasm, a large portion of the proteoglycans that we isolated from the cell lysate were probably targetted for the cell membrane and extracellular space and in the process of Golgi trafficking for these locations. In this sense, alterations in proteoglycans isolated from the cell lysate may be reflecting the changes in molecules targetted for the cell surface of the extracellular matrix. This may be applicable to the observations of changes in the ion-exchange elution profile of cellular proteoglycans from cells treated with TGF-β and low molecular weight HA. Proteoglycans destined for the cell surface and extracellular space may have been altered but were not observable in preparations of these cell fractions under the conditions of our experiment. However, using this argument we would also expect to see alterations in the cellular proteoglycans derived from IL-1β treated cells. This was not the case, and this discrepancy remains unresolved.

Although we did not observe angiogenic effects, such as increased cell number or increased cellular processes, due to low molecular weight HA, this is an established characteristic of these molecules [56,57]. Due to the nature of our experimental culturing conditions, which used cells that were 90% confluent, angiogenesis may not have been possible in this setting. However, initial alterations in cell adhesiveness may have been permitted under these

conditions. Since PGs may act as cell adhesion molecules, a relative decrease in the amount of more highly negative proteoglycans could lead to low affinity interactions with the cell substratum, facilitating cellular migration associated with angiogenesis. Likewise, the relative increase in production of more highly charged species observed with TGF-β treatment may promote high affinity interactions and cell adhesion.

Since HSPGs have affinities for many substrates, including growth factors, and β-APP/A4, a perturbation in the composition of charges contained by PGs could influence the physiologic functions of these interactions. HSPG acts as a low affinity receptor and a reservoir for bFGF [145], an interaction that is mediated by the negative charges conferred by the sulfate groups of HS, and alterations in the binding affinity of HSPG for FGF probably lead to modulation of FGF activity. It has been found that developmental changes in the carbohydrate composition of HSPG appear to regulate the presentation of the different forms FGF to neural cell surfaces [15]. Similarly, the alteration in the cellular composition of proteoglycans that we have observed due to stimulation by factors related to immune system function may result in the modulation of FGF activity.The binding of HSPG to β-APP is also influenced in part by the sulfate residues of HS that align with positively charge amino acids on β-APP [146], making the regulation of these negative charges important for the physiologic function of APP.

In the samples where alterations in the ion-exchange profile were observed, we further analyzed these proteoglycans according to the sizes of the intact proteoglycans and the GAG chains prepared from these proteoglycans according to gel filtration. In this instance, the dual labelling approach employed in these experiments proved very useful in analyzing our results. The sizes of the GAG chains cleaved from their protein core were precisely matched for

proteoglycans from stimulated and control samples in every instance. GAG chains prepared from proteoglycans with higher net negative charges had higher molecular weights than the proteoglycans with lower net negative charges as determined by their elution position on gel filtration chromatography. This is consistent with the view that longer chains may have a greater number of highly sulfated heparan sulfate subunits, conferring a more net overall charge on the GAG.

Our analysis of the binding affinities of both intact proteoglycans and GAG chains to A4 demonstrated binding by the intact proteoglycans, and individual GAG chains approximately the same value (figure 16a). This was determined by assuming that the binding affinity of HSPG and A4 can be extrapolated from the salt concentration required to disrupt binding. The salt concentration required to disrupt this affinity was 0.65 M. This is considerably lower than the affinity of bovine glomerular vacular HSPG (0.85 M NaCl) or neuroblastoma derived proteoglycans (0.85-0.95 M NaCl) for A4 as reported by our laboratory [97,117].

In summary, we observed specific alterations in the regulation of proteoglycans produced by endothelial cells in the presence of factors thought to play a role in immune responses involved in AD. An alteration of the relative ratio between proteoglycans of high net negative charge compared to proteoglycans with a lower net charge as determined by ion-exchange chromatography was observed in several instances. The exact manifestations of these alterations is unclear, but due to the important role that proteoglycans, in particular, heparan sulfate proteoglycans, plays in regulating the binding of growth factors and other proteins in the cellular microenvironment it would not be surprising if changes in proteoglycan metabolism, such as those observed here, had dramatic effects on the state of a cell. Due to the important role that

proteoglycans play in many normal physiologic functions and diseased states these issues deserves further investigation.

Figures

Figure 1. Immunohistochemistry of vascular heparan sulfate proteoglycan in AD (a,b,e,f) and control brain (c,d). Note the faint staining of diffuse plaques in the dentate gyrus (a), and widespread staining of neurofibrillary tangle islands in the entorhinal cortex (arrowheads in b), as well as diffuse plaque-like structures in layer 6 (asterisk, see figure 1f for high magnification). Heavy accumulation of HSPG occurs in some vessels (1f).

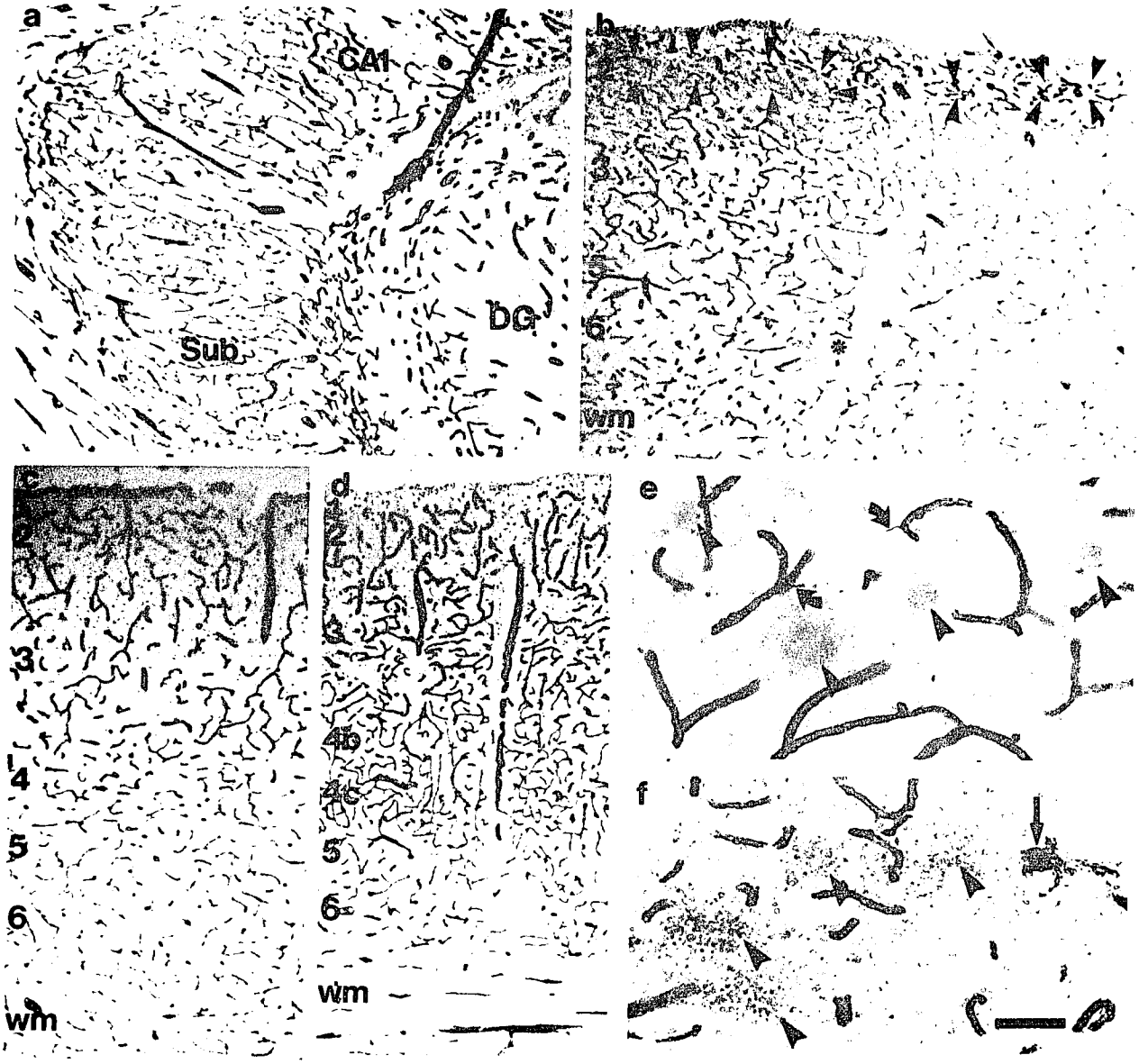
a
CA1
DG
Sub
b
3
5
wm
c
3
4
5
6
wm
d
3
4b
4c
5
6
wm
e
f

Figure 2. Immunohistochemistry using anti-vHSPG antibody in an aged squirrel monkey brain. Large accumulations of vHSPG closely associated with blood vessels, in cerebrovascular amyloid-like structures are representative of many angiopathic alterations seen in other regions.

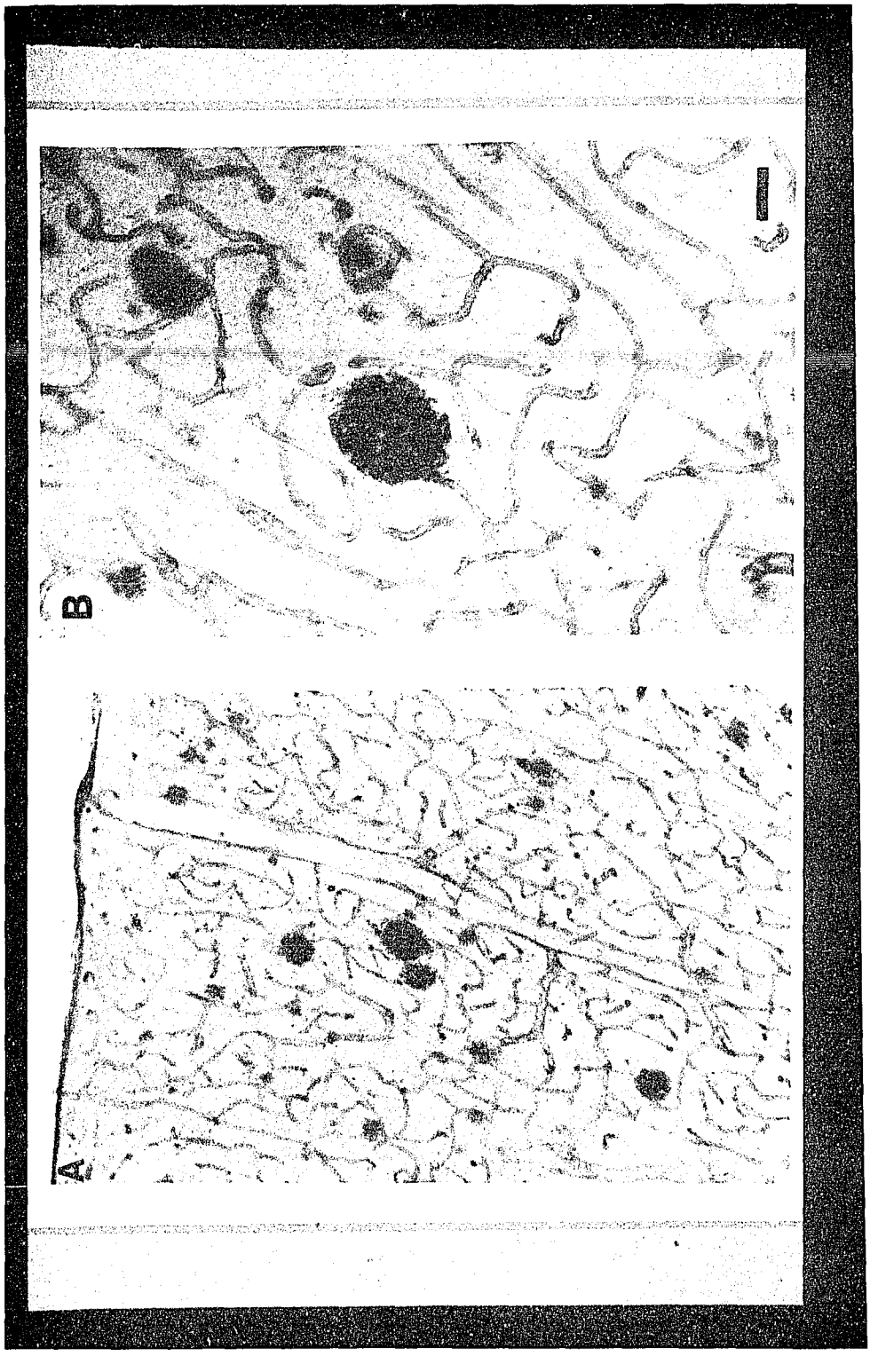
B
A

Figure 3. High magnification (400X) views of anti-vHSPG (a-d) immunohistochemistry in aged squirrel monkey brain. Sections e and f, double-labelling with anti-vHSPG rabbit polyclonal antibody and anti-A4 antibody.

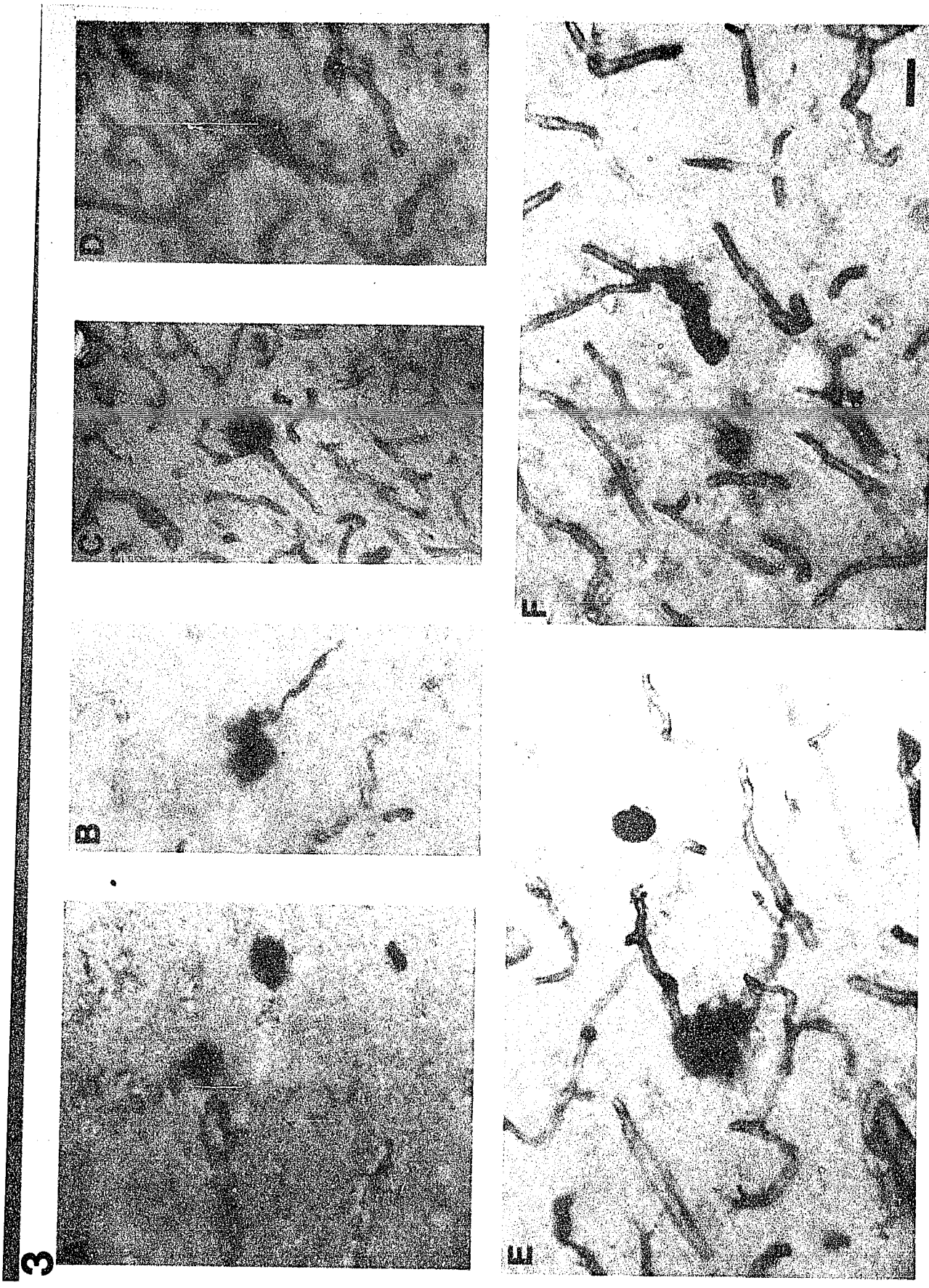

3

Figure 4. ELISA to determine the antibody titration curves and the level of cross-reactivity beween anti-vHSPG an anti-perlecan antibodies. In 4a. vHSPG was plated as the antigen, and in b., perlecan was the antigen. In 4c snPG was plated as the antigen. In 4d vHSPG was plated as antigen, and anti-vHSPG was inhibited with vHSPG and perlecan. In 4e-g inhibitions of anti-vHSPG were performed with varying concentrations of heparan sulfate.

4a

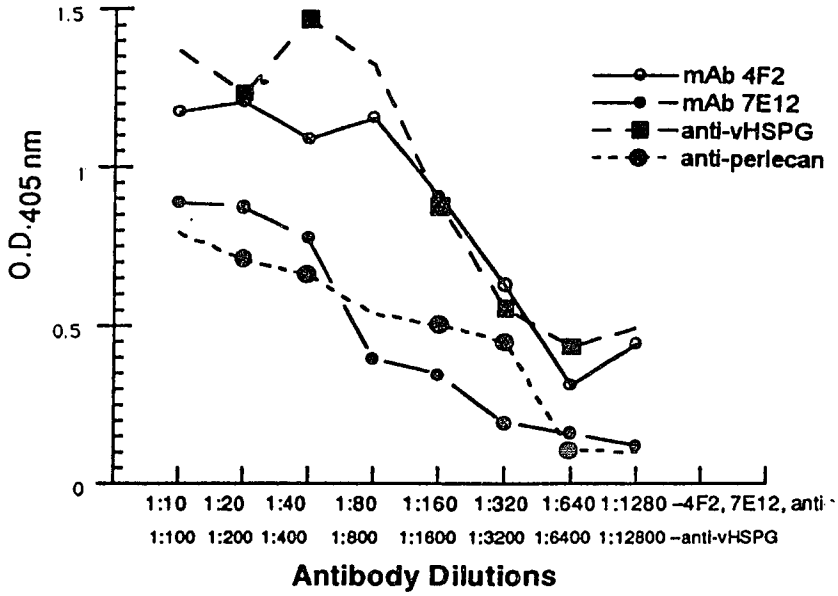
1.5
1
0.5
0
O.D.405 nm
mAb 4F2
mAb 7E12
anti-vHSPG
anti-perlecan
1:10 1:20 1:40 1:80 1:160 1:320 1:640 1:1280 –4F2, 7E12, anti
1:100 1:200 1:400 1:800 1:1600 1:3200 1:6400 1:12800 –anti-vHSPG
Antibody Dilutions

b

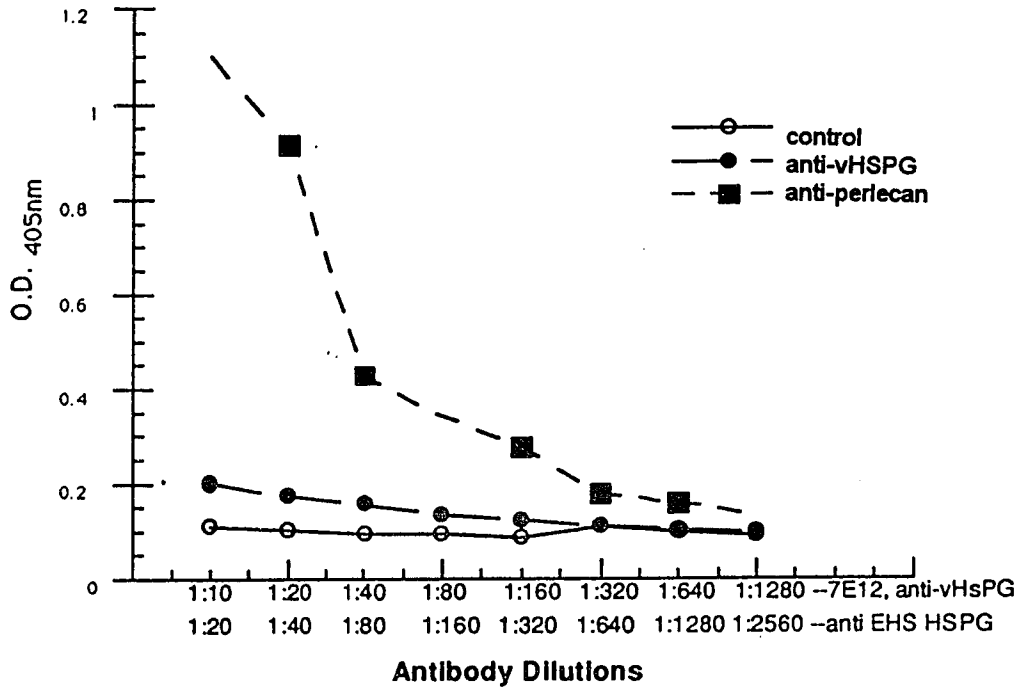
1.2
1
0.8
0.6
0.4
0.2
0
O.D. 405nm
control
anti-vHSPG
anti-perlecan
1:10 1:20 1:40 1:80 1:160 1:320 1:640 1:1280 –7E12, anti-vHsPG
1:20 1:40 1:80 1:160 1:320 1:640 1:1280 1:2560 –anti EHS HSPG
Antibody Dilutions

4c

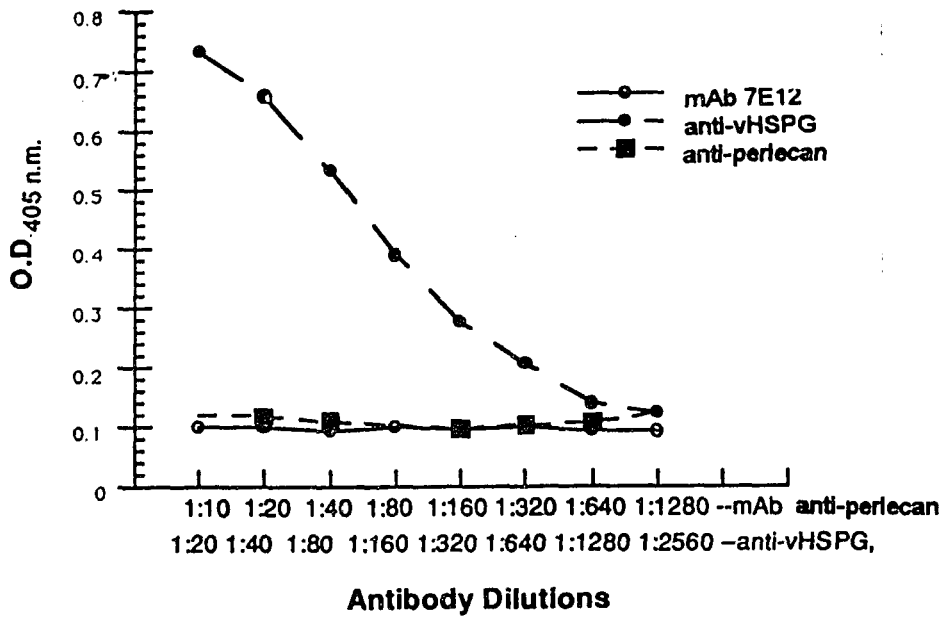
0.8
0.7
0.6
0.5
0.4
0.3
0.2
0.1
0
O.D.405 n.m.
mAb 7E12
anti-vHSPG
anti-perlecan
1:10 1:20 1:40 1:80 1:160 1:320 1:640 1:1280 --mAb anti-perlecan
1:20 1:40 1:80 1:160 1:320 1:640 1:1280 1:2560 –anti-vHSPG,
Antibody Dilutions

4d

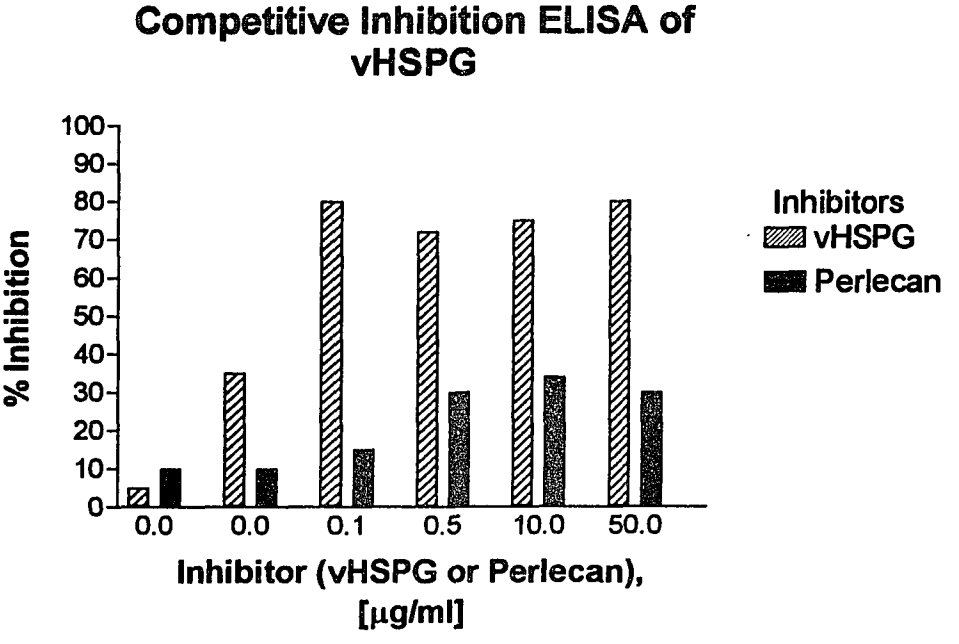
Competitive Inhibition ELISA of vHSPG
% Inhibition
100
90
80
70
60
50
40
30
20
10
0
0.0
0.0
0.1
0.5
10.0
50.0
Inhibitor (vHSPG or Perlecan), [µg/ml]
Inhibitors
vHSPG
Perlecan

4e

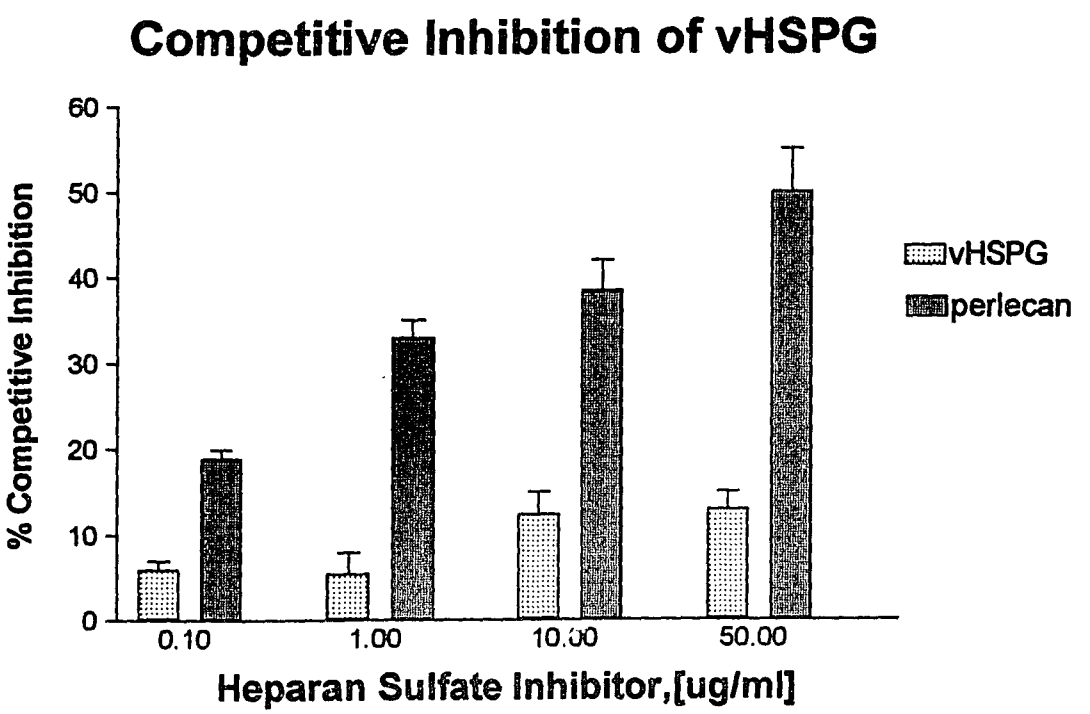
Competitive Inhibition of vHSPG
% Competitive Inhibition
60
50
40
30
20
10
0
0.10
1.00
10.00
50.00
Heparan Sulfate Inhibitor,[ug/ml]
vHSPG
perlecan

4 f

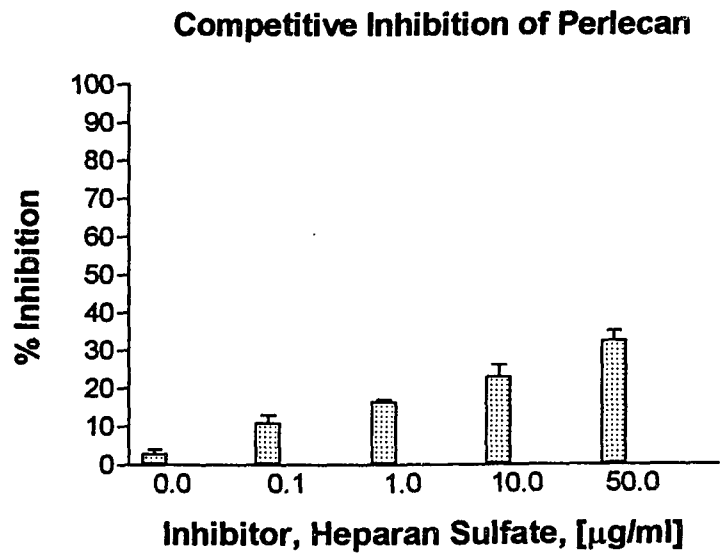
Competitive Inhibition of Perlecan
% Inhibition
100
90
80
70
60
50
40
30
20
10
0
0.0
0.1
1.0
10.0
50.0
Inhibitor, Heparan Sulfate, [µg/ml]

4g

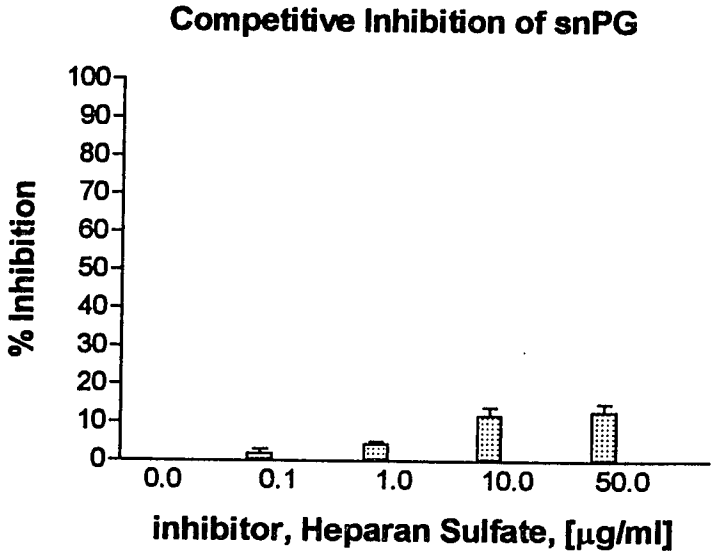
Competitive Inhibition of snPG
% Inhibition
100
90
80
70
60
50
40
30
20
10
0
0.0
0.1
1.0
10.0
50.0
inhibitor, Heparan Sulfate, [µg/ml]

Figure 5. In 5a, and b, vHSPG, and perlecan were loaded in lane 1 and 3, respectively (10μg) in SDS sample buffer, electrophoresed, and blotted as described in the text. The blots were reacted with anti-vHSPG, and anti-perlecan antibodies, respectively (5a and 5b) followed by anti-rabbit IgG conjugated to alkaline-phosphatase, and developed colorimetrically with BCIP in the presence of NBT. Lanes 4-6 were processed exactly the same except for that primary antibody was not used. In 5c, lane 4 contains snPG derived from peak B of the ion-exchange chromatography step as described. As expected, vHSPG migrates in accordance with its molecular weight of approximately 200 kDa, however the migration is not in a tight band due to the molecular heterogeneity of the proteoglycans. In lane 4, Peak A of the vascular heparan sulfate proteoglycan preparation was loaded (10 ml of a 1 mg/ml solution in SDS sample buffer). Lane 6 contains vHSPG (10 μl of a 1 mg/ml solution in SDS sample buffer). The blot was reacted with anti-vHSPG (1:1000)

Lanes 1, 2, and 3 were prepared exactly like lanes 4, 5, and 6 except that they were only incubated with goat anti-mouse IgG and no primary antibody. They represent the conjugate control for this experiment. This immunoblot demonstrates that the monoclonal antibody 7E12 which has been shown to be specific for vHSPG does not recognize the EHS HSPG.

5A

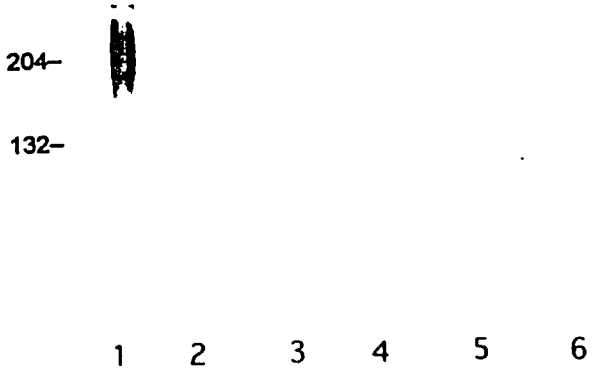

B

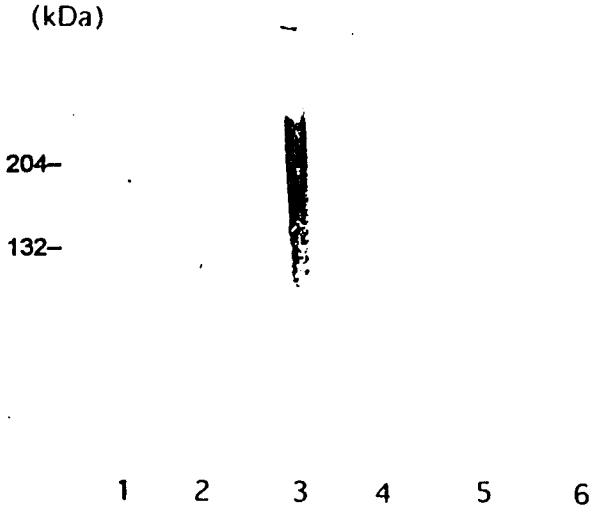

5C

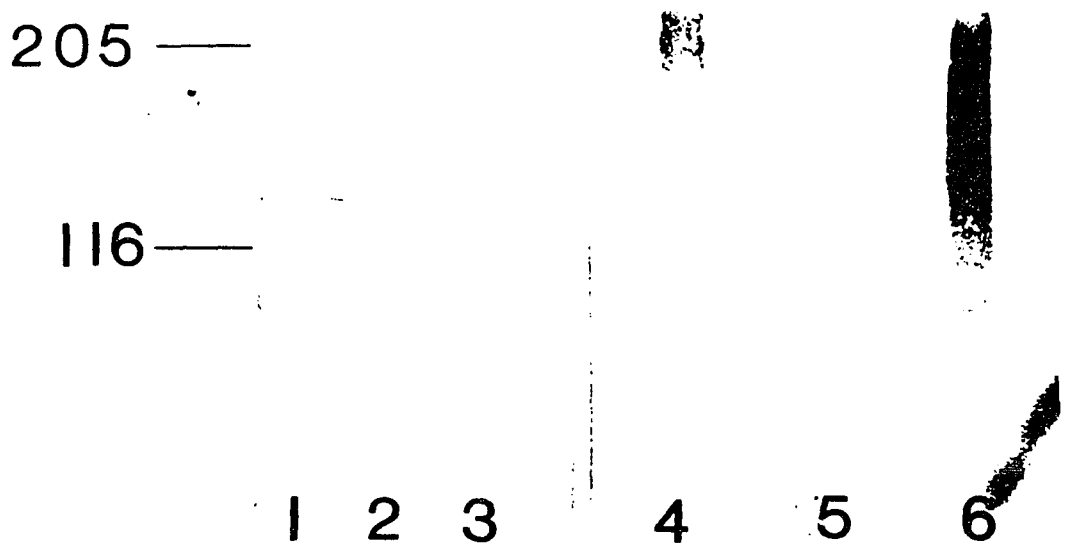

D

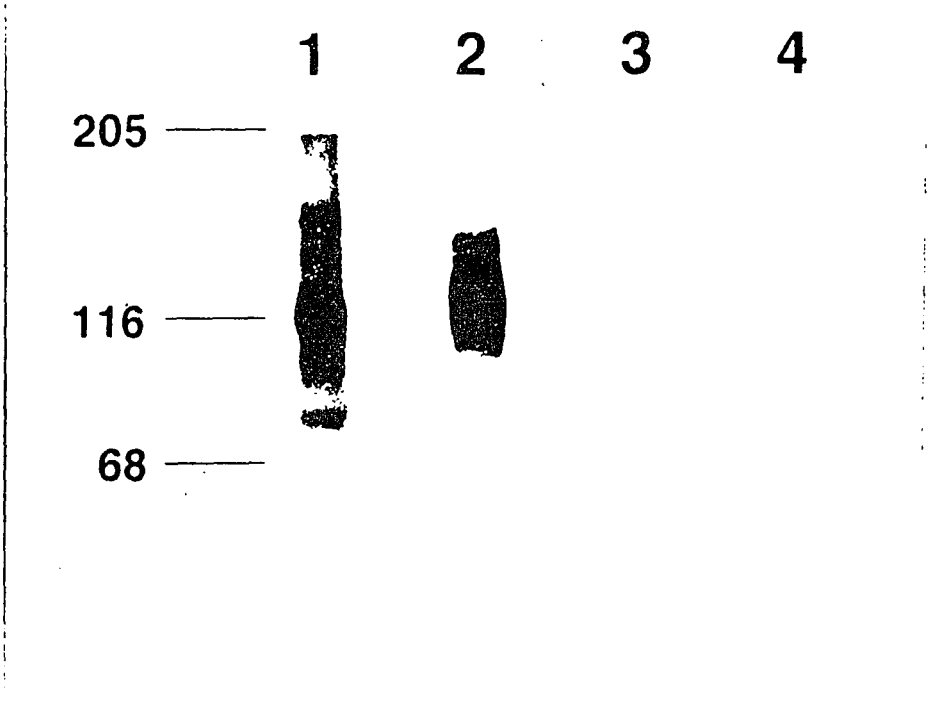

Figure 6. Autoradiographs (1 and 2) and immunoblots of immunoprecipitations with anti-vHSPG of labelled and unlabelled MAE conditioned culture media, electrophoresed on 3-10% SDS-PAGE. Lane A. was reacted with anti-vHSPG, lane B with anti-perlecan antibodies, and lane C was reacted anti-rabbit IgG alkaline phosphatase antibody.

Immunoprecipitation of Labelled and Unlabelled endothelial cell media with vHSPG antibodies

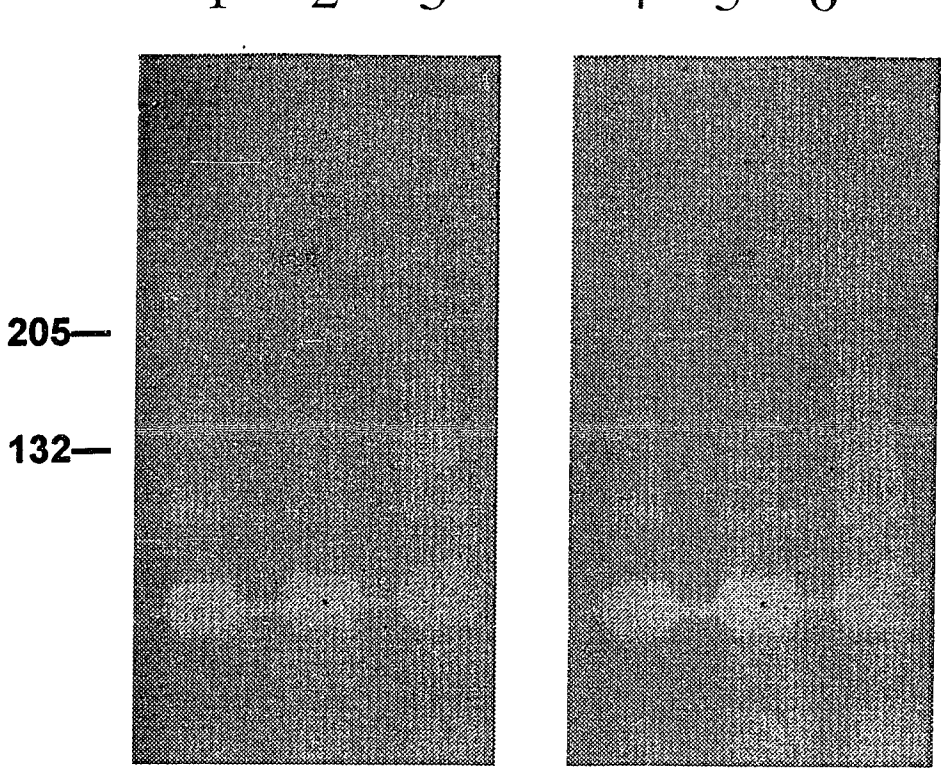

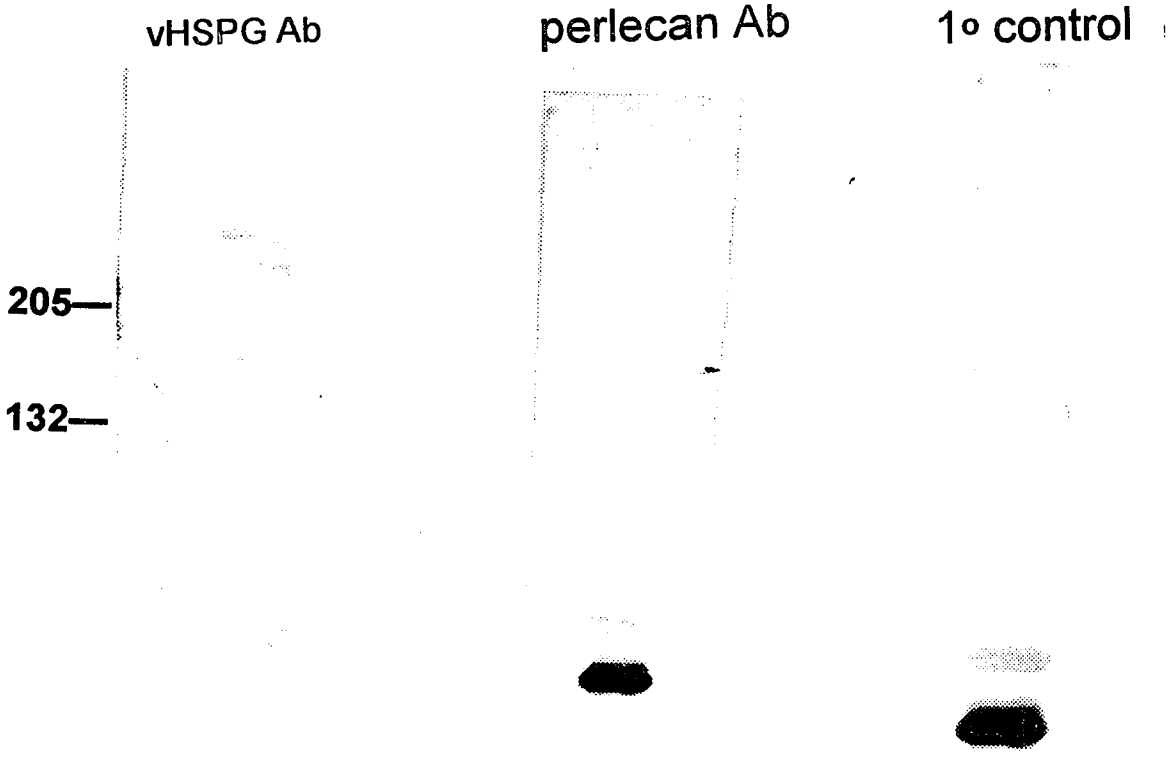

Figure 7a. Fluorographs of immunoprecipitates from mouse aortic endothelial cells pulsed with 500 μCi/ml ^{35}S methionine/cysteine and ran3-10% SDS/PAGE. Cell lysate, culture media immunoprecipitated with anti-vHSPG, lanes 1 and 3. Immunoprecipitate with normal sera in lane 2. Immunoprecipitate with anti-perlecan in lane 4.

Metabolic precursors of vHSPG and perlecan (20 minute pulse with ^{35}S methionine)

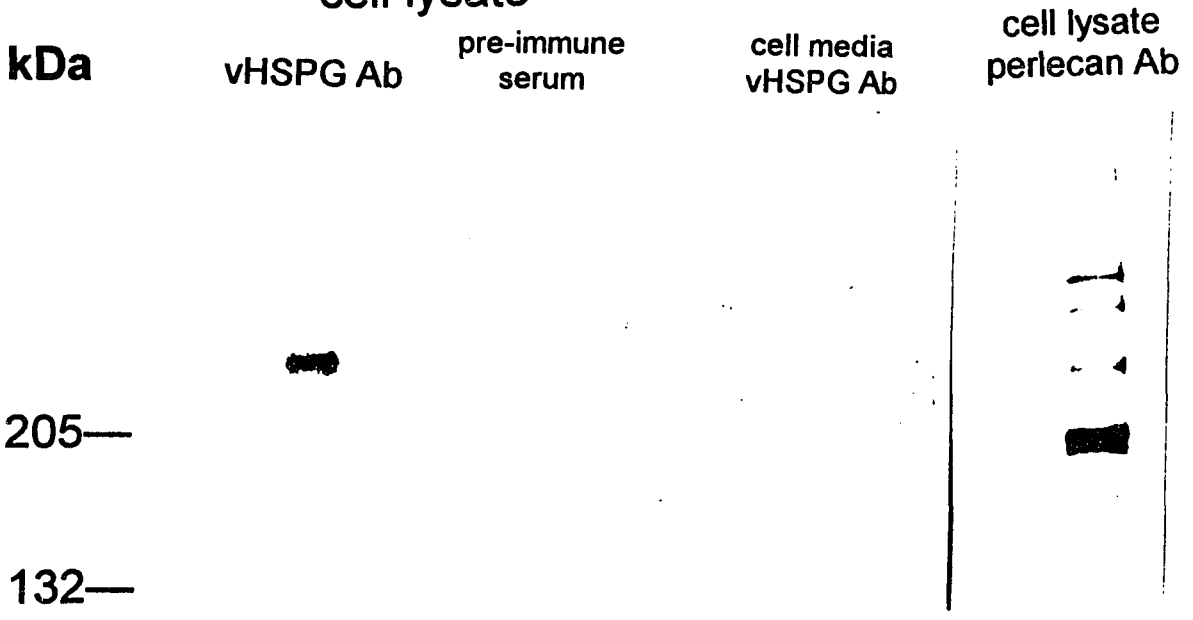

Figure 7b. Northern blot analysis of RNA from neuroblastoma, mouse aortic endothelial, bovine capillary endothelial cell, and EHS cells in lanes probed with (^{32}P) BPG5.

Northern Blot

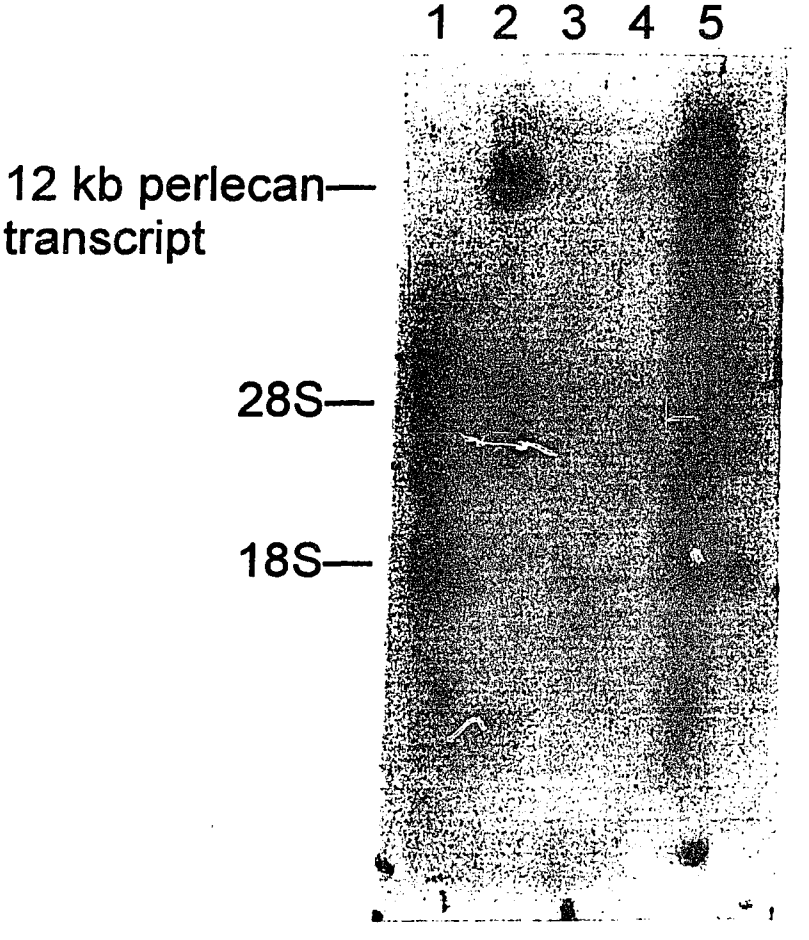

Figure 8. (a) Cartoon of the subcloning strategy for the preparation of the perlecan riboprobe BPG7/322. A 322 bp EcoR I/Pst I restriction fragment was subcloned into the corresponding site in pBluescript SK. (b) Comparison of the published sequence of perlecan with the DNA sequence obtained of the BPG7/322 subclone.

8a

Subcloning of BPG7 EcoR1/Pst1 fragment into pBlueScript

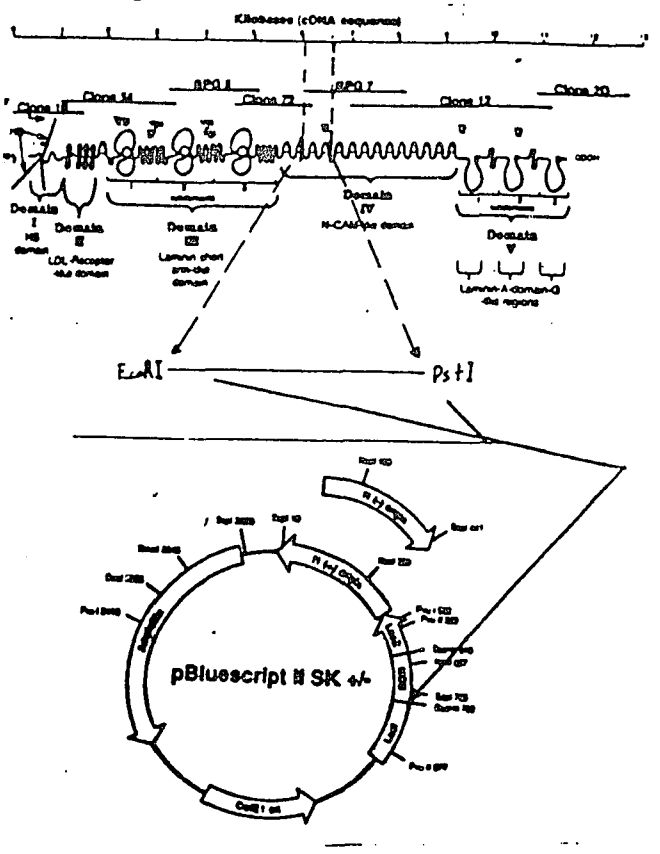

b

Mouse basement membrane proteglycan mRNA, partial cds, clone BPG 7.
99.7% identity in 322 bp overlap

```
                10        20        30        40        50        60
Bpg7.3 CACCCTCCACAGCTCACCGTGCAGCCGGGACAACAGGCTGAGTTCCGCTGTAGCGCCACG
       ||||||||||||||||||||||||||||||||||||||||||||||||||||||||||||||
Muspgc CACCCTCCACAGCTCACCGTGCAGCCGGGACAACAGGCTGAGTTCCGCTGTAGCGCCACG
                10        20        30        40        50        60

                70        80        90       100       110       120
Bpg7.3 GGCAACCCCACCCCCATGCTGCAATGGATAGGGGGTCCTAGCGGCCAGCTTCCTGCGAAG
       ||||||||||||||||||||||||||||||||||||||||||||||||||||||||||||||
Muspgc GGCAACCCCACCCCCATGCTGCAATGGATAGGGGGTCCTAGCGGCCAGCTTCCTGCGAAG
                70        80        90       100       110       120

               130       140       150       160       170       180
Bpg7.3 GCTCAGATCCACAACGGCATCCTGCGCTTGCCAGCCATTGAACCCTCGGATCAGGGCCAG
       ||||||||||||||||||||||||||||||||||||||||||||||||||||||||||||||
Muspgc GCTCAGATCCACAACGGCATCCTGCGCTTGCCAGCCATTGAACCCTCGGATCAGGGCCAG
               130       140       150       160       170       180

               190       200       210       220       230       240
Bpg7.3 TACCTGTGCCGTGCCCTCAGCAGCGCTGGGCAGCATGTGGCCAGGGCTATGCTTCAGGTG
       ||||||||||||||||||||||||||||||||||||||||||||||||||||||||||||||
Muspgc TACCTGTGCCGTGCCCTCAGCAGCGCTGGGCAGCATGTGGCCAGGGCTATGCTTCAGGTG
               190       200       210       220       230       240

               250       260       270       280       290       300
Bpg7.3 CACGGGGGCAGTGGACCCAGGGTCCAGGTTAGCCCCGACAGCACCCAGGTGCATGAAGCC
       ||||||||||||||||||||||||||||||||||||||||||||||||||||||||||||||
Muspgc CACGGGGGCAGTGGACCCAGGGTCCAGGTTAGCCCCGACAGCACCCAGGTGCATGAAGCC
               250       260       270       280       290       300

               310       320
Bpg7.3 CGCACAGTGAGGCTGTACTGCA
       ||||||||||||||||||||||
Muspgc CGCACAGTGAGGCTGTACTGCA
               310       320
```

Figure 9. (a.) Autoradiograph of acrylamide gel electrophoresis of individual riboprobes. Lane 1, cyclophilin, 117 base pairs. Lane 2, c-Fos, 305 base pairs. Lane 3, BPG7/322, 322 base pairs. (b.) Standard curve of BPG7/322 riboprobe. Lane 1 molecular weight marker, lambda/Hind III digest. Lane 2-8; 0, 0.25, 0.5, 1.0, 2.5, 5.0, 10.0pg of (+) strand RNA hybridized with excess (-) strand BPG7/322 riboprobe. (c.) Standard curve as determined by scintillation counts of protected bands from known quantities of (+) strand RNA.

9a

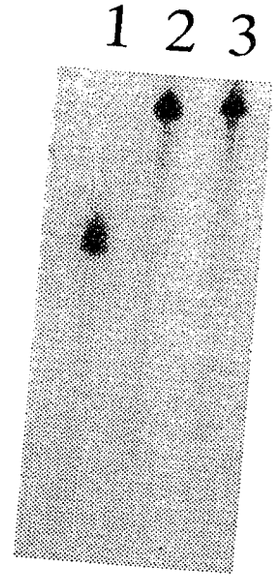

b

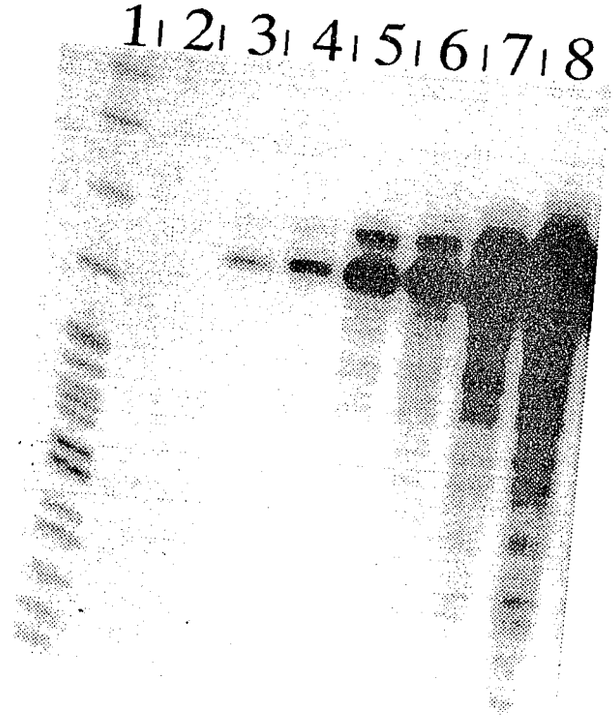

9c

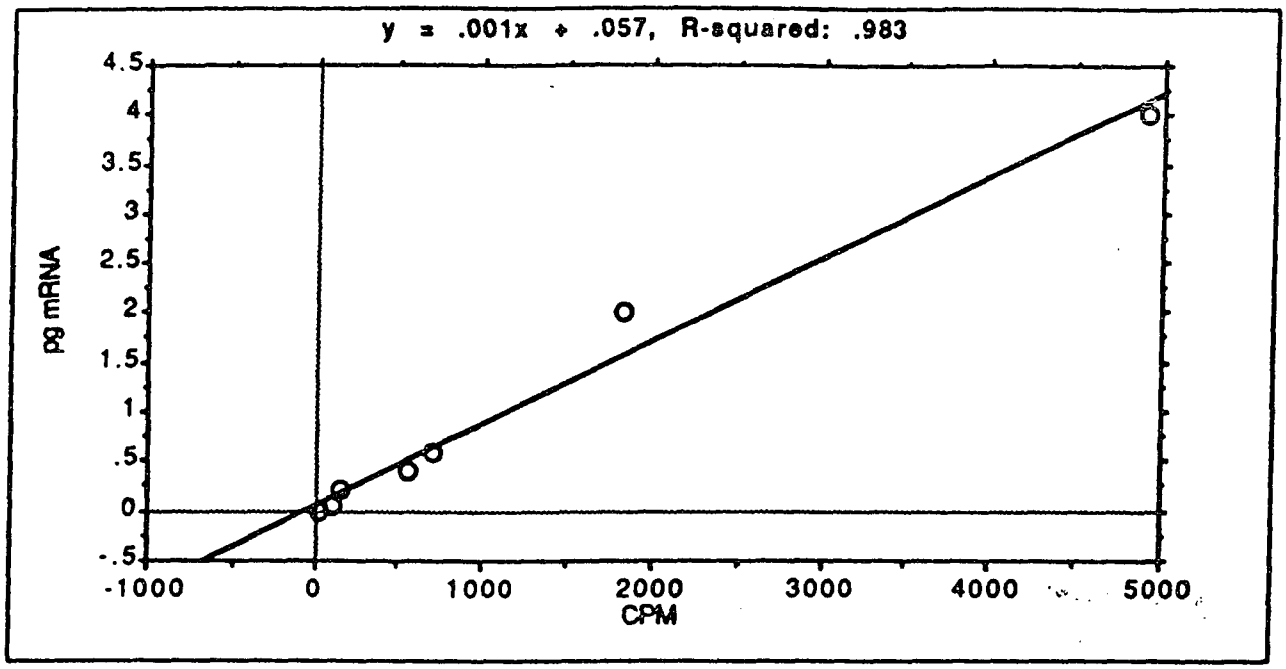
y = .001x + .057, R-squared: .983
pg mRNA
4.5
4
3.5
3
2.5
2
1.5
1
.5
0
-.5
-1000
0
1000
2000
3000
4000
5000
CPM

Figure 10.(a) Autoradiograph of solution hybridization of c-fos protected band from RNA prepared from mouse aortic endothelial cells treated with IL-1β (10 ng/ml), for 0.5 hours (lanes 5-8). Lanes 1-4 are samples of RNA treated under the same conditions for 2 hr; c-fos protected band is no longer present. (b) Autoradiograph of protected BPG7/322 riboprobe from RNA prepared from mouse aortic endothelial cells treated with IL-1β (10 ng/ml), TGF-β (5 ng/ml), and low molecular weight hyaluronic acid, (1mg/ml), for 0.5, 2, 24, and 48 hr. At each time point control was the absence of treatment by any factor. (d) Perlecan mRNA levels (pg/μg total RNA)from MAE cells treated with IL-1β (10 ng/ml), TGF-β (5 ng/ml), and low molecular weight hyaluronic acid, (1mg/ml) extrapolated from the standard curve.

10 a

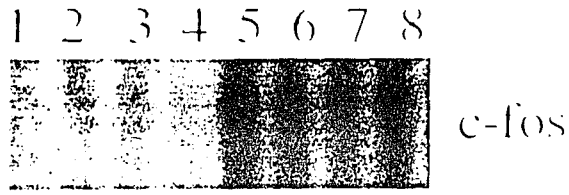
1 2 3 4 5 6 7 8
c-fos

b

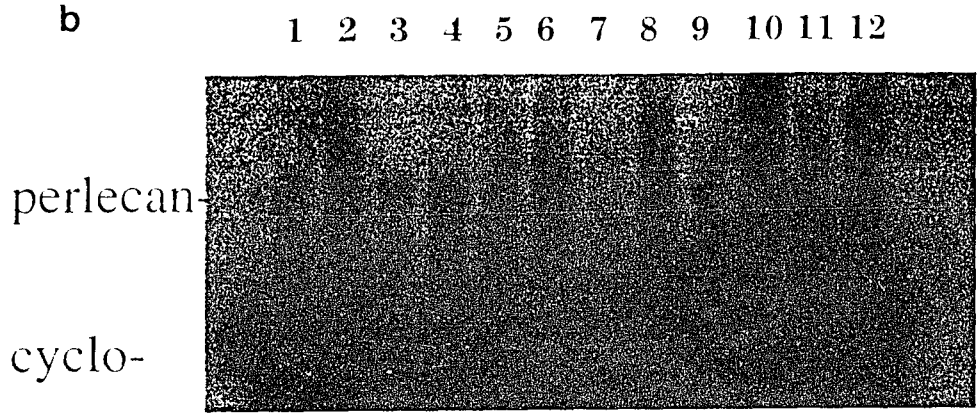
1 2 3 4 5 6 7 8 9 10 11 12
perlecan-
cyclo-

c

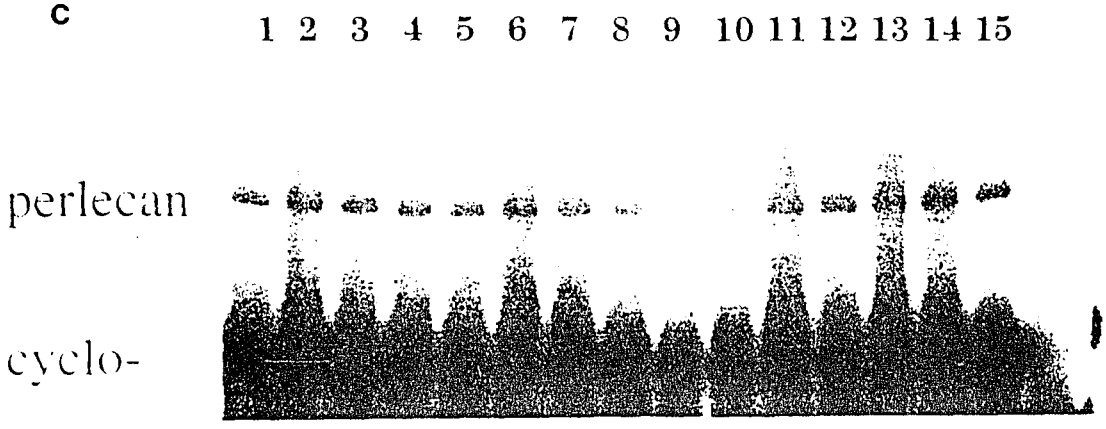
1 2 3 4 5 6 7 8 9 10 11 12 13 14 15
perlecan
cyclo-

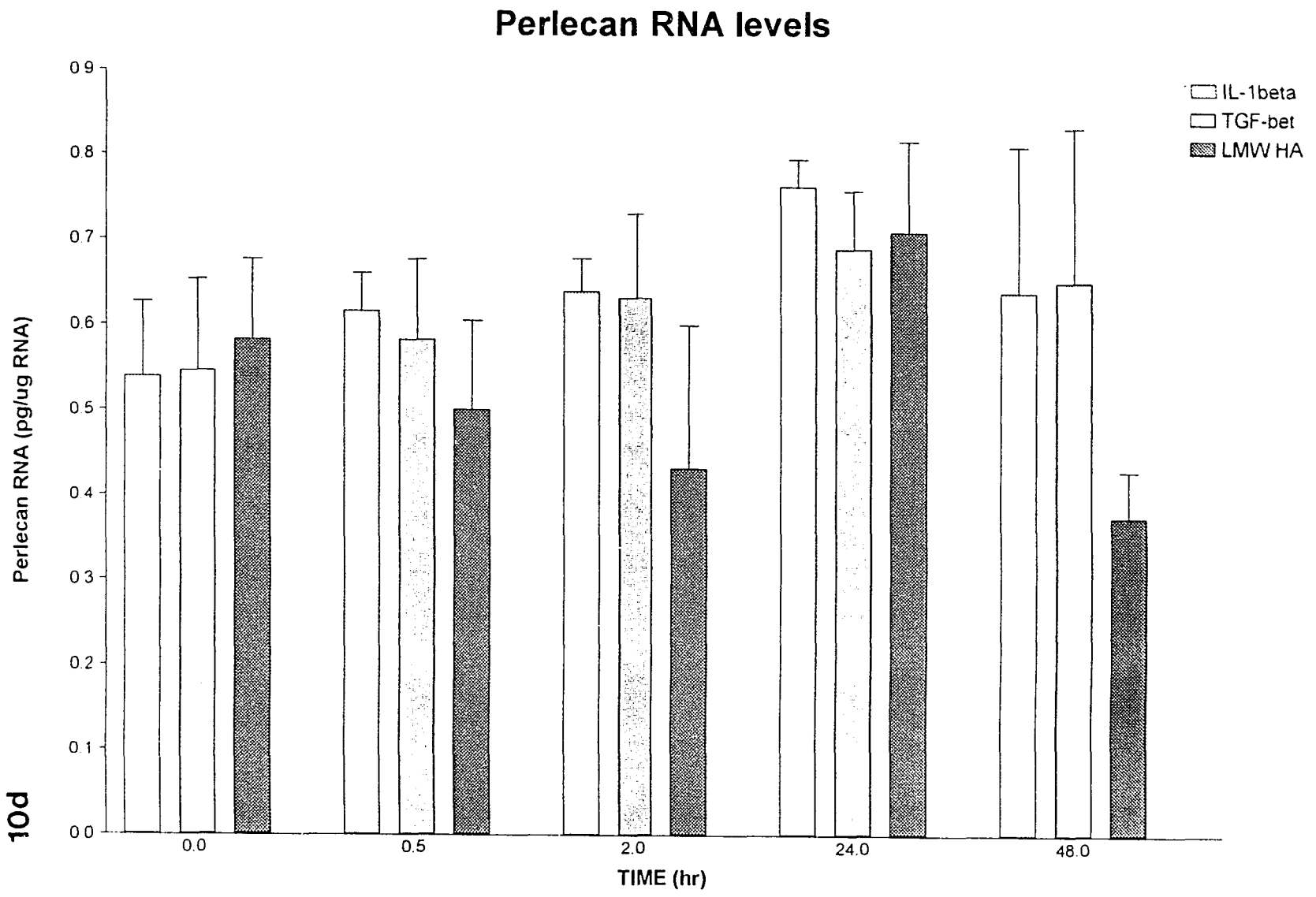
Perlecan RNA levels
IL-1beta
TGF-bet
LMW HA
Perlecan RNA (pg/ug RNA)
0.0
0.1
0.2
0.3
0.4
0.5
0.6
0.7
0.8
0.9
0.0
0.5
2.0
24.0
48.0
TIME (hr)

10d

Figure 11.DEAE-ion exchange chromatography of radiolabelled proteoglycans from metabolically MAE cells labelled with ^{14}C-glucosamine for control, and ^{3}H-glucosamine for cells treated with IL-1β (10 ng/ml) for 24 hours. Samples were loaded on a 10 ml column of DEAE-Sepharose CL-6B, and bound material was eluted with a 100 ml linear gradient of 0.15-1.0 M NaCl. Fractions of 1 ml were collected and analyzed by dual labelling scintillation counting. (a) cellular lysates (b) secreted pool.The absorbance (280 nm) tracing (Isco Absorbance detector) is included above to demonstrate the corresponding protein peaks.

11 a

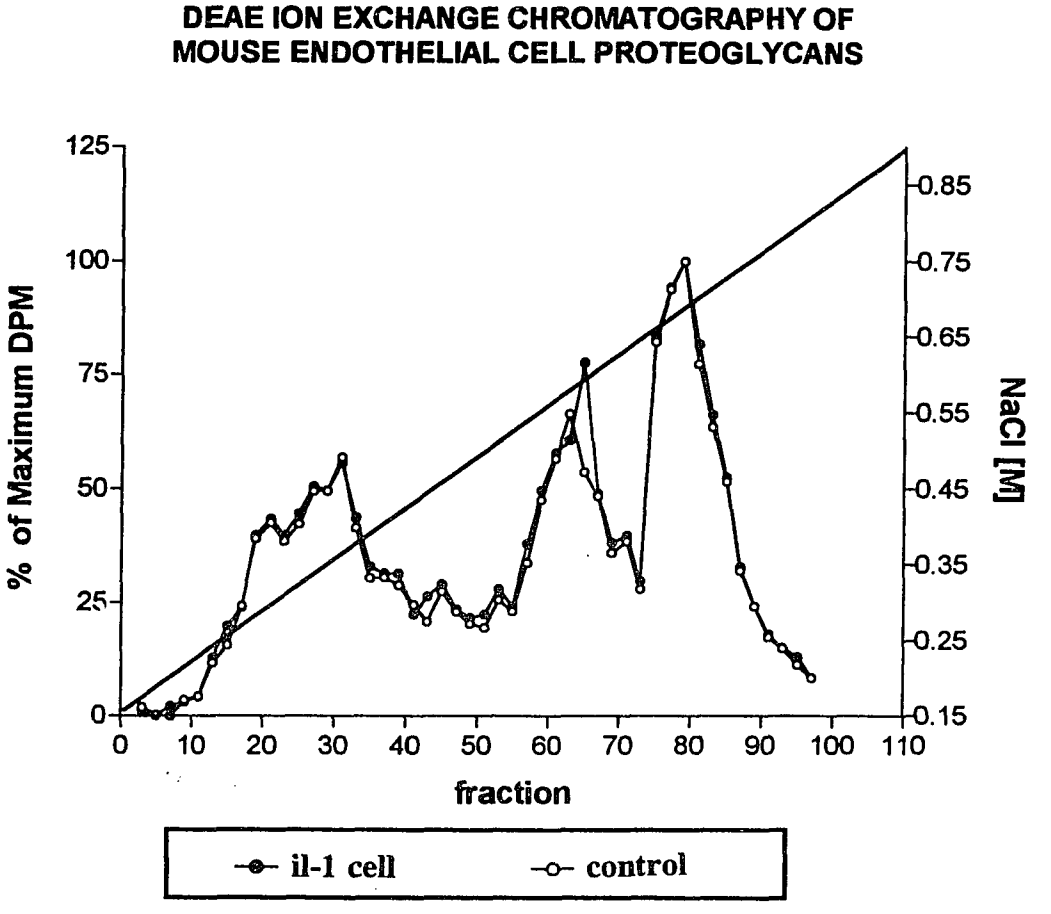
DEAE ION EXCHANGE CHROMATOGRAPHY OF
MOUSE ENDOTHELIAL CELL PROTEOGLYCANS
% of Maximum DPM
125
100
75
50
25
0
0
10
20
30
40
50
60
70
80
90
100
110
fraction
NaCl [M]
0.85
0.75
0.65
0.55
0.45
0.35
0.25
0.15
il-1 cell
control

11b

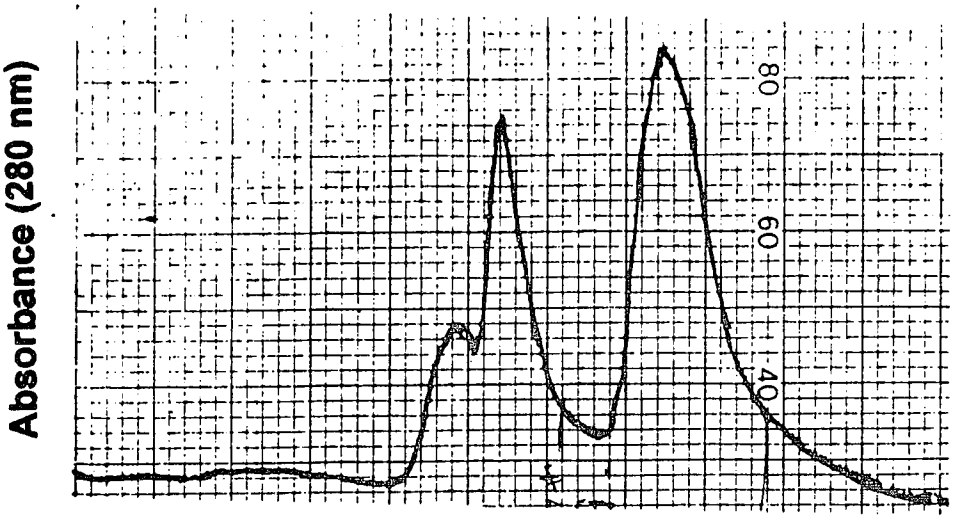

DEAE ION EXCHANGE CHROMATOGRAPHY OF
MOUSE ENDOTHELIAL CELL PROTEOGLYCANS

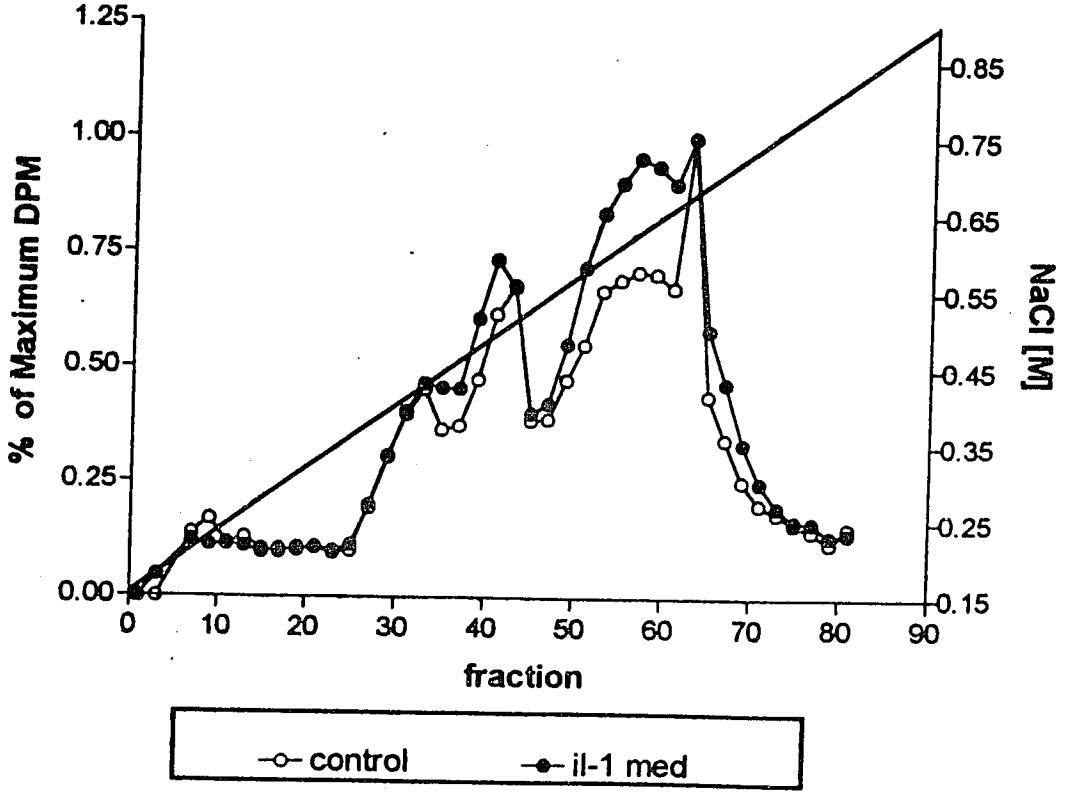

Figure 12. DEAE-ion exchange chromatography of radiolabelled proteoglycans from metabolically MAE cells labelled with ^{14}C-glucosamine for control, and ^{3}H-glucosamine for cells treated withTGF- β (5ng/ml) for 24 hours. Samples were processed exactly as in figure 11. (a) cellular proteoglycans (b) secreted.

12a

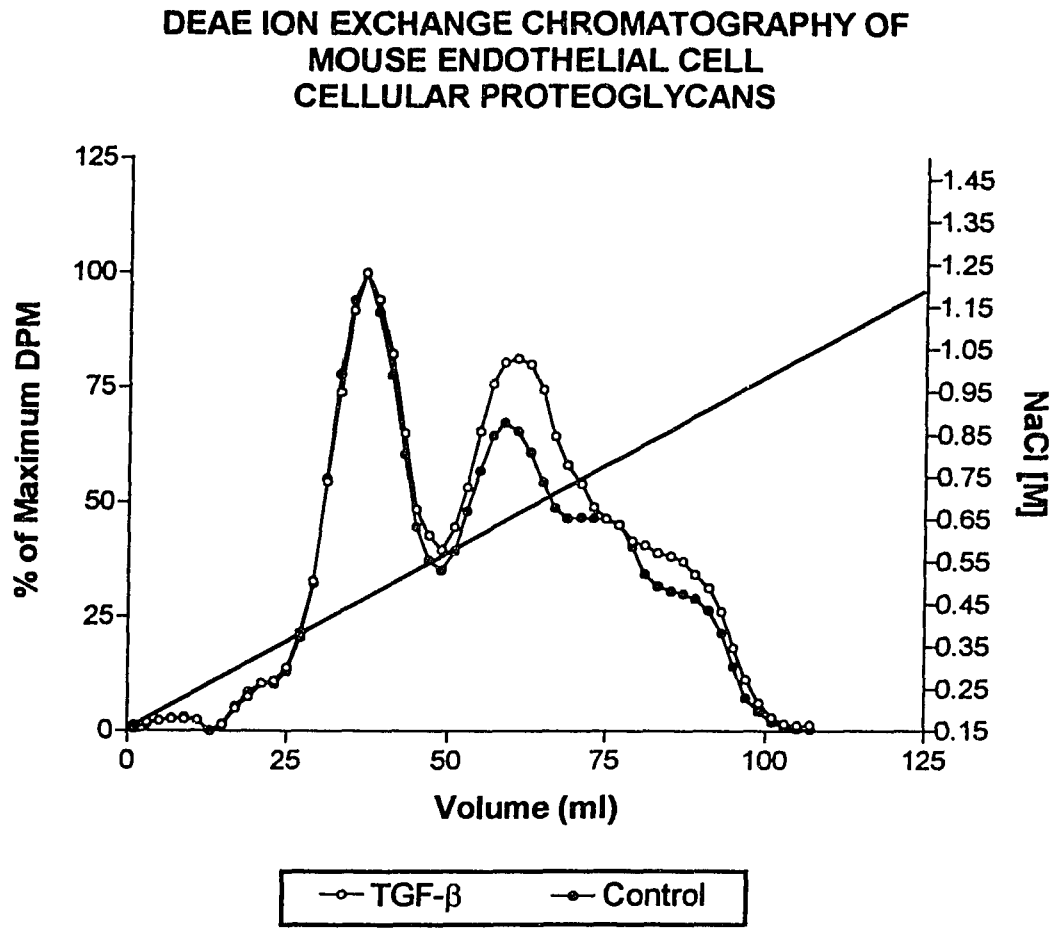
DEAE ION EXCHANGE CHROMATOGRAPHY OF
MOUSE ENDOTHELIAL CELL
CELLULAR PROTEOGLYCANS
% of Maximum DPM
125
100
75
50
25
0
0
25
50
75
100
125
Volume (ml)
NaCl [M]
1.45
1.35
1.25
1.15
1.05
0.95
0.85
0.75
0.65
0.55
0.45
0.35
0.25
0.15
TGF-β
Control

12b

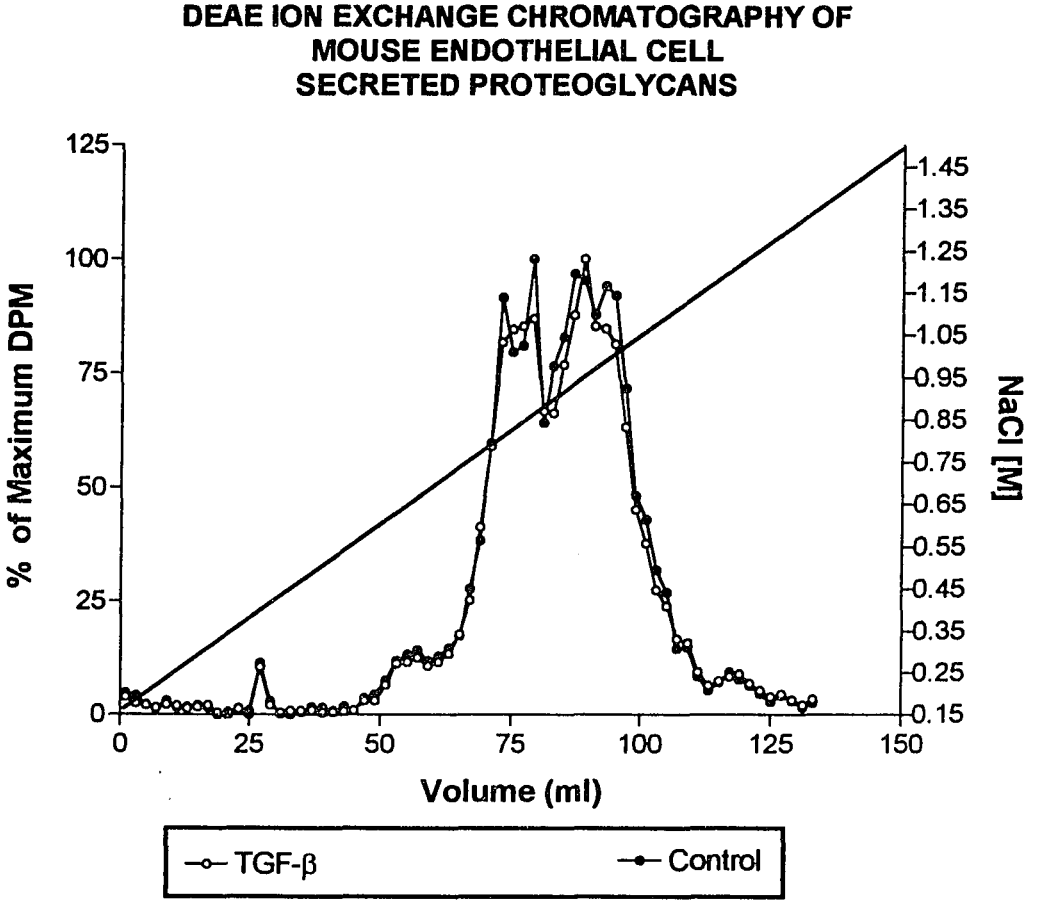
DEAE ION EXCHANGE CHROMATOGRAPHY OF
MOUSE ENDOTHELIAL CELL
SECRETED PROTEOGLYCANS
% of Maximum DPM
125
100
75
50
25
0
0
25
50
75
100
125
150
Volume (ml)
1.45
1.35
1.25
1.15
1.05
0.95
0.85
0.75
0.65
0.55
0.45
0.35
0.25
0.15
NaCl [M]
TGF-β
Control

Figure 13. DEAE-ion exchange chromatography of radiolabelled proteoglycans from metabolically MAE cells labelled with ^{14}C-glucosamine for control, and ^{3}H-glucosamine for cells treated with low molecular weight hyaluronic acid (1 μ g/ml). Samples were processed exactly as in figure 11. (a) cellular proteoglycans, (b) secreted proteoglycans.

13a

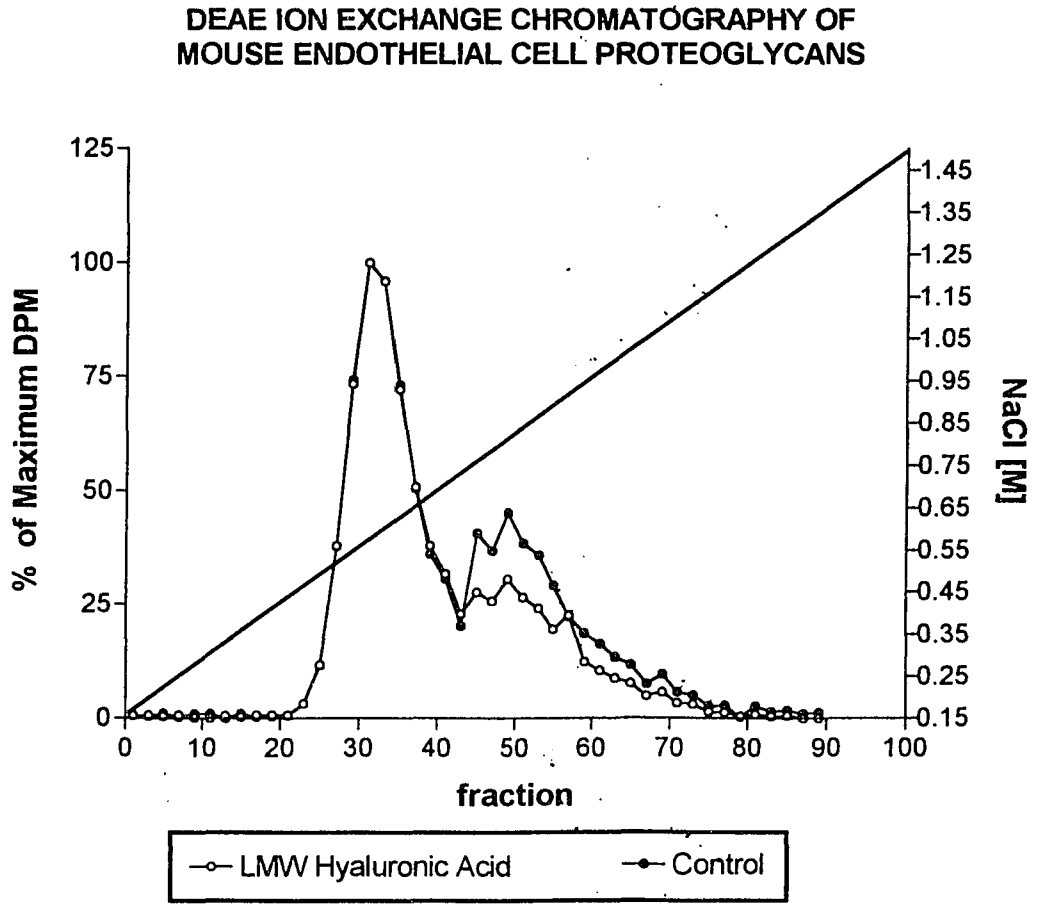
DEAE ION EXCHANGE CHROMATOGRAPHY OF
MOUSE ENDOTHELIAL CELL PROTEOGLYCANS
% of Maximum DPM
125
100
75
50
25
0
0
10
20
30
40
50
60
70
80
90
100
fraction
NaCl [M]
1.45
1.35
1.25
1.15
1.05
0.95
0.85
0.75
0.65
0.55
0.45
0.35
0.25
0.15
LMW Hyaluronic Acid
Control
DEAE.PZM:Graph-5 - Sat Jul 16 08:42:14 1994

13b

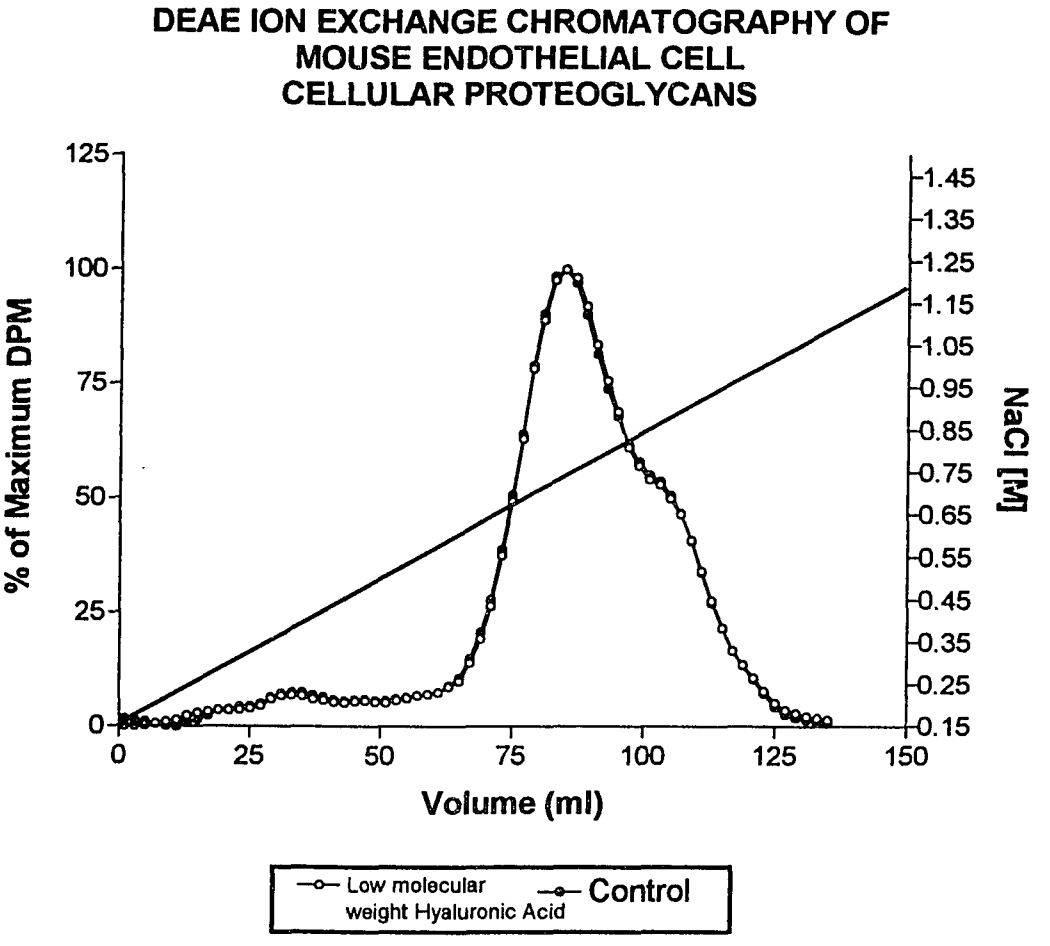
DEAE ION EXCHANGE CHROMATOGRAPHY OF
MOUSE ENDOTHELIAL CELL
CELLULAR PROTEOGLYCANS
% of Maximum DPM
125
100
75
50
25
0
0
25
50
75
100
125
150
Volume (ml)
NaCl [M]
1.45
1.35
1.25
1.15
1.05
0.95
0.85
0.75
0.65
0.55
0.45
0.35
0.25
0.15
Low molecular weight Hyaluronic Acid
Control

Figure 14. Gel filtration chromatography of GAG lyase digestions of pooled proteoglycan fractions.

Proteoglycan fractions from DEAE-ion exchange chromatography (Peak A and B) were pooled and submitted to enzymatic digestion of glycosaminoglycans using specific GAG lyases. Each peak as obtained by collecting fractions was submitted to digestion with heparitinase I, and III in combination, and chondroitinase ABC, each at a concentration of 100 mUnits/ml with PMSF to inhibit degradation, at 37 ^{o}C for 2 hours, and then the enzymes were inactivated by boiling for 5 minutes. Samples were then analyzed by gel filtration on Sepharose CL-4B. The column was equilibrated in 7M urea buffer, and the column flow rate was 11.6 ml/hr. Fractions (0.5 ml) were collected (2.58 min/fraction) and 0.25 ml of each fraction was counted in a scintillation counter. (a) Peak A proteoglycans are sensitive to chondroitinase ABC, and a chondroitin sulfate peak is evident eluting at a position that corresponds to low molecular weight material. Peak B proteoglycans are sensitive to heparitinase I, and III as evidenced by the peak representing heparan sulfate disaccharides.

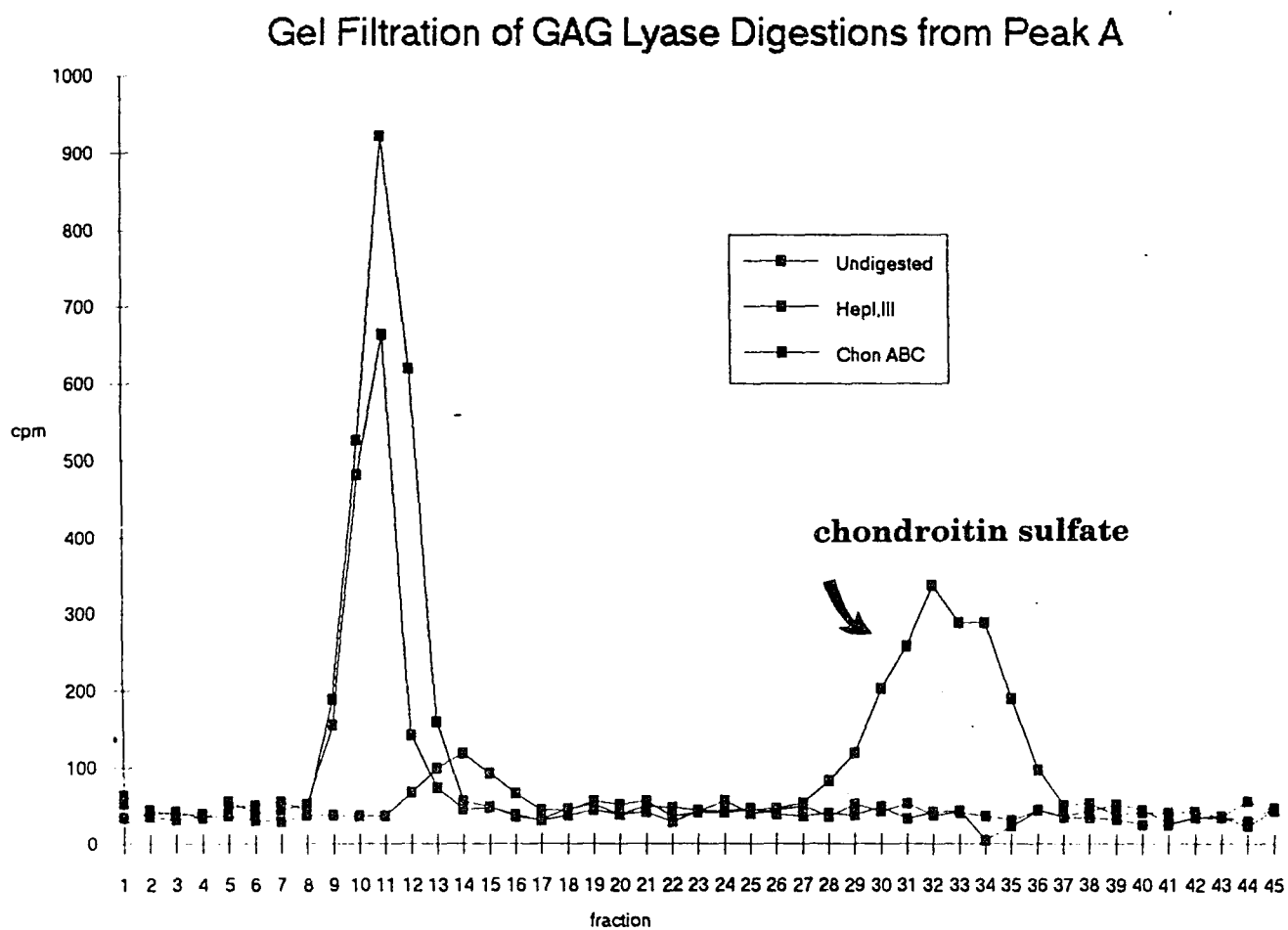
Gel Filtration of GAG Lyase Digestions from Peak A
cpm
1000
900
800
700
600
500
400
300
200
100
0
1 2 3 4 5 6 7 8 9 10 11 12 13 14 15 16 17 18 19 20 21 22 23 24 25 26 27 28 29 30 31 32 33 34 35 36 37 38 39 40 41 42 43 44 45
fraction
Undigested
HepI.III
Chon ABC
chondroitin sulfate

14a

Gel Filtration Chromatography of GAG Lyase Digestions of Peak B fractions

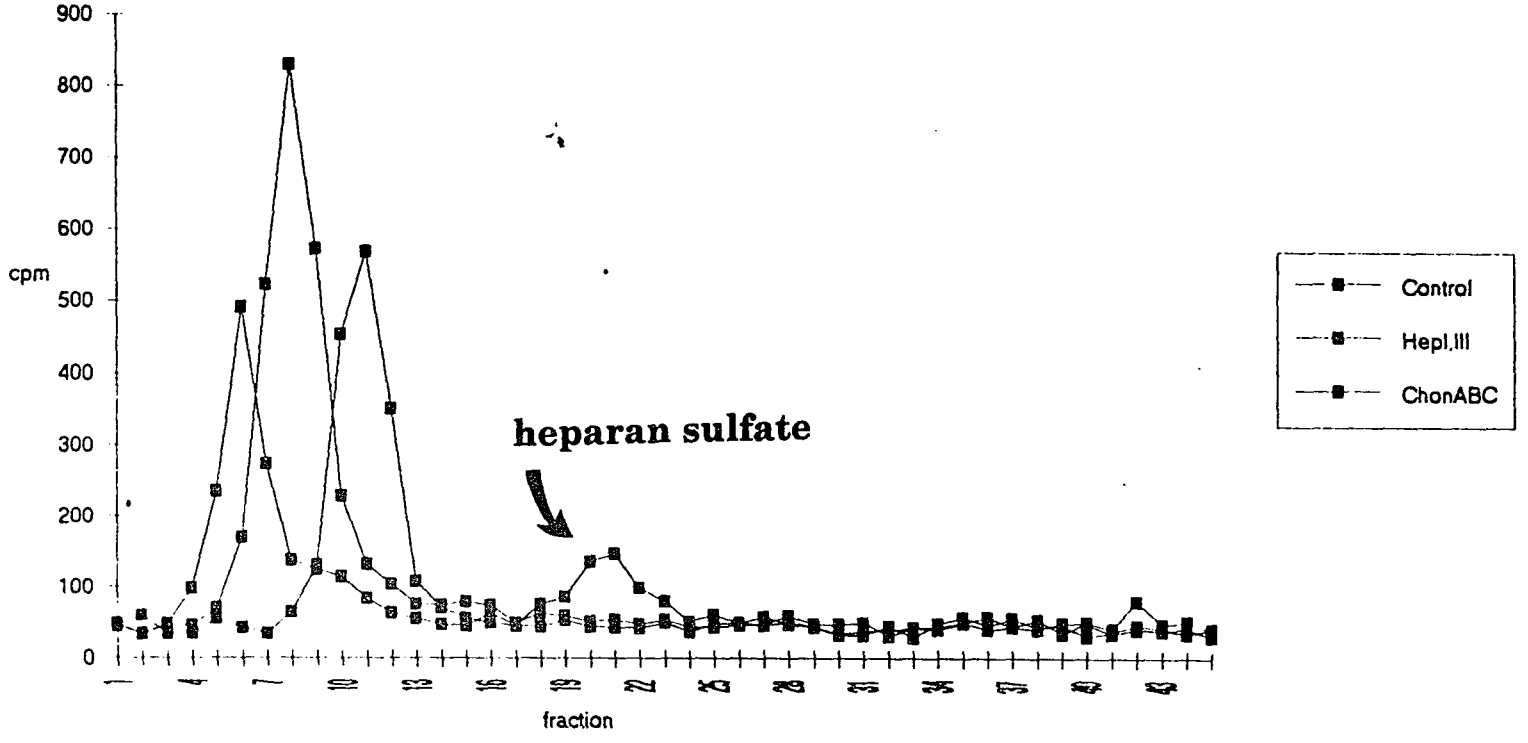

14b

Figure 15. Gel filtration chromatography on Sephadex G-150 of GAG chains chemically cleaved from the intact proteoglycans. Proteoglycan fractions from individual peaks of DEAE-ion exchange chromatography were pooled and GAG chains were reomoved with 1 M sodium borohydride (pH10) at 37 ^{o}C overnight. The material was dialyzed in H_2O, lyophilized and dissolved in PBS. Samples were then loaded on Sephadex G-150 (flow rate 10 ml/hr). Fractions (0.2ml) were collected and counted on scintillation counter.

Sephadex G-150 Gel Filtration Chromatography
of GAG chains chemically cleaved from protein cores

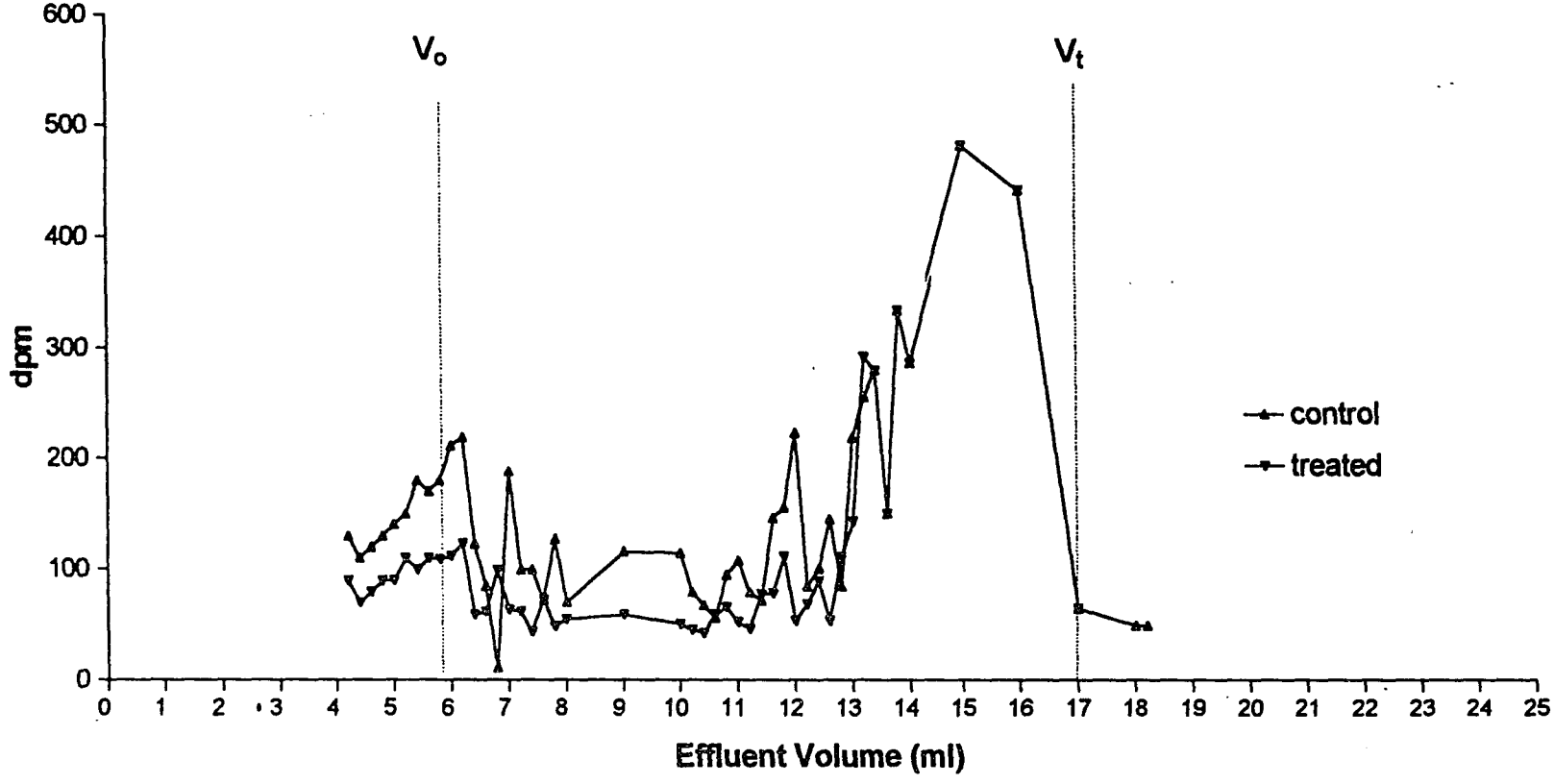

15a

Gel Filtration Chromatograpphpy (Sephadex G-150) of Glycosaminoglycans derived from Endothelial Cell Proteoglycans

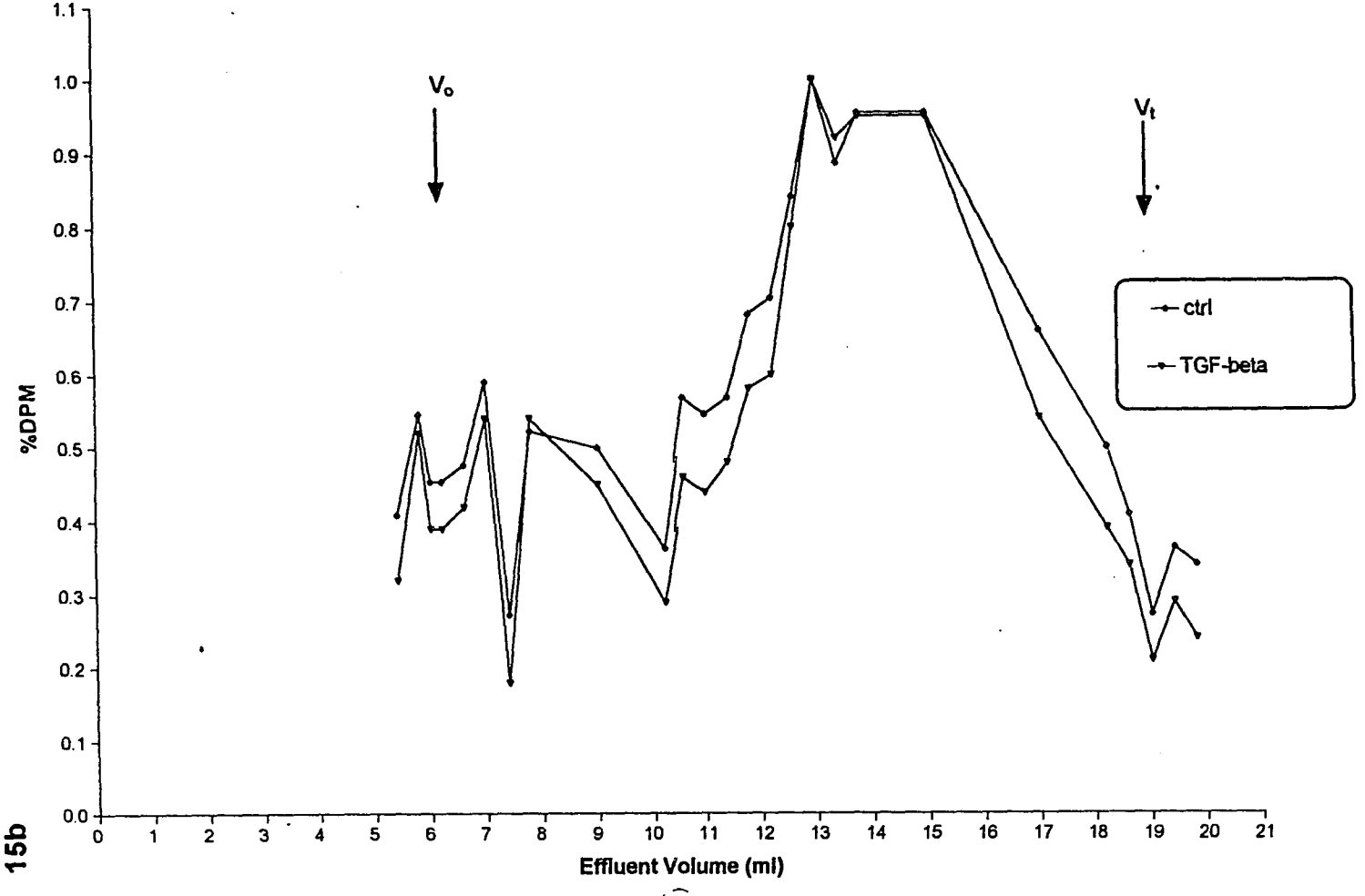

15b

Gel Filtration Chromatograpphpy (Sephadex G-150) of Glycosaminoglycans derived from Endothelial Cell Proteoglycans

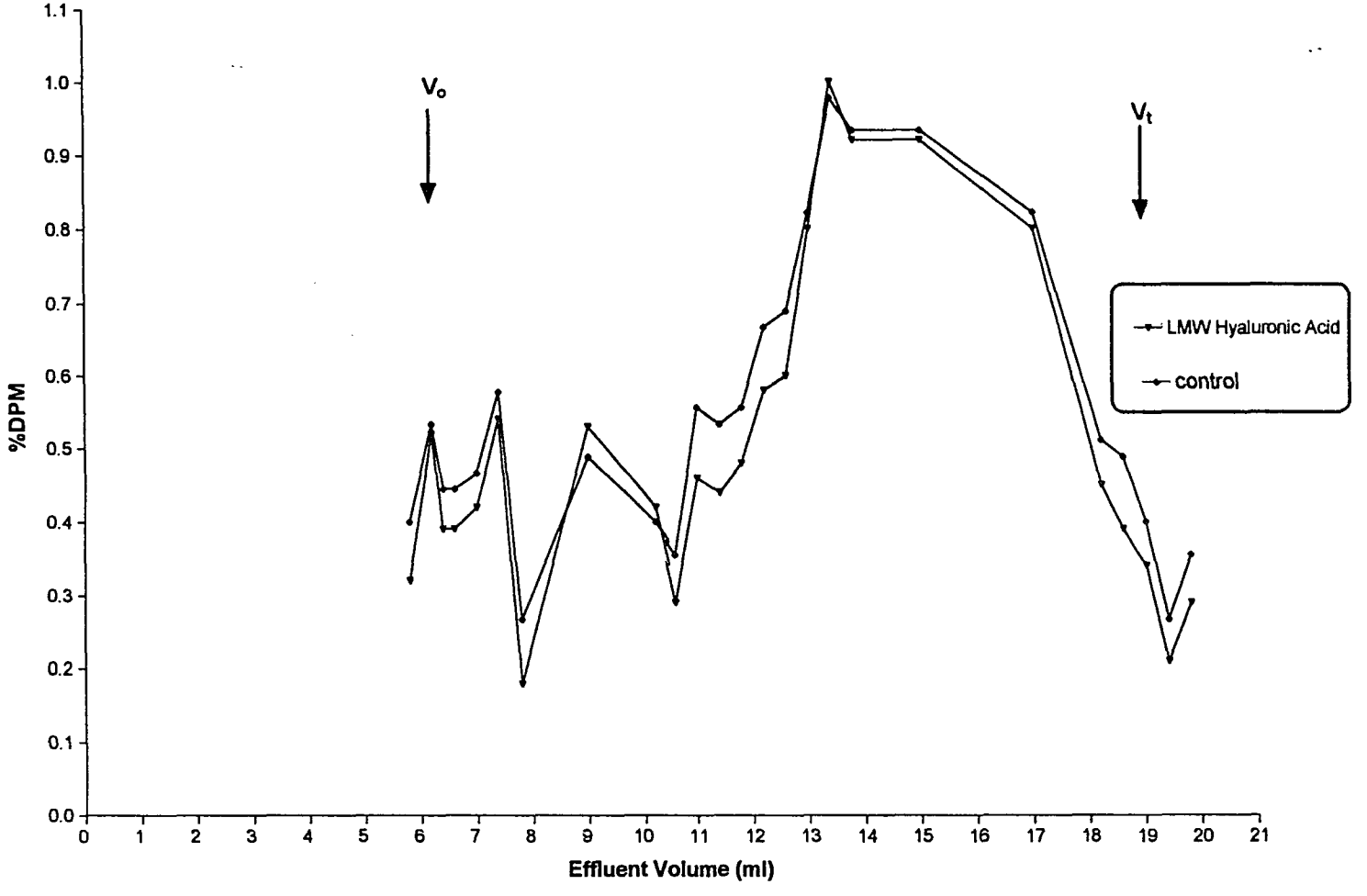

15c

Figure 16. A4 affinity chromatography of GAG chains derived from intact proteoglycans. One half of the sample of prepared GAGs (sodium borohydride cleavage of the GAG chains from the protein core) was used for A4 affinity chromatography. Samples were loaded on the A4 affinity column and eluted with a linear salt gradient (0.15 M-2.0 M NaCl). Fractions (0.5 ml) were collected and counted in a scintillation counter.

A4 Affinity Chromatography of Glycosaminoglycans derived from Endothelial Cells Treated with Interleukin-1β

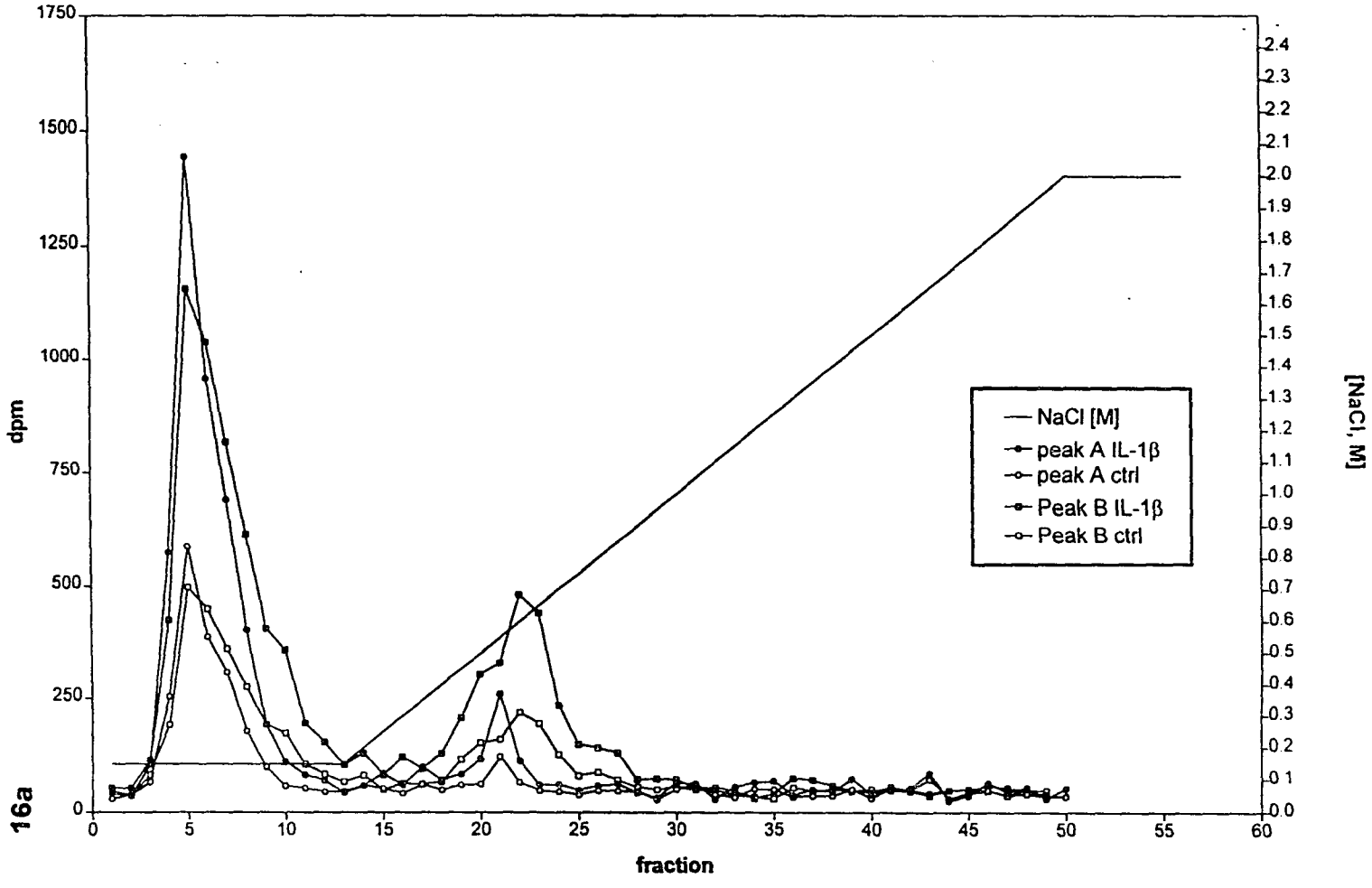

16a

A4 Affinity Chromatography of Glycosaminoglycans derived from Endothelial Cells Treated with Transforming Growth Factor-β

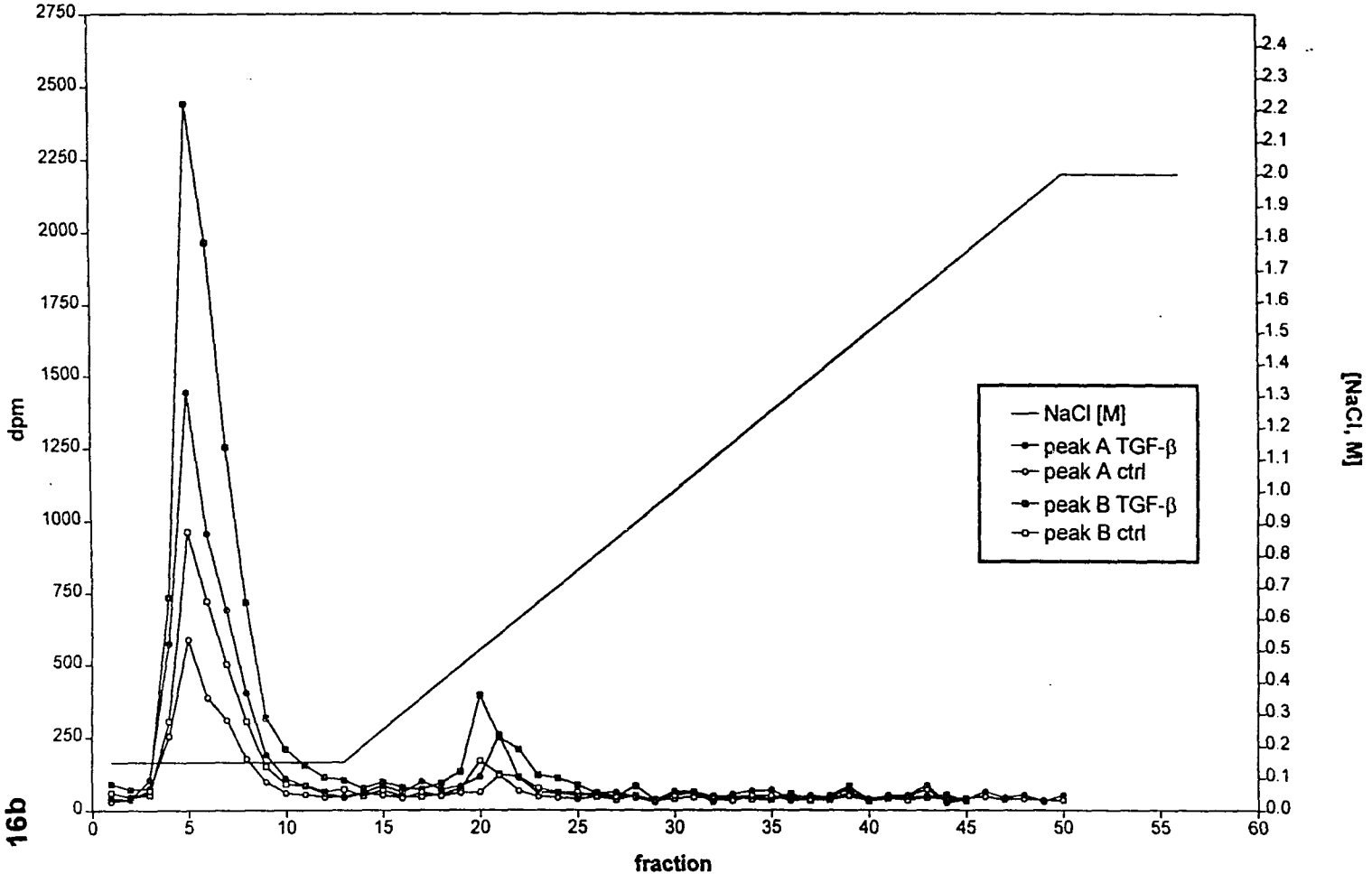

16b

A4 Affinity Chromatography of Glycosaminoglycans derived from Endothelial Cells Treated with Hyaluronic Acid (HA, low molecular weight)

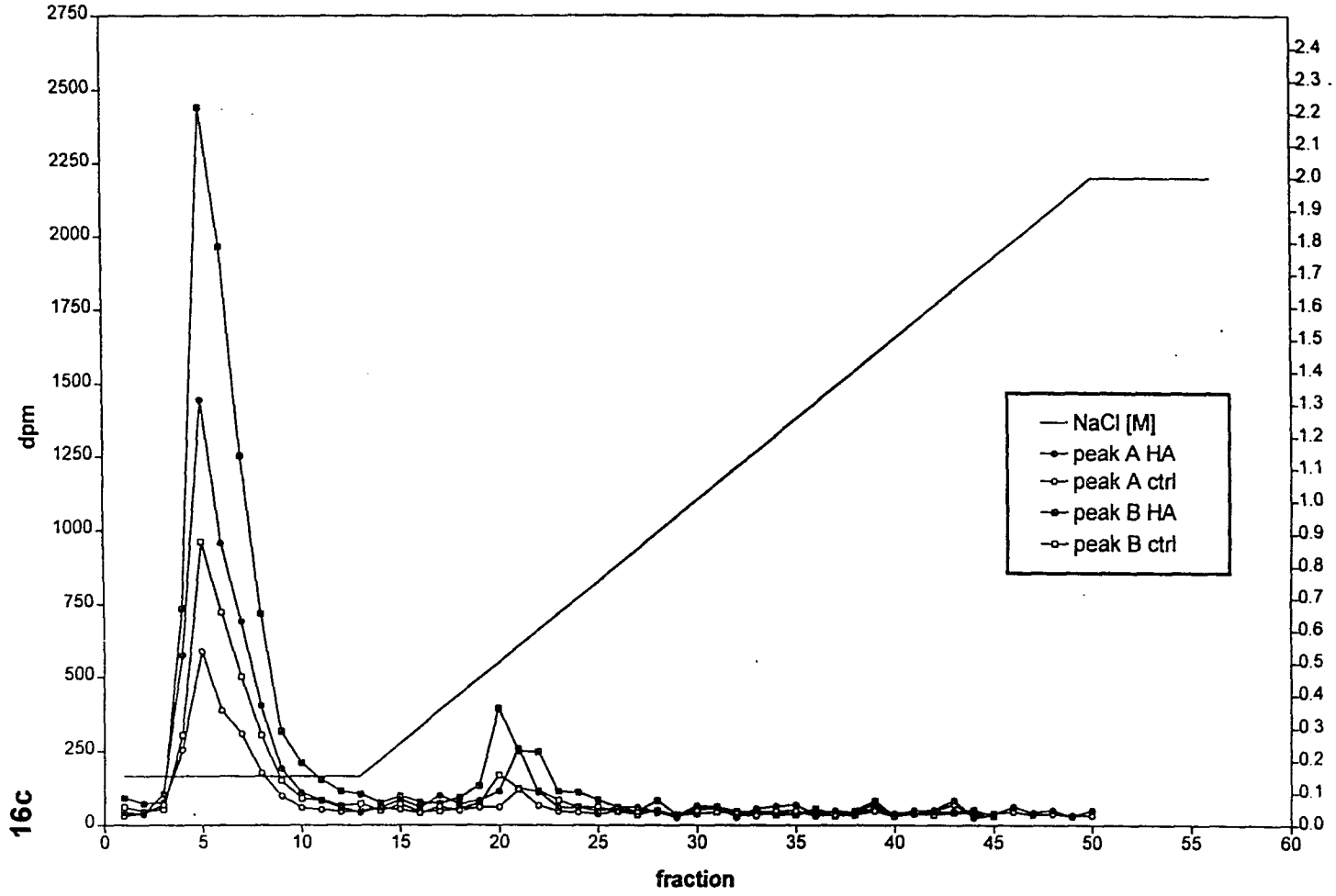

16c

References

1 Hascall VC: Proteoglycans:structure and function; in Ginsburg V (ed): Biology of Carbohydrates. New York, Wiley and Sons, 1981, pp 1

2 Kjellen L, Lindahl U: Proteoglycans: structures and interactions. Ann Rev Biochem 1991;60:443-475.

3 Nader HB, Ferreira TM, Toma L, et al: Maintenance of heparan sulfate structure throughout evolution:Chemical and enzymatic degradation, and ^{13}C-NMR-spectral evidence.. Carb Res 1988;184:292-300.

4 Bernfield M, Kokenyesi R, Kato M, et al: Biology of the Syndecans: A Family of Transmembrane Heparan Sulfate Proteoglycans. Annu Rev Cell Biol 1992;8:365-393.

5 Wagner WD: Proteoglycan structure and function as related to atherosclerosis; in Lee KT (ed): Ann. N. Y. Acad. Sci. New York, NY Acad. Sci., 1985, pp 52-68.

6 Kuettner KE, Kimura JH: Proteoglycans: An overview. J Cell Biol 1985;27:327

7 Poole AR: Proteoglycans in health and disease: structures and functions. Biochem J 1986;236:1-14.

8 Gallagher JT, Lyon M, Steward WP: Structure and function of heparan sulfate proteoglycans. Biochem J 1986;236:313-325.

9 Hassell JR, Kimura JH, Hascall VC: Proteoglycan core protein families. Ann Rev Biochem 1986;55:539-567.

10 Wight TN: Cell biology of arterial proteoglycans. Arteriosclerosis 1989;9:1-20.

11 Saksela O, Rifkin D: Release of Basic Fibroblast Growth Factor-Heparan Sulfate Complexes from Endothelial Cells by Plasminogen Activator-mediated Proteolytic Activity. The Journal of Cell Biology 1990;110:767-775.

12 Yayon A, Klagsbrun M, Esko J, et al: Cell Surface, Heparin-like Molecules are required for Binding of Basic Fibroblast Growth Factor to its High Affinity Receptor. Cell 1991;64:841-848.

13 Flaumenhaft R, Rifkin D: Extracellular matrix regulation of growth factor and protease activity. Current Opinion in Cell Biology 1991;3:817-823.

14 Saksela O, Moscatelli D, Sommer A, et al: Endothelial cell-derived heparan sulfate binds basic fibroblast growth factor and protects it from proteolytic degradation. J Cell Biol 1988;107:743-751.

15 Nurcombe V, Ford MD, Wildschut JA, et al: Developmental Regulation of Neural Response to FGF-1 and FGF-2 by Heparan Sulfate Proteoglycan. Science 1993;260:103-106.

16 Lee MK, Lander AD: Analysis of affinity and structureal selectivity in the binding of proteins to glycosaminoglycans: development of a sensitive electrophoretic approach.. P N A S 1994;88(7):2768-2772.

17 Ruoslahti E, Yamaguchi Y: Proteoglycans as modulators of growth factor activities. Cell 1991;64:867-869.

18 Nietfeld JJ: Cytokines and proteoglycans. Experientia 1993;49:456-469.

19 Kemeny E, Fillit HM, Damle SP, et al: Monoclonal antibodies to heparan sulfate proteoglycan : development and application to the study of normal tissue and pathologic human kidney biopsies. Conn Tiss Res 1988;18:1-12.

20 Mohan PS, Spiro RG: Characterization of heparan sulfate proteoglycan from calf lens capsule and proteoglycans synthesized by cultured lens epithelial cells. J Biol Chem 1991;266:8567-8575.

21 Hassell JR, Leyshon WC, Ledbetter SR, et al: Isolation of two forms of basement membrane proteoglycans. J Biol Chem 1985;260:8098-9105.

22 Klein DJ, Brown DM, Oegema TR, et al: Glomerular Basement Membrane Proteoglycans are Derived from a Large Precursor. J Cell Biol 1988;106:963-970.

23 Parthasarathy N, Spiro RG: Isolation and characterization of the heparan sulfate proteoglycan of the bovine glomerular basement membrane. J Biol Chem 1984;259:12749-12755.

24 Kato M, Koike Y, Ito Y, et al: Mulitple Forms of Heparan Sulfate Proteoglycans in the Engelbreth-Holm-Swarm Mouse Tumor. The Journal of Biological Chemistry 1987;262,No.15,May 25:7180-7188.

25 Jackson RL, Busch SJ, Cardin AD: Glycosaminoglycans: Molecular properties, protein interactions, and role in physiological processes. Physiol Rev 1991;71:481-539.

26 Kanwar YS, Farquhar MG: Role of glycosaminoglycans in permeability of glomerular basement membrane. Fed Proc 1980;39:334

27 Kanwar YS, Linker A, Farguhar MG: Increased permeability of glomerular basement membrane to ferritin after removal of glycosaminoglycans (heparan sulfate) by enzyme digestion. J Cell Biol 1980;86:688

28 Mynderse LA, Hassell JR, Kleinman HK, et al: Loss of heparan sulfate proteoglycan from glomerular basement of nephrotic rats. Lab Invest 1983;48:292-302.

29 Sasisekharan S, Moses M, Nugent M, et al: Heparinase inhibits neovascularization. Proc Natl Acad Sci USA 1994;91:1524-1528.

30 Hynes RO, Lander AD: Contact and Adhesive Specificities in the Associations, Migrations, and Targetting of Cells and Axons. Cell 1992;68:303-322.

31 Dow KE, Riopelle RJ, Kisilevsky R: Domains of neuronal heparan sulfate proteoglycans involved in neurite growth on laminin. Cell Tissue Res 1991;265:345-351.

32 Noonan DM, Fulle A, Valente P, et al: The complete sequence of perlecan, a basement membrane heparan sulfate proteoglycan, reveals extensive similarity with laminin A chain, low density lipoprotein-receptor, and the neural cell adhesion molecule. J Biol Chem 1991;266:22939-22947.

33 Letourneau P, Condic M, Snow D: Interactions of Developing Neurons with the Extracellular Matrix. the journal of neuroscience 1994;14(3):915-928.

34 Halfter W: A Heparan Sulfate Proteolgycan in Developing Avian Axonal Tracts. Journal of Neuroscience 1993;7:2863-2873.

35 Hascall VC, Kimura JH: Proteoglycans: isolation and characterization; in Cunningham LW, Frederiksen DW (eds): Methods in Enzymology. New York, Academic Press, 1982, pp 769-800.

36 Hassell JR, Gehron-Robey P, Barrach H-., et al: Isolation of a heparan-sulfate proteoglycan from basement membrane. Proc Natl Acad Sci 1980;77:4494-4498.

37 Stow JL, Farquhar MG: Distinctive Populations of Basement Membrane and Cell Membrane Heparan Sulfate Proteoglycans are Produced by Cultured Cell Lines. The Journal of Cell Biology 1987;105:529-539.

38 van den Heuvel L, van den Bom J, van de Velden T, et al: Isolation and partial characterization of heparan sulfate proteoglycan from the human glomerular basement membrane. Biochem J 1989;264:457-465.

39 Miettinen A, Stow JL, Mentone S, et al: Antibodies to basement membrane heparan sulfate proteoglycans bind to the laminae rarae of the glomerular basement membrane (GBM) and induce subepithelial GBM thickening. J Exp Med 1986;163:1064-1084.

40 Parthasarathy N, Spiro RG: Characterization of the glycosaminoglycan component of the renal glomerular basement membrane and its relationship to the peptide portion. J Biol Chem 1981;674:96

41 Rubin E, Farber JL: Pathology. Lippincott Comp., Philadephia. 1988.

42 Nitsch RM, Slack BE, Farber SA, et al: Receptor-coupled Amyloid Precursor Protein Processing. Ann.N.Y.Acad.Sci. 1994;122-127.

43 Pober J: Cytokine-Mediated Activation of Vascular Endothelium: Physiology and Pathology. American Journal of Pathology 1988;133,No.3,Dec.:426-450.

44 Rothwell N, Relton J: Involvement of Cytokines in Acute Neurodegeneration in the CNS. Neuroscience and Biobehavioral Reviews 1993;17:217-227.

45 McGeer PL, Akiyama H, Itagaki S, et al: Immune system response in Alzheimer's disease. Can J Neurol Sci 1989;16:516-527.

46 Selkoe DJ: Molecular Pathology of Amyloidogenic Proteins and the Role of Vascular Amyloidosis in Alzheimer's Disease.. Neurobiology of Aging 1989;10:387-395.

47 Bartfai T, Schultzberg M: Cytokines in Neuronal Cell Types. Neurochem Int 1993;22,No.5:435-444.

48 Nathan C, Spom M: Cytokines in context. J Cell Biol 1991;113:981-986.

49 Berkenbosch F, Robakis N, Blum M: IL-1 in the central nervous system: a role in the acute phase response and in brain injury, brain development and the pathogenesis of Alzheimer's disease; in Frederickson RCA, McGaugh JL, Felten DL (eds): Peripheral signaling of the brain. Role in neural-immune interactions, leaming and memory. Toronto, Hogrefe & Huber Publ., 1991, pp 131-145.

50 Jarvelainen H, Kinsella M, Wight T, et al: Differential Expression of Small Chondroitin/Dermatan Sulfate Proteoglycans, PG-I/Biglycan and PG-II/Decorin, by Vascular Smooth Muscle and Endothelial Cells in Culture. The Journal of Biological Chemistry 1991;266,No.34:23274-23281.

51 Jackson RL, Busch SJ, Cardin AD: Glycosaminoglycans: Molecular properties, protein interactions, and role in physiological processes. Physiol Rev 1991;71:481-539.

52 Chakrabarti B, Park JW: Glycosaminoglycans: structure and function. CRC Crit Rev Biochem 1980;8:225-313.

53 Margolis RK, Margolis RU: Structure and distribution of glycoprotein and glycosaminoglycans; in Margolis RU, Margolis RK (eds): Complex cabohydrates of nervous tissue. New York, Plenum Press, 1979, pp 45-72.

54 Bignami A, Hosley M, Dahl D: Hyaluronic acid and hyaluronic acid-binding proteins in brain extracellular matrix. Anat Embryol Berl 1993;188:419-433.

55 West D, Hampson I, Arnold F, et al: Angiogenesis Induced by Degradation Products of Hyaluronic Acid. Science 1985;228:1324-1326.

56 West D, Kumar S: The Effect of Hyaluronate and its Ologosaccharides on Endothelial Cell Proliferation and Monolayer Integrity. Experimental Cell Research 1989;183:179-196.

57 Rooney P, Wang M, Kumar P, et al: Angiogenic oligosaccharides of hyaluronan enhance the production of collagens by endothelial cells. Journal of Cell Science 1993;105:213-218.

58 Banks WA, Kastin AJ: Aluminum increases permeability of the blood-brain barrier to labelled DSIP and beta-endorphin: possible implications for senile and dialysis dementia. Lancet 1983;ii:1227-1229.

59 Hardy J, Adolfsson R, Alafuzoff I, et al: Transmitter deficits in Alzheimer's disease. Neurochem Int 1985;7:545-563.

60 Bondareff W, Mountjoy CQ, Roth M: Loss of neurons of origin of the adrenergic projection to cerebral cortex (nucleus locus ceruleus). Neurology 1982;32:164-168.

61 Kidd M: Alzheimer's disease. An electronmicroscope study. Brain 1964;87:307-327.

62 Gottfries CG: Alzheimer's Disease: a critical review. Compr Gerontol 1988;2:47-62.

63 Selkoe DJ: The molecular pathology of Alzheimer's disease. Neuron 1991;6:487-498.

64 Abraham CR, Selkoe DJ, Potter H: Immunochemical identification of the serine protease inhibitor alpha-one antichymotrypsin in the brain amyloid deposits of Alzheimer's disease. Cell 1988;52:487-501.

65 Selkoe D: Biochemistry of altered brain proteins in Alzheimer's disease. Ann Rev Neurosci 1989;12:463-490.

66 Hefti F, Mash DC: Localization of NGF receptors in the normal human brain and in Alzheimer's disease. Neurobiology of Aging 1989;10:75-87.

67 Mufson EJ, Bothwell M, Kordower JH: Loss of NGF receptor containing neurons in Alzheimer's disease: a quantitative analysis across subregions of basal forebrain. Exp Neurol 1989;105:221-232.

68 Woolf NJ, Gould E, Butcher LL: NGF receptor is associated with cholinergic neurons of the basal forebrain but not the pontomesencephalon. Neuroscience 1989;30:143-152.

69 Katoh-Semba R, Oohira A, Kashiwamata S: Nerve growth factor-induced changes in the structure of sulfated proteoglycans in PC12 pheochromocytoma cells. J Neurochem 1992;59:282-289.

70 Hof PR, Cox K, Morrison JH: Quantiative analysis of a vulnerable subset of pyramidal neurons in Alzheimer's disease. I. Superior frontal and inferior temporal cortex. J Comp Neurol 1990;301:44-54.

71 Homer WG, Dickson DW, Gleeson J, et al: Regional Synaptic Pathology in Alzheimer's Disease.. Neurobiology of Aging 1992;13:375-382.

72 Perlmutter LS, Barron E, Saperia D, et al: Association between vascular basement membrane components and the lesions of Alzheimer's disease. J Neurosci Res 3092;1991:673-681.

73 Buee L, Hof PR, Bouras C, et al: Pathological alterations of the cerebral microvasculature in Alzheimer's disease and related dementing disorders. Acta Neuropathol 1994;87:469-480.

74 Stow JL, Sawada H, Farquhar MG: Basement membrane heparan sulfate proteoglycans are concentrated in the laminae rarae and in podocytes of the rat renal glomerulus. Proc Natl Acad Sci 1985;82:3296

75 Kang J, Lemaire HG, Unterbeck A, et al: The precursor of Alzheimer's disease amyloid A4 protein resembles a cell-surface receptor. Nature 1987;325:733-736.

76 Bauer J, Ganter U, Strauss S, et al: The participation of IL-6 in the pathogenesis of Alzheimer's disease. Res Immunol 1992;143:650-657.

77 Sisodia SS, Koo EH, Beyreuther K, et al: Evidence that b-amyloid protein in Alzheimer's disease is not derived by normal processing. Science 1990;248:492-495.

78 Selkoe DJ, Abraham CR, Podlisny MB, et al: Isolation of low molecular weight proteins from amyloid plaques fibres in Alzheimer's disease. J Neurochem 1986;45:1820-1834.

79 Glenner GC, Wong CW: Alzheimer's disease: initial report of the purification and characterization of a novel cerebrovascular amyloid protein. Biochem Biophys Res Comun 1984;120:885-890.

80 Kalaria R: The Blood-Brain Barrier and Cerebral Microcirculation in Alzheimer Disease. Cerebrovascular and Brain Metabolism Reviews 1992;4:226-260.

81 Snow AD, Wight TN: Proteoglycans in the pathogenesis of Alzheimer's disease and other amyloidoses. Neurobiol Aging 1989;10:481-497.

82 Snow A, Bramson R, Henderson M, et al: A Temporal and Ultrastructural Relationship Between Heparan Sulfate Proteoglycans and AA Amyloid in Experimental Amyloidosis. The Journal of Histochemistry and Cytochemistry 1991;39,No.10:1321-1330.

83 Crutcher K, Anderton B, Barger S, et al: Cellular and Molecular Pathology in Alzheimer's Disease. Hippocampus 1993;3,Special Issue:271-288.

84 Kisilevsky R: Proteoglycans, glycosaminoglycans, amyloid-enhancing factor, and amyloid deposition. J Int Med 1992;232:515-516.

85 Snow AD, Bramson R, Mar H, et al: A temporal and ultrastructural relationship between heparan sulfate proteoglycans and AA amyloid in experimental amyloidosis. J Histochem Cytochem 1991;399999:1321-1330.

86 Snow AD, Kisilevsky R: Temporal relationship between glycosaminoglycan accumulation and amyloid deposition during experimental amyloidosis. Lab Invest 1985;53:37-44.

87 Kisilevsky R: Heparan sulfate proteoglycans in amyloidogenesis: an epiphenomenon, a unique factor, or the tip of a more fundamental process?. Lab Invest 1990;63:589-591.

88 Suzuki K, Katzman R, Korey S: Chemical studies on Alzheimer's disease. J Neuropathol Exp Neurol 1965;141:211-222.

89 Brandan E, Inestrosa N: Extracellular Matrix Components and Amyloid in Neuritic Plaques of Alzheimer's Disease. Gen Pharmac 1993;24,No.5:1063-1068.

90 Perry G, Siedlak SL, Richey P, et al: Association of heparan sulfate proteoglycan with the neurofibrillary tangles of Alzheimer's disease. J Neurosci 1991;11:3679-3683.

91 Snow AD, Willmer J, Kisilevsky R: Sulfated glycosaminoglycans:a common constituent of all amyloids?. Lab Invest 1987;56:120-123.

92 Snow AD, Willmer JP, Kisilevsky R: Sulfated glycosaminoglycans in Alzheimer's disease. Human Pathol 1987;18:506-510.

93 Siedlak SL, Cras P, Kawai M, et al: Basic fibroblast growth factor binding is a marker for extracellular neurofibrillary tangles in Alzheimer disease. J Histochem Cytochem 1991;39:899-904.

94 Perry G, Richey P, Siedlak SL, et al: Basic fibroblast growth factor binds to filamentous inclusions of neurodegenerative diseases. Brain Res 1992;579:3350-352.

95 Kisilevsky R: Theme and variations on a string of amyloid. Neurobiol Aging 1989;10:499-500.

96 Narindrasorasak S, Lowery D, Altman RA, et al: Characterization of high affinity binding between laminin and Alzheimer's disease amyloid precursor proteins. Lab Invest 1992;67:643-652.

97 Buee L, Ding W, Delacourte A, et al: Binding of secreted human neuroblastoma proteoglycans to the Alzheimer amyloid A4 peptide. Brain Res 1992;in press:

98 Buée L, Ding W, Delacourte A, et al: Binding of secreted neuroblastoma proteoglycans to the Alzheimer's amyloid A4 peptide. Brain Res 1993;601:154-163.

99 Fillit H, Lahita R: Antibodies to vascular heparan sulfate proteoglycan in patients with systemic lupus erythematosus. Autoimmunity 1991;9:159-164.

100 Dziadek M, Fujiwara S, Paulsson M, et al: Immunological characterization of basement membrane types of heparan sulfate proteoglycan. EMBO J 1985;4:905-912.

101 Ledbetter S, Tyree B, Hassell J, et al: Identification of the Precursor Protein to Basement Membrane Heparan Sulfate Proteoglycans. The Journal of Biological Chemistry 1985;260,No.13,July5:8106-8113.

102 Laemmli UK: Cleavage of structural proteins during the assembly of the head of bacteriophage T4. Nature 1970;227:680-685.

103 Snow A, Mar H, Nochlin D, et al: Early Accumulation of Heparan Sulfate in Neurons and in the Beta-amyloid Protein-containing Lesions of Alzheimer's Disease and Down's Syndrome. American Journal of Pathology 1990;137,No.5:1253-1270.

104 Perlmutter LS, Chui HC: Microangiopathy, the vascular basement membrane and Alzheimer's disease: a review. Brain Res Bull 1990;24:677-686.

105 Mancardi GL, Perdelli F, Rivano C, et al: Thickening of the basement membrane of cortical capillaries in Alzheimer's disease. Acta Neuropathol 1980;49:79-85.

106 Van Hoesen GW, Hyman BT, Damasio AR: Entorhinal Cortex Pathology in Alzheimer's Disease.. Hippocampus 1991;1:1-8.

107 Lippa CF, Hamos JE, Pulaski-Salo D, et al: Alzheimer's Disease and Aging: Effects on Perforant Pathway Perikarya and Synapses. Neurobiology of Aging 1992;13:405-411.

108 Bouras C, Hof PR, Morrison JH: Neurofibrillary tangle densities in the hippocampal formation in a non-demented population define subgroups of patients with differential early pathologic changes.. Neuroscience Letters 1993;153:131-135.

109 Vickers JC, Delacourte A, Morrison JH: Progressive transformation of teh cytoskeleton associated with normal aging and Alzheimer's disease.. Brain Res 1992;594:273-278.

110 Sambrook J, Fritsch EF, Maniatis T: Molecular Cloning: A Laboratory Manual. Cold Spring Harbor Laboratory Press, 1989.

111 Rothwell NJ: Functions and mechanisms of interleukin-1 in the brain. TIPS 1991;12:430-436.

112 Dinarello CA: Bioloy of interleukin 1.. FASEB J 1988;2:108-115.

113 Edge A, Faltynek C, Hof L, et al: Deglycosylation of Glycoproteins by Trifluoromethanesulfonic Acid. Analytical Biochemistry 1981;118:131-137.

114 Heinegard D, Bjorne-Persson A, Coster L, et al: The core proteins of large and small interstitial proteoglycans from various connective tissues form distinct subgroups. Biochem J 1985;230:181-194.

115 Kinsella MG, Wight TN: Structural characterization of heparan sulfate proteoglycan subclassess isolated from bovine aortic endothelial cell cultures. Biochemistry 1988;27:2136-2144.

116 Oohira A, Wight TN, Bornstein P: Sulfated Proteoglycans Synthesized by Vascular Endothelial Cells in Culture. The Journal of Biological Chemistry 1983;258:2014-2021.

117 Buee L, Ding W, Anderson JP, et al: Binding of vascular heparan sulfate proteoglycan to Alzheimer's amyloid precursor protein is mediated in part by the N-terminal region of A4 peptide. Brain Res 1993;627:199-204.

118 Snow A, Sekiguchi R, Nochlin D, et al: An important role of heparan sulfate proteoglycan (perlecan) in a model system for the deposition and persistence of fibrillar AB-Amyloid in rat brain. Neuron 1994;12:219-234.

119 Narindrasorasak S, Lowery D, Gonzalez-DeWhitt P, et al: High affinity interactions between the Alzheimer's beta amyloid precursor proteins and the basement membrane form of heparan sulfate proteoglycan. J Biol Chem 1991;266:12878-12883.

120 Templeton D: Protegylcans in Cell Regulation. Critical Reviews in Clinical Laboratory Sciences 1992;29(2):141-184.

121 Small DH, Nurcombe V, Moir R, et al: Association and Release of the Amyloid Precusror of Alzheimer's Disease from Chick Brain Extracellular Matrix.. Journal of Neuroscience 1992;12:4143-4150.

122 Wong CW, Quaranta V, Glenner GG: Neuritic plaques and cerebrovascular amyloid in Alzheimer disease are antigenically related. Proc Natl Acad Sci 1985;82:8729-8732.

123 Roher AE, Lowenson JD, Clarke S, et al: B-Amyloid-(1-42) is a major component of cerebrovascular amyloid deposits: Implications for the pathology of Alzheimer disease. PNAS 1993;90:10836-10840.

124 Wisniewski HM, Kozlowski PB: Evidence for blood-brain barrier changes in senile dementia of Alzheimer's type. Ann.N.Y.Acad.Sci. 1982;386:119-129.

125 Pardridge WM: Does the brain's gatekeeper falter in aging?. Neurobiol Aging 1988;9:44-46.

126 Vinters HV, Pardridge WM: The blood-brain barrier in Alzheimer's disease. Can J Neurol Sci 1986;13:446-448.

127 Kanwar YS, Farquhar MG: Anionic sites in the glomerular basement membrane. In vivo and in vitro localization to the laminae rarae by cationic probes. J Cell Biol 1979;81:137

128 Kanwar YS, Hascall VC, Farquhar MG: Partial characterization of newly ssynthesized proteoglycans isolated from the glomerular basement membrane. J Cell Biol 1981;90:527

129 Kanwar YS, Farquhar MG: Presence of heparan sulfate in the glomerular basement membrane. Proc Natl Acad Sci 1979;76:1303

130 Olgemoller B, Schleichler E, Nerlich A, et al: Isolation, Characterization and Immunological Determination of Basement Membrane-Associated Heparan Sulfate Proteoglycan. Biol Chem 1989;370:1321-1329.

131 Murdoch A, Dodge G, Cohen I, et al: Primary Structure of the Human Heparan Sulfate Proteoglycan from Basement Membrane (HSPG2/Perlecan). The Journal of Biological Chemistry 1992;267,No.12,April 25:8544-8557.

132 Klein DJ, Brown DM, Oegema T, Jr.: Partial characterization of heparan and dermatan sulfate proteoglycans synthesized by normal rat glomeruli. J Biol Chem 1986;261:16636-16652.

133 Hagen SG, Michael AF, Butkowski RJ: Immunochemical and biochemical evidence for distinct basement membrane heparan sulfate proteoglycans. J Biol Chem 1993;268:7261-7269.

134 Campanelli JT, Ferns M, Hoch W, et al: Agrin: a synaptic basal lamina protein that regulates development of the neuromuscular junction. Cold Spring Harb Symp Quant Biol 1992;57:461-472.

135 Haralson MA: Extracellular Matrix and Growth Factors: An Integrated Interplay Controlling Tissue Repair and Progression to Disease. Laboratory Investigation 1993;69:369-372.

136 Berenson GS, Radhakrishnamurthy B, Srinivasan SR, et al: Recent advances in molecular pathology Carbohydrate-protein macromolecules and arterial wall integrity -A role in atherogenesis. Exp Mol Pathol 1984;41:267-287.

137 Linker A, Carney HC: Presence and Role of Glycosaminoglycans in Amyloidosis.. Laboratory Investigations 1987;57:297-305.

138 Snow AD, Wight TN, Nochlin D, et al: Immunolocalization of Heparan Sulfate Proteglycans to the Prion Protein Amyloid Plaques of Gerstmann-Straussler Syndrome,Creutzfeldt-Jakob Disease and Scrapie.. Laboratory Investigation 1990;63:601-611.

139 Guiroy DC, Yanagihara R, Gajdusek DC: Localization of amyloidogenic proteins and sulfated glycosaminoglycans in nontransmissibble and transmissible cerebral amyloidoses.. Acta Neuropathol 1991;82:87-92.

140 Snow AD, Kisilevsky R, Stephens C, et al: Characterization of tissue and plasma glycosaminoglycans during experimental AA amyloidosis and acute inflammation. Lab Invest 1987;56:665-675.

141 Altstiel L, Sperber K: Cytokines in Alzheimer's Disease. Prog Neuro-Psychopharmacol & Biol Psychiat 1991;15:481-495.

142 Kalaria R: The Immunopathology of Alzheimer's Disease and Some Related Disorders. Brain Pathology 1993;3:333-347.

143 Dickson D, Rogers J: Neuroimmunology of Alzheimer's Disease: A Conference Report. Neurobiology of Aging 1991;13:793-798.

144 Vandenabeele P, Fiers W: Is amyloidogenesis during Alzheimer's disease due to an IL-1-/IL-6-mediated 'acute phase response' in the brain?. Immunology Today 1991;12:217-220.

145 Bernfield M, Sanderson R: Syndecan, a developmentally regulated cell surface proteglycan that binds extracellular matrix and growth factors. Phil Trans R Soc Lond 1990;B 327:171-186.

146 Small D, Nurcombe V, Reed G, et al: A Heparin-binding Domain in the Amyloid Protein Precursor of Alzheimer's Disease is involved in the Regulation of Neurite Outgrowth. the journal of neuroscience 1994;14(4),April:2117-2126.